



PROCEEDINGS



The Montana Tunnels mine in Jefferson City, Montana. Photo by J.H. Dilles, Oregon State University. All Rights Reserved.

Montana Mining and Mineral Symposium 2017
October 11–October 14, 2017
Montana Bureau of Mines and Geology
Open-File Report 699

TABLE OF CONTENTS

Technical Papers and Abstracts

In the Field with the Hard Rock Mining Bureau: An Update on Mining in Montana.....	<i>Garrett Smith</i> 3
On the Origin of Montana Sapphires	<i>Richard B. Berg</i> 11
Geology and Mineralogy of the Southeastern Margin of the Butte Pluton near Pipestone, Montana..... <i>Richard I. Gibson</i> 15
Mineralogy, Fluid Inclusion, and S-Isotope Data for the Heddleston Porphyry Cu-Mo Deposit, Montana
.....	<i>B. Schubert and Christopher H. Gammons</i> 19
Ringing Rocks, Montana: A Modern Gas Diapir?	<i>John W. Gabelman</i> 31
Timing of Pluton Emplacement and Mineralization of the Boulder Batholith.....
.....	<i>Stanley L. Korzeb and Kaleb C. Scarberry</i> 39
The Black Butte Copper Deposits, Central Montana: Their Geology and Development.....
.....	<i>Jerry A. Zieg</i> 45
Petrology and Mineralogy of the Mount Rosa Complex, El Paso County, Colorado
.....	<i>Philip M. Persson</i> 49
Using Your Smartphone for Field Work	<i>Jesse G. Mosolf</i> 53
Nature of the Mineralization and Alteration Mapped at the Clementine Porphyry Copper Prospect in	the Northern Pioneer Mountains of Southwest Montana
.....	<i>George H. Brimhall and Bruce D. Marsh</i> 55
Experiments on the Hydrothermal Solubility of Gold and Iron, and the Origin of	Iron–Oxide–Copper–Gold (IOCG) Deposits.....
.....	<i>Christopher H. Gammons and Nick Allin</i> 59
Exploration at the Madison Au-Cu-Ag Skarn, Silver Star, Montana.....	<i>Jenna M. Kaplan</i> 61
Supergene Minerals from the Mayflower Mine, Madison County, Montana	<i>Richard I. Gibson</i> 67
Copperopolis, Copper City, and Copper Cliff: Microminerals from Three of Montana’s Obscure	Copper Deposits.....
.....	<i>Michael J. Goble</i> 69
MBMG’s Abandoned and Inactive Mines (AIM) Inventory and Sampling Program—8,000 Mines	and So Little Time.....
.....	<i>Phyllis Hargrave</i> 81
Geology, History, and Remediation in the Carpenter–Snow Creek Mining District, Neihart, Montana
.....	<i>Sara Edinberg</i> 83
The Early History (1982-2000) of Butte Mine Flooding.....	<i>John Metesh</i> 87
Modeling Areas Susceptible to Ground Subsidence Due to Mine Drift and Shaft Collapse in	Butte, Montana.....
.....	<i>Christopher P. Smith and Paul R. Thale</i> 91

Posters and Abstracts

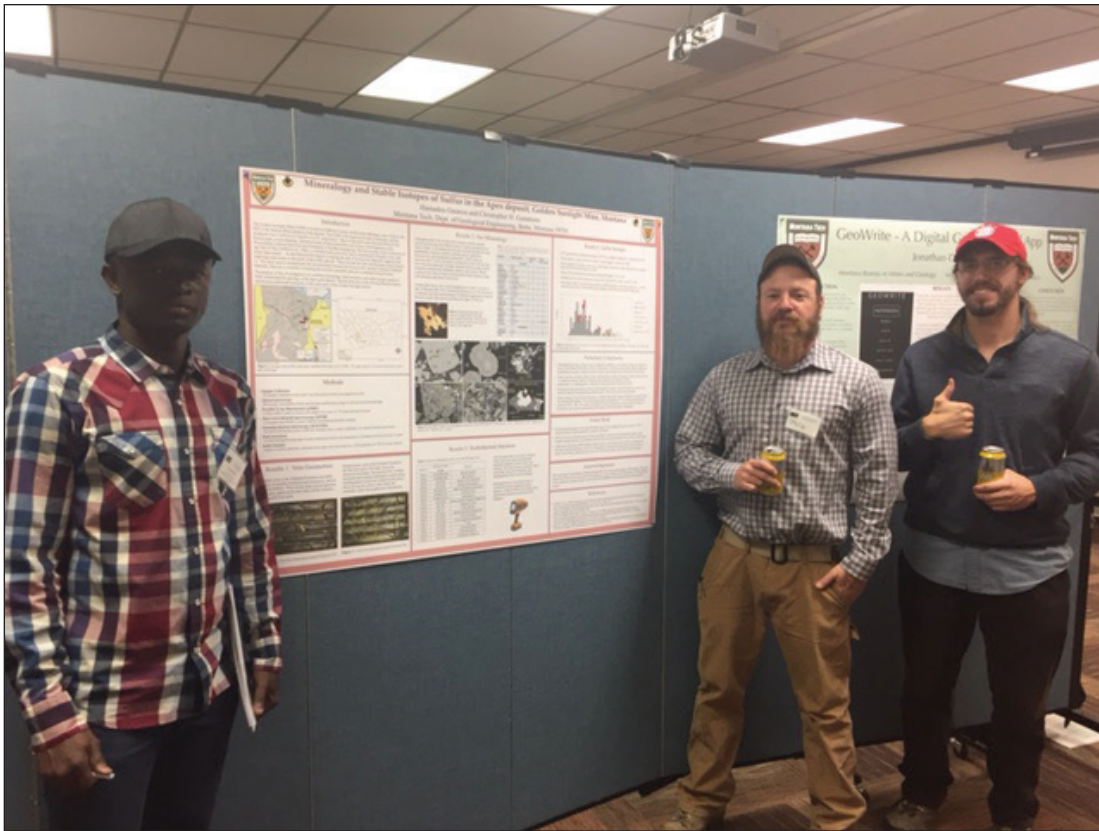
Thermochemical Arsenite Reduction and the Origin of Hydrothermal Arsenide Minerals
.....	<i>Nick Allin</i> 97
An Occurrence of Cu-Ni-Co-Au-PGE in the Grouse Mountain Dike, Troy District, Lincoln County,	Montana
.....	<i>John E. Etienne</i> 97
Identifying Environmental Tracers Using Water Chemistry and Stable Isotopes, Moulton Road Area,	Butte, Montana.....
.....	<i>Matt Berzel</i> 100
Mapping Hydrothermal Alteration in the Belt Supergroup Using a pXRF	<i>Philip Dalhof</i> 100
GeoWrite: A Digital Field Notebook	<i>Jonathan Dupuis</i> 101
Mineralogy and Stable Isotope Geochemistry of the Apex Gold Deposit near the Golden Sunlight	Mine, Montana.....
.....	<i>Hamadou Gnanou and Christopher H. Gammons</i> 101

Distribution of Sulfide Minerals in Metasedimentary Deposits of the Apple Creek Formation, Salmon River Mountains, Idaho	<i>Francis Grondin</i>	102
Using Fluid Inclusions and C, O, H and Sr Isotopes to Understand the Genesis of Dolomite-Hosted Talc Mineralization in Montana.....	<i>Garrett W. Hill and Christopher H. Gammons</i>	102
Eocene Ignimbrite Flare-Up in the Northeastern U.S. Cordillera: Timing and Style of Volcanism in the Lowland Creek Volcanic Field of Southwestern Montana	<i>Kaleb C. Scarberry</i>	103
Hydrothermal Water-Rock Interactions: From Mineralogy to Water Chemistry.....	<i>Shanna Law and Alysia Cox</i>	104
Montana Lamprophyre Occurrences.....	<i>Jake McCane</i>	104
Secondary Pb-Zn Mineralogy of the Summit Mine, Radersburg District, Broadwater County, Montana	<i>Kyle Eastman and Nick Allin</i>	105
Field Trip: Silver Star		
Field Trip to the Madison Au-Cu Deposit, Silver Star, Montana	<i>Jenna M. Kaplan and Christopher H. Gammons</i>	109
Presenter Biographies		117

**PROCEEDINGS,
MONTANA MINING AND MINERAL SYMPOSIUM 2017
TECHNICAL PAPERS AND ABSTRACTS**

Edited by Kaleb C. Scarberry and Susan Barth
Montana Bureau of Mines and Geology

Open-File Report 699



Montana Tech Geologic Engineering M.S. student Hamadou Gnanou (left) with his poster and Colorado State University M.S students Philip Dalhof and Jake McCane (right). Photo by K. Scarberry, MBMG.



MBMG geologists Dick Berg (left) and Petr Yakovlev (center) judge student posters at the poster session. Photo by A. Roth, MBMG.

In the Field with the Hard Rock Mining Bureau: An Update on Mining in Montana

Garrett Smith

Geochemist, Montana Department of Environmental Quality, Helena, Montana

Background and Duties

The Hard Rock Mining Bureau (HRMB) is the program within the Montana Department of Environmental Quality (DEQ) that regulates the mechanized exploration and development of all ore, rock, or mineral substances from hard rock sources. Although that definition encompasses a wide variety of operations, the resources that are excluded from the HRMB's authority include bentonite, clay, coal, natural gas, oil, peat, sand and alluvial gravel, scoria, soil materials, and uranium. In general, the HRMB oversees operations conducted under small miner exclusion statements (SMES, ≤ 5 acres), exploration licenses, and operating permits.

Administrative duties and permitting procedures that apply to the HRMB originate primarily from the Metal Mine Reclamation Act (MMRA) and Montana Environmental Policy Act (MEPA); see 82-4-301, Montana Code Annotated (MCA), and 75-1-101, MCA. These duties include issuing timely and complete decisions for permit applications and modifications, and ensuring permitted mineral development occurs with adequate protection of air and water resources. This is often coordinated with other permits obtained through State or Federal agencies. The HRMB also reviews annual reports or renewal statements submitted by operators and conducts annual inspections to review mining and reclamation status at each site and to offer compliance assistance. Performance bonds (i.e., financial assurances) are held for operating permits, exploration projects, and some SMES sites, in order to perform any potential reclamation work that is not completed by the operator. The bonds are reviewed annually and recalculated at a minimum of every 5 years or following significant permit modifications.

Operating Permit Updates

The following discussion focuses primarily on hard rock operating permits and proposed projects that are currently under review, but it does not address the many active SMES (>400) and exploration projects (>150) underway across the state. As of September 2017, there are currently 69 operating permits administered by HRMB, with another 7 permits in the process of closure, and 9 permits that are under HRMB review or awaiting actions from the operator or cooperating agencies before work can begin. There are also several permits that include multiple mining locations under one operating and reclamation plan. This is more common with quarries and surficial rock picking operations that acquire specific types of rock from relatively small locations spread over a large region. Considering these additional locations, there are 226 active sites covered by operating permits and inspected by HRMB staff (see fig. 1).

The total land area now permitted for hard rock mining and milling operations in Montana is approximately 85,000 acres (<0.1% of Montana), but a smaller fraction of that land is disturbed by the actual operations. Many of the sites contain a disturbance area within a relatively larger permit area, which often corresponds to property ownership boundaries. Operators that produce rock products (e.g., riprap, railroad ballast, construction, and decorative stone) comprise the vast majority of sites, and account for 44% of all land permitted for hard rock mining. Base metal (e.g., Cu, Pb, Zn) mines cover 23% of all permitted land, while precious metal (e.g., Au, Ag, Pt, Pd, Rh) mines cover just under 20%. The remaining land is permitted for mining, milling, and processing a wide variety of products that include cement materials, talc, limestone, garnets, and sapphires.

Reviewing the number of operations that are currently active (i.e., generating material and revenue) highlights that markets for rock products and industrial minerals are less volatile than those for base and precious metals. Perhaps more affected by commodity prices, most of the metal mines are now in care and maintenance status or in the process of final closure. In contrast, many industrial mineral mines have amended their permits to extend production plans, while quarries and rock picking operations continue to expand and experience increasing competition from neighboring operators. What follows is an update of some of the major developments at active operations and pending projects in Montana.

Hard Rock Operating Permits 2017

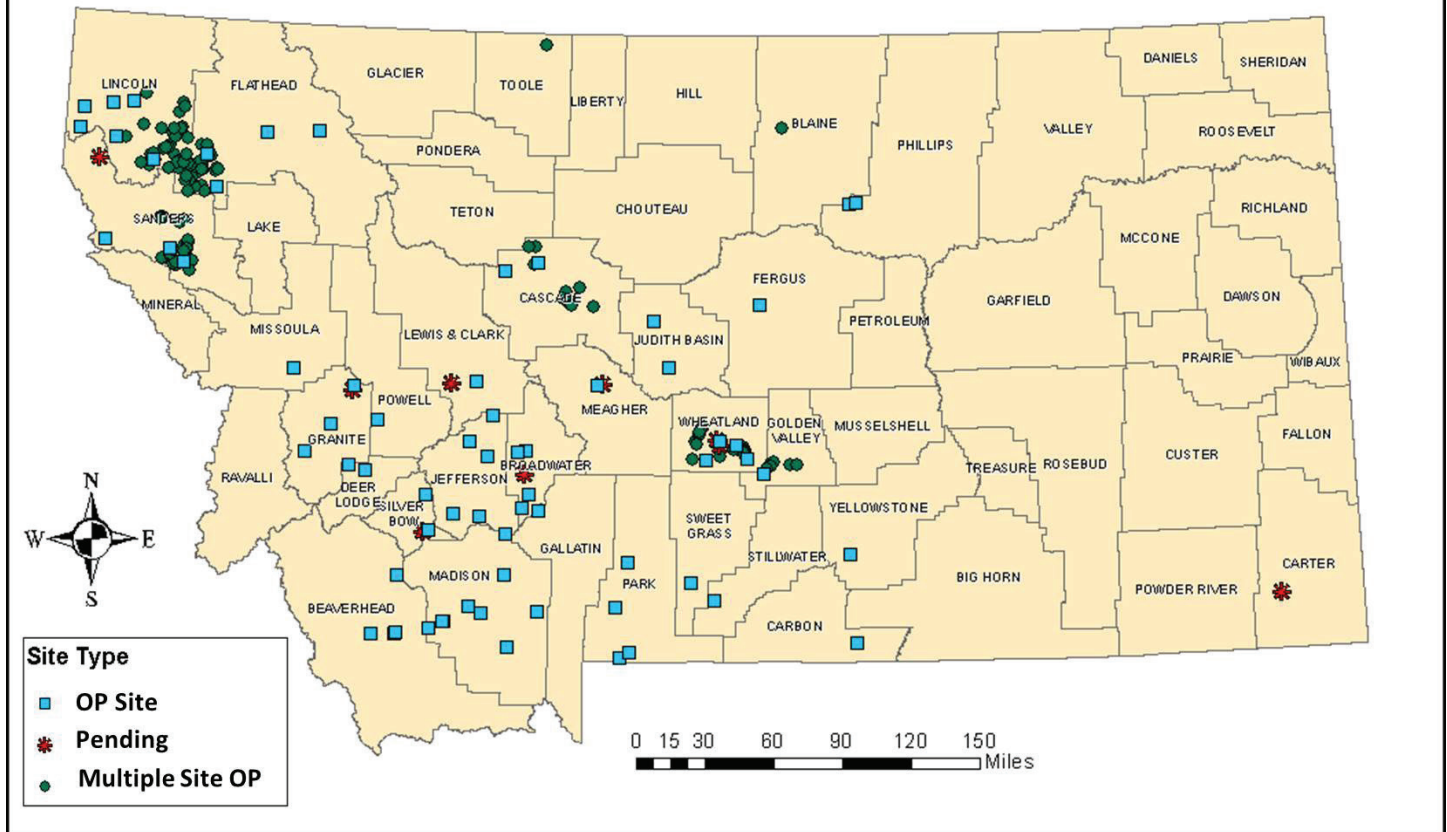


Figure 1. Map showing the location of Operating Permit (OP) sites, multiple quarry sites that are grouped under one OP, and pending sites that are dependent on a response from the operator or permitting action from the agency before work can begin.

Continental Mine, Montana Resources (Cu, Mo, Ag)

With copper prices recovering after a 5-year decline, Montana Resources in Butte continued to produce ore from the D-North area of the Continental Pit, while stripping overburden in the D-East expansion area to expose additional ore reserves. The overburden is used as construction material around the site, particularly for raising the tailings embankment. Copper concentrates were produced from leach pad solutions at the Horseshoe Bend precipitation plant, and the nearby water treatment plant continued to treat the effluent stream for re-use in the mill circuit.

In late 2016, HRMB approved a revision to permits that would allow Montana Resources to potentially receive waste material removed from the Parrot Tailings area, near the Butte Silver Bow county shops and Civic Center. Waste removal would be conducted under the direction of the Natural Resource Damage (NRD) Program, but that work has not yet begun. Montana Resources would allow NRD contractors to stockpile waste on the site, which would then likely be disposed within the tailings facility. The company also submitted a revision to the operating permits to allow for additional soil salvage around the tailings facility and stockpiling the soil to create berms along a nearby county road. In the summer of 2017, soil was removed in advance of the D-East expansion and then used to initiate reclamation on the south end of the East Dump Complex.

Montana Resources is preparing to submit a permit amendment application to HRMB to raise the tailings facility embankment to an elevation of 6,450 feet. Among other construction logistics, this expansion would necessitate water management on the west side of the facility, to prevent tailings pond seepage and potential degradation of groundwater beneath the nearby ridge. Prior to HRMB review, the baseline studies and engineering designs for the expansion have been reviewed by an Engineer of Record and Independent Review Panel, as specified in 2015 legislation.

Golden Sunlight Mine, Barrick Gold Corp. (Au, Ag)

In late 2015, Golden Sunlight shifted its focus from production from small pits and low-grade stockpiles, to producing ore from only the underground workings within Mineral Hill Pit. This underground development continues and the mill operates in batch mode. The mill also continues to receive low-grade material brought in by third parties, often originating from historic waste dumps from across southwest Montana. This program generates revenue and provides an environmental benefit to the waste removal sites, but some small operators have been limited by gold prices, which continue to follow 5-year fluctuations between \$1,100 and \$1,300 per ounce.

New revisions to the permit include development of a small excavation near the Far East Dump, to produce limestone riprap for use across the site. Another revision allows reclamation cover testing on the Northeast Dump, to determine the effect that compost amendment may have on the prevalence of annual weeds. Reclamation repair work also took place on some areas of the active tailings facility embankment, with soil grading and revegetation. Following years of exploration drilling, Golden Sunlight submitted an amendment application in 2017 for the development of new underground workings in the Apex area, located north of Mineral Hill Pit. Ore mineralogy in the Apex area is like that in the Mineral Hill Pit, but the underground mining method would target pods of ore located within 100 to 900 feet below ground surface. The application is currently going through the HRMB deficiency review process.

Stillwater Mine (Nye), Sibanye-Stillwater Ltd. (Pt, Pd, Rh, Au, Cu, Ni)

Stillwater Mining Co. was acquired by Sibanye Gold Ltd. of South Africa in mid-2017, becoming Sibanye-Stillwater Ltd., the third largest producer of palladium and platinum in the world. Normal operations continued through 2017 at the Stillwater Mine near Nye. The Tunnel Boring Machine located at the 5000 East Portal is being utilized for advancing underground workings as part of the Blitz project. Expansion of the East Waste Rock Dump continued, with liner placement occurring in phases before the waste rock is placed and then contoured, soiled, and seeded. Cone penetration tests were conducted on the Nye impoundment, as part of the data collection phase in preparing for final reclamation of the impoundment. A minor revision was submitted for infiltration testing and a dye tracer study in preparation for possible infiltration ponds at the Hertzler impoundment. Another minor revision was approved for a slope stabilization project around the 5900 West portal, which involved the installation of rock netting over the uphill slope on the access road just before the portal, and an extension of the steel structure at the portal entrance. Another minor revision was approved for a redesign and upgrade of the locomotive load outs at the 5000 East Portal.

East Boulder Mine, Sibanye-Stillwater Ltd. (Pt, Pd, Rh, Au, Cu, Ni, Co)

Like the Stillwater Mine, the East Boulder Mine continued normal operations through the formation of Sibanye-Stillwater Ltd. Minor facility upgrades have been proposed, including installation of an electronically operated security gate near the guard shack entrance. A minor revision for a groundwater mixing zone was approved by HRMB and the Forest Service that will address non-point release of nitrogen to groundwater. The mixing zone will allow the company to address cumulative contributions to a groundwater nitrate plume from various sources within the permit boundary. These internal sources include meteoric water infiltration through the waste rock-built tailings embankment. The mixing zone will allow termination of the administrative order on consent that the mine is currently under. Other recent site activities include raising the tailings impoundment through Stages 4 and 5, which should provide capacity to 2030. Preliminary designs and investigations are ongoing for the Stage 6 expansion, which would increase the storage area to the west of the current impoundment footprint. The company is also developing plans for a waste rock storage site and associated water management features in Lewis Gulch.

Troy Mine, Hecla Mining Co. (Cu, Ag) Closure

After acquiring the Troy Mine in 2015, Hecla began closing the operation by removing remaining mining equipment and infrastructure from the underground workings. Water will be allowed to flood the workings,

beginning with the decline to the lower “I Beds” deposit that was never completed during operations. Hecla will continue to implement the reclamation plan by eventually demolishing the mill and other surface structures, and maintaining the pipeline to convey mine water to the impoundment, and by covering and vegetating other portions of the impoundment. An amendment was submitted in 2017 to change the soil capping thickness on the impoundment, and an EA for that amendment is currently underway.

Black Butte Copper Project, Tintina Resources Inc. (Cu) Pending

Tintina Resources submitted an operating permit application to HRMB in late 2015. The project proposes to develop the upper and lower Johnny Lee deposits, located north of White Sulphur Springs. The underground mine would utilize “cut and fill” methods to extract ore and backfill completed stopes with cemented paste tailings. The proposed facility would include a lined surface impoundment to contain cemented paste tailings and waste rock, storage ponds for process water and storm water collection, a water treatment plant, groundwater infiltration galleries for treated water discharge, a cement plant, and a mill facility with crushing and flotation capabilities.

After multiple deficiency reviews, the HRMB determined that the application was complete and compliant with MMRA requirements and a draft permit was issued in September 2017. This initiates a 1 year timeline for DEQ to complete an Environmental Impact Statement (EIS) for the project. Further development of the Black Butte Copper Project would require additional permits and approved plans outside the authority of HRMB, covering air quality, public water supply well, treated water discharge, water rights, and consumptive use mitigation.

Yellowstone Mine, Imerys S.A. (Talc)

Imerys notified DEQ in late 2016 that construction to relocate the primary site access road to the south of its current location would begin. The construction of a new road is needed before the East Overburden Disposal Area expands to the southeast and covers the existing road. The road was approved, in concept, in Amendment 7 (2006), but more details were provided prior to the start of construction. Subsequent HRMB inspections have documented the salvage of substantial soil resources during preparation of the new road footprint. The pit layback, known as “Phase 6,” is also currently underway, which will involve removing overburden from the north end of the pit over the next 10 years. This area is shown at the far end of the pit, in the center of figure 2. As ore is exposed by the Phase 6 layback, the next phase of development will start at the south end of the pit, requiring a new location for the onsite mill facility. Reclamation work is underway at the north end of the site, and as the old North Main pit is backfilled, the final reclaimed surface will be contoured to promote drainage from the area.

Barretts Minerals Inc., Minerals Technologies, Inc. (Talc)

In April 2017, HRMB approved a layback expansion within the Treasure Chest Pit at the Treasure Mine. The expansion will encompass an area of about 15 acres in the existing pit. The layback will modify pit topography by deepening the bottom elevation, but it will also contribute more material for use as backfill on the west side of the adjacent pit. At the Regal Mine, an amendment to the permit is in preparation to expand the Regal Pit to access more talc at depth. However, expansion would necessitate a flow mitigation plan or diversion structure for nearby Hoffman Creek to offset any impacts to surface water or connected groundwater that may be intercepted by the pit. At Barretts Mill, a series of minor revisions was submitted for the excavation of two ponds that contain mill tailings. Ponds F and G were cleaned out and the containment berms raised, to increase tailings storage capacity. Excavated mill tailings were disposed in dry dump areas, adjacent to the active ponds.

Geyser Mine, CRH (Gypsum)

Due to decreasing reserves at the current quarry location, an amendment application was received to expand the gypsum mine located to the south of Geyser in Judith Basin County. The gypsum layer at the site is approximately 7 feet thick, under an equivalent thickness of overburden, and is mapped within the Heath Shale



Figure 2. Looking north across the Yellowstone talc mine, operated by Imerys S.A. The Phase 6 pit layback has commenced at the far north end of the pit (upper center of photo), which will expose additional talc ore beneath the upper layers of volcanic tuff and dolomitic waste rock.

of the Mississippian Big Snowy Group. Mining at the Geyser site typically occurs based on demand, but CRH now anticipates producing up to 25,000 tons of ore per year. Gypsum ore is hauled by truck to the CRH cement plant in Trident, located about 150 miles south of the mine. The pending amendment would increase the permit area by 19 acres, and allow the company to produce gypsum from an area to the east of their current quarry and extend production by approximately 3 years. The eastern extension would be located on land administered by the Montana Department of Natural Resource Conservation (DNRC), so additional arrangements must be made regarding a mineral lease.

Red Wash Quarry, Garnet USA, LLC (Garnet)

Garnet USA operates the Red Wash site and processing plant near Alder, located in Madison County. Historic production in the area relied on garnet found in alluvial deposits and by processing historically dredged placer tailings. The current operation produces garnet from a bedrock source of garnet-bearing amphibolite and garnet-quartz-feldspar gneiss that contains 10–60% garnet. A number of permit revisions were approved in 2017, a few of which addressed updates to the water monitoring plan, including new monitoring wells and new sampling locations near the processing plant and the Red Wash Quarry site. Another revision allowed for the southward expansion of the quarry in the “Middle 80,” to access higher quality ore. Upgrades have been proposed around the plant site, including moving the main entrance gate and adding an expansion to walkways and the parking area for haul trucks.

Rock Products, Various Companies

There were multiple operating permit applications submitted to HRMB in 2017 for rock product operations. The pending sites include the Homestead Quarry (Kootenai Rocks) and Gordon Jones Ranch, both located south of Harlowton in Wheatland County, and the “Brownfield Sandstone” site near Hammond, which would be operated by Carter County to produce rock for construction and maintenance projects.

E.S. Stone and Structure continues to produce rock from many sites across north-central Montana. The most recently approved sites (#19 and #20) are located north and south of Vaughn, respectively. Excavators are used at these locations to remove large slabs of sandstone from the top 5 feet of the ground surface (figs. 3, 4). The rock may be sold directly for decorative use or sized and shaped for construction purposes. An amendment was submitted by E.S. Stone and Structure in 2017 to permit site #21, located between their other permit areas to the south of Harlowton. This amendment is now going through the deficiency review process. The permits for Venture Stone and Block Mountain Slate and Stone were finalized upon receipt of the performance bonds for each operation. Venture Stone operations consist of an office and mill site near Vaughn and five rock picking locations south and southeast of Great Falls, in Cascade County. Block Mountain Slate and Stone operations consist of seven rock picking and quarry sites near Plains, in Sanders County.



Figure 3. An excavator is used to remove slabs of sandstone from shallow depths in a field north of Vaughn. The stone is hauled to another location to be sorted and shaped. The ground disturbance is then graded and seeded to establish vegetation.



Figure 4. Depending on market demands, the larger rock slabs may be sold directly or they may be sized and shaped with a pneumatic rock chopper before being stacked on pallets for shipping.



Department of Environmental Quality geochemist G. Smith. Photo by A. Roth, MBMG.



Looking at rocks in the Boulder batholith near Boulder, MT. Photo by D. Herman, MBMG.

On the Origin of Montana Sapphires

Richard B. Berg

Montana Bureau of Mines and Geology

With historic production exceeding 70 tonnes, and continuing production, Montana leads the U.S. in total sapphire production. Because of the importance of Montana sapphires, research has focused on the geology of the deposits, their bedrock sources, and the origins of the gemstones. As used here, origin applies to how the corundum (sapphire) initially formed—by magmatic metasomatic, or metamorphic processes—and further, whether the formation occurred in the crust or in the mantle. This report does not include a summary of research on the magmatic transport of sapphires to the surface or the distribution of sapphire deposits in Montana. This summary is devoted exclusively to the proposed origins of sapphires in Montana.

The most famous Montana deposit is that at Yogo (fig. 1), where sapphires occur in a lamprophyre dike (fig. 2). However, most historic production is from alluvial deposits in southwestern Montana, where evidence for a bedrock source is limited. Sapphires from the Yogo dike are simply referred to as Yogo sapphires in the gemstone trade, whereas sapphires from the alluvial deposits are referred to as Montana sapphires. The following summary of the origins of sapphires in Montana is arranged in chronological order, beginning with articles on the Yogo sapphires, and proceeding to articles related to Montana sapphires in alluvial deposits.

Yogo Sapphires

Clabaugh (1952, p. 56, 57) suggested the reaction between silica-deficient lamprophyre magma and included pre-Belt metamorphic rocks, some containing aluminous minerals such as kyanite, as a possible way to generate Yogo sapphires (fig. 2). Brownlow and Komorowski (1988) suggested that they formed by partial melting of a mantle rock to form an aluminum-rich melt, followed by magmatic differentiation resulting in sapphire crystallization. Dahy (1991, p. 53) favored formation by partial melting and desilication of a crustal pelitic schist by lamprophyre magma to produce a plagioclase, pyroxene, corundum rock. Further assimilation of this

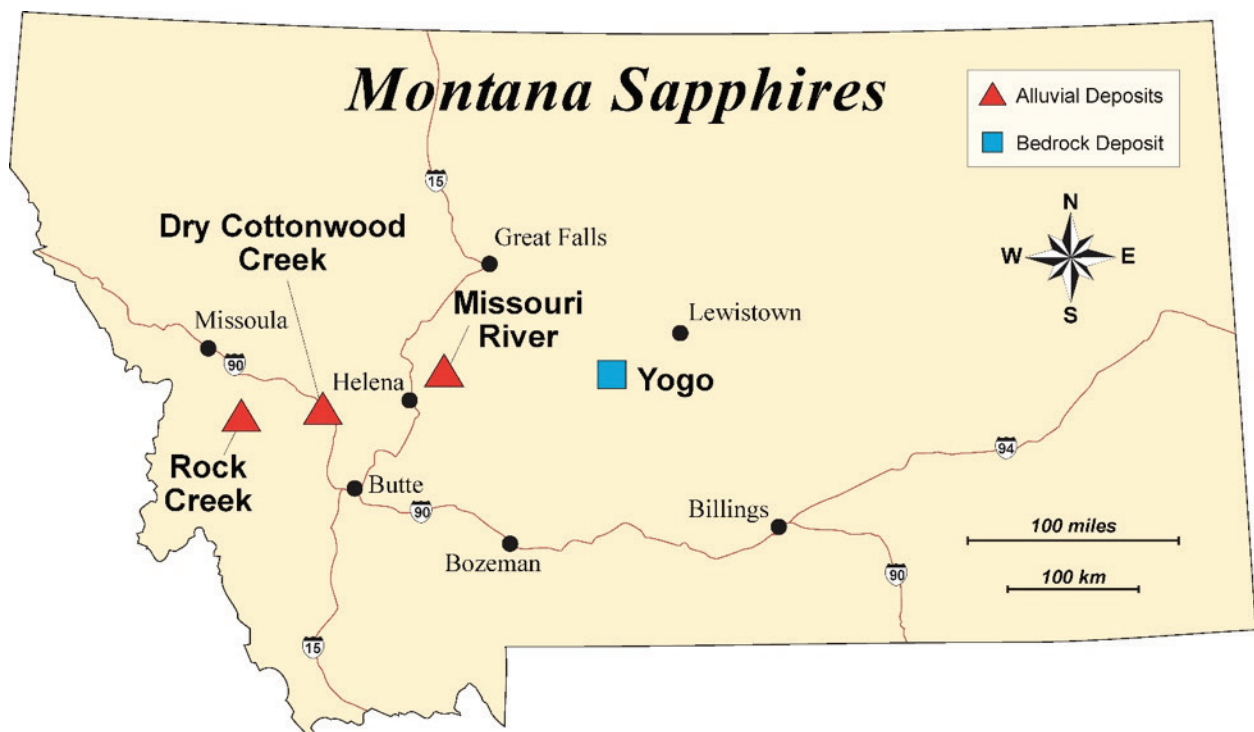


Figure 1. Montana sapphire deposits.



Figure 2. Sapphire in Yogo lamprophyre dike (R.B.B. photo)

rock resulted in liberation of the more refractory corundum. Gauthier (1995) concluded that the sapphires are xenocrysts with crustal origins, based on analysis of a garnet–clinopyroxene–plagioclase metamorphic xenolith. Cade and Groat (2006, p. 106) compared the geochemistry of garnet inclusions in Yogo sapphires to eclogitic garnets and concluded that mantle eclogites were the probable sapphire source. Palke and others (2016) postulated that partial melting of an Al-rich protolith by lamprophyre magmas at the base of the crust formed these sapphires. Thermodynamic modelling identified anorthosite, or troctolite, as the most likely Al-rich protoliths.

Montana Sapphires (Alluvial Deposits in Southwestern Montana)

Berg and Dahy (2002, p. 203, 204) concluded that Montana sapphires are of a metamorphic origin based on sapphire-bearing metamorphic xenoliths found in a sill near Helena. Assimilation of similar metamorphic xenoliths liberated refractory sapphire xenocrysts found in the sill. Garland (2002) analyzed mineral inclusions in sapphires from the Rock Creek and Dry Cottonwood Creek deposits and concluded that they formed in metamorphic rocks at mid-crustal levels. Berg and others (2008) reported $\delta^{18}\text{O}$ values for sapphires from Rock Creek, Dry Cottonwood Creek, and the Silver Bow area west of Butte. The $\delta^{18}\text{O}$ data showed that these Montana sapphires are isotopically similar to sapphires from a metamorphic source (e.g., Giuliani and others, 2005). Zwaan and others (2015) used a geochemical approach to conclude that Montana sapphires may have metasomatic origins. Trace element concentrations in many Montana sapphires are similar to those of sapphire-bearing plumasite in the Umba River Valley in northeast Tanzania (Peucat and others, 2007). The Tanzania plumasite host rock may have formed by reaction of an anorthosite and desilication caused by an adjacent serpentinite forming corundum (Solesbury, 1967). Palke and others (2017) used chemical compositions to distinguish between primary and secondary glassy melt inclusions in sapphires. Primary melt inclusions are samples of the melt produced during partial melting of an anorthosite protolith, which leaves a corundum (sapphire) residuum. Secondary melt inclusions are samples of magma that carried the corundum to the surface.

The most significant conclusion that can be reached regarding the origins of Montana sapphires is that their origins are not fully understood. The reader is encouraged to refer to the cited articles for detailed discussion of evidence for the proposed hypotheses.

Future Research Topics

1. Age determinations of zircon crystals included in sapphires. A Precambrian age will not be definitive because they could be inherited zircons from a Precambrian source. However, a Tertiary zircon would show that the sapphire can be no older than Tertiary.
2. Petrographic analysis of corundum-bearing xenoliths in igneous rocks such as the Eocene Lowland Creek Volcanics.
3. Comparison of sapphire-bearing dikes in the Yogo district to dikes that are barren in the district.

4. Search for sapphires in igneous rocks, particularly in the numerous lamprophyre dikes, in the Central Montana Alkalic Province.
5. Detailed study of the chemistry and inclusion mineralogy of metamorphic corundum in the Wyoming Archean Province.
6. Comparison of trace element chemistry of corundum in Montana plumasite to that of Montana sapphires in southwestern Montana. This small plumasite body is in the metamorphic rocks of the northern Tobacco Root Mountains (Christensen, 1956).

References Cited

- Berg, R.B., and Dahy, J.P., 2002, Montana sapphires and speculation on their origin, *in* Scott, P.W., and Bristow, C.M., eds., *Industrial Minerals and the Extractive Industry Geology*: Geological Society, London, p. 199–204.
- Berg, R.B., Gammons, C.H., and Arehart, G.B., 2008, Preliminary oxygen isotope values for Montana sapphires [abs.]: *Geological Society of America Abstracts with Programs*, v. 40, no. 6, p. 254.
- Brownlow, A.H., and Komorowski, Jean-Christophe, 1988, Geology and origin of the Yogo sapphire deposit, Montana: *Economic Geology*, p. 875–880.
- Cade, A., and Groat, L.A., 2006, Garnet inclusions in Yogo sapphires [abs.]: 2006 Gemological Research Conference, *Gems and Gemology*, v. 42, p. 106.
- Christensen, E.W., 1956, Petrography of plumasite, altered enstatite, and metamorphosed quartz-rich rocks from the Gilliam prospect, Madison County, Montana: Bloomington, Indiana University, M.A. thesis, 41 p., 18 figs.
- Clabaugh, S.E., 1952, Corundum deposits of Montana: U.S. Geological Survey Bulletin 983, 100 p. and maps.
- Dahy, J.P., 1991, Geology and igneous rocks of the Yogo sapphire deposit, Little Belt Mountains, Montana, *in* Baker, D.W., and Berg, R.B., eds., *Guidebook of the central Montana alkalic province: Geology, ore deposits, and origin*: Montana Bureau of Mines and Geology Special Publication 100, p. 45–54.
- Garland, M.I., 2002, The alluvial sapphire deposits of western Montana: Toronto, Ontario, University of Toronto, Ph.D. dissertation, 381 p., 4 pls.
- Gauthier, G., 1995, Mineralogy, geochemistry, and geochronology of the Yogo dike sapphire deposit, Montana: Vancouver, University of British Columbia, M.S. thesis, 289 p.
- Giuliani, G., Fallick, A.E., Garnier, V., France-Lanord, C., Ohnenstatter, D., and Schwarz, D., 2005, Oxygen isotope composition as a tracer for the origins of rubies and sapphires: *Geology*, v. 33, no. 4, p. 249–252.
- Palke, A.C., Renfro, N.D., and Berg, R.B., 2016, Origin of sapphires from a lamprophyre dike at Yogo Gulch, Montana, U.S.A.: *Lithos*, 260, p. 339–344.
- Palke, A.C., Renfro, N.D., and Berg, R.B., 2017, Melt inclusions in alluvial sapphires from Montana, U.S.A.: Formation of sapphires as a restitic component of lower crustal melting?: *Lithos*, v. 278–281, p. 43–53.
- Peucat, J.E., Raffault, P., Frisch, E., Bouhnik-Le Coz, Simonet, M., and Lasnier, B., 2007, Ga/Mg ratio as a new geochemical tool to differentiate magmatic from metamorphic blue sapphires: *Lithos*, 98, p. 261–274.
- Solesbury, F.W., 1967, Gem corundum pegmatites in NE Tanganyika: *Economic Geology*, v. 42, p. 983–991.
- Zwaan, J.C., Buter, E., Mertz-Kraus, R., and Kane, R.E., 2015, Alluvial sapphires from Montana: Inclusions, geochemistry, and indications of a metasomatic origin: *Gems and Gemology*, v. 51, no. 4, p. 370–391.



MBMG field geologists Colleen Elliott (left), Dick Berg (second from left), and Katie McDonald (center). Photo by A. Roth, MBMG.



MBMG geologist Dick Berg. Photo by A. Roth, MBMG.

Geology and Mineralogy of the Southeastern Margin of the Butte Pluton near Pipestone, Montana

Richard I. Gibson

Geologist, Butte, Montana, rigibson@earthlink.net

The Eastern Margin of the Butte Pluton

Controversy continues as to the nature of the eastern contact of the Butte Pluton with adjacent rocks (fig. 1): is it an igneous contact along a pre-existing basement structure? Is it a compressive fault contact, and if so, is the fault a deep-seated detachment or to a simpler high-angle reverse fault? Although the contact zone is narrow, ranging from about a kilometer at Toll Mountain to less than 100 meters at Delmoe Road, the southeastern margin of the Butte Pluton, near Pipestone (fig. 1), is marked by an intense magnetic gradient (fig. 2). The magnetic signal suggests that the contact zone has a strong magnetic susceptibility contrast that extends over a significant vertical distance, on the order of a few kilometers. This paper briefly reviews ideas related to the contact zone and focuses on the mineralogy of part of the contact at Bald Mountain, along the Delmoe-Pipestone Road, and at a nearby railroad cut (fig. 1).

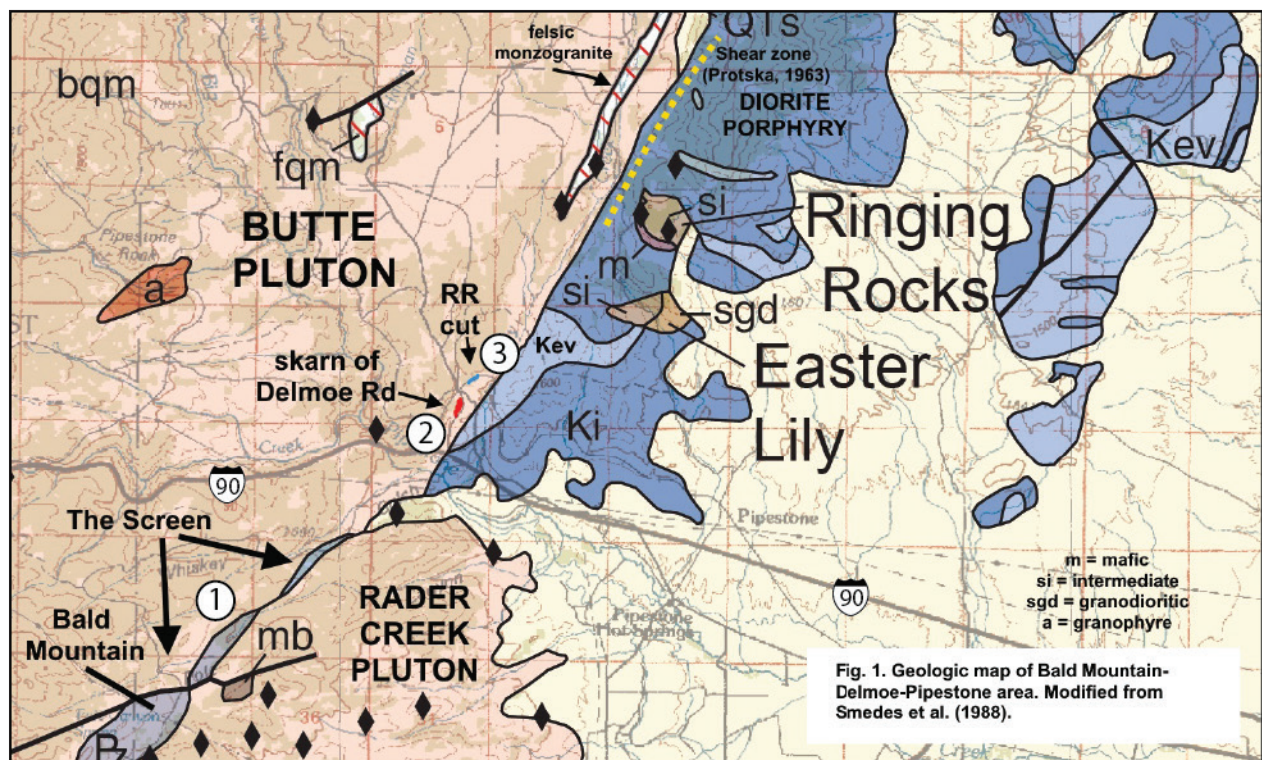


Figure 1. Geologic location map modified from Smedes and others (1988). Alteration mineralogy locations are shown by circles, labeled 1–3. Toll Mountain (not shown) is located a few kilometers southwest of Bald Mountain.

A zone of skarns in metasediments are caught between the 76 Ma Butte pluton and the 80 Ma Rader Creek pluton. This zone was traditionally thought of as roof pendants, but with geochemical and radiometric age discrimination of the plutons, the zone has been called a “screen” of metasedimentary rocks, at least since 1974 (Hamilton and Myers, 1974) (fig. 1). The belt of metamorphosed sedimentary rocks is discontinuous northeastward from Toll Mountain about eight kilometers to Bald Mountain (fig. 1, location 1). These rocks are mapped as Precambrian (Belt) sediments and Paleozoic rocks (Smedes and others, 1988). Despite amphibolite grade metamorphism (Elliott, personal communication, 2017), the sequence at Bald Mountain might be construed as contact metamorphosed Belt (Grayson shale?), Cambrian Flathead sandstone, Cambrian Wolsey shale/carbonate, and Cambrian Meagher limestone. The sequence could also be interpreted as tectonically juxtaposed metamorphic packages, or thrust wedges, with no clear stratigraphic implications.

Northeast of Bald Mountain, and north of Interstate 90 (fig. 1, location 2), the screen continues as a narrow series of outcrops that include a metasedimentary skarn along the Delmoe-Pipestone Road. Less than a kilome-

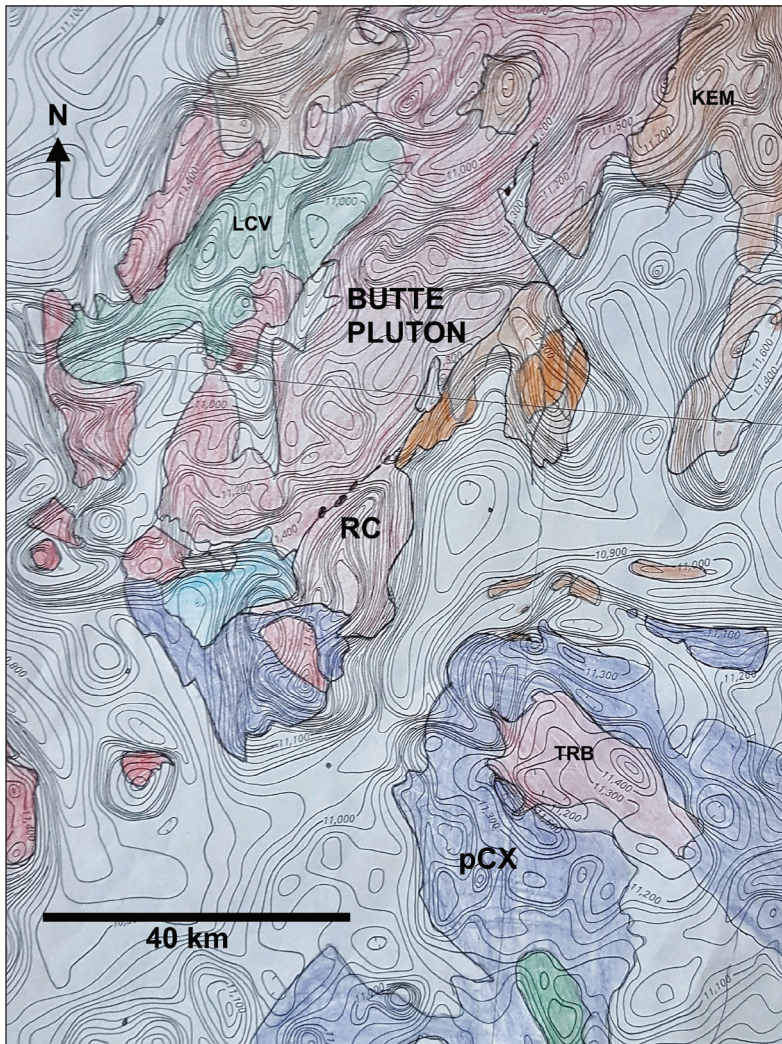


Figure 2. Magnetic anomaly map (from Zietz and others, 1980), with screen outcrops shown as black dots northeast of Rader Creek Pluton. Abbreviations: RC, Rader Creek Pluton; LCV, Lowland Creek Volcanics; KEM, Elkhorn Mountains Volcanics; TRB, Tobacco Root Batholith; pCX, Archaean-Paleoproterozoic crystalline rocks.

locations.

The railroad cut (fig. 1, location 3) contains conspicuous epidote, axinite (fig. 3B), rare and tiny well-formed apatite crystals, and rare titanite. Pegmatites on the order of one meter across are present within tens of meters east of the railroad cut, and contain microcline crystals to 10 cm and crusts of epidote. Axinite (calcium Fe-Mg-Mn aluminoborosilicate) probably forms in preference to schorl or other Na-dominant tourmaline group members in more calcium-rich systems. Axinite's presence in the mafic zone along the railroad cut suggests a northeastward chemical continuation of the typical calc-silicate skarns at Bald Mountain and Delmoe Road (fig. 1, locations 1 and 2, respectively). Most axinite specimens include clinocllore or other chlorite-group minerals and in places the crystals appear to be pseudomorphs of chlorite after axinite. I believe that the axinite crystals are inclusions rather than a replacement mineral. In experimental studies, axinite forms at 300-500° C (Deer and others, 1997) and well above zeolite facies temperatures in which chlorite is typical (although higher-temperature forms of clinocllore exist).

Acknowledgements

Thanks to Colleen Elliott, Susan Vuke, Dick Berg, Chris Gammons, Petr Yakovlev, and Kaleb Scarberry for encouragement, advice, and ideas on this topic; to Chris Gammons for Raman spectroscopy and x-ray diffraction; to Jon Szarkowski for x-ray diffraction analysis; and to Kaleb Scarberry for a valuable review.

ter northeast, along a railroad cut (fig. 1, location 3), mafic rocks crop out and are interpreted as part of an endoskarn within the igneous country rock. Here, the contact zone occurs between the 76 Ma Butte Pluton and 83 Ma to 85 Ma igneous rocks (ages from Olson and others, 2017). Prostka (1963) and Smedes and others (1998) mapped these igneous rocks as diorite porphyry intrusions of the lower member Elkhorn Mountains Volcanics (EMV) (Klepper and others, 1957). Olson and others (2016) mapped the diorite porphyry as dacite lavas based on observation of flow-banding, flow breccia, and ramp structures, and assigned the sequence to the lower member EMV.

Alteration Mineralogy

Reuss (1976) and Knudsen (2011) described the mineralogy of the contact zone near the "screen" at Bald Mountain (fig. 1, location 1); it is famous for occurrences of diopside, grossular garnet, and blue calcite. The current study observes clinoptilolite (confirmed by Raman spectroscopy), titanite, and probable thomsonite at Bald Mountain (fig. 1, location 1). Altered rock along the Delmoe-Pipestone Road (fig. 1, location 2) contains abundant scapolite (meionite, confirmed by x-ray diffraction; generally, fluoresces deep red; fig. 3A), zeolites (stilbite and possibly heulandite), vesuvianite, grossular, and rarer thulite (pink manganian Mn⁺³ zoisite) and schorl. Crystalline igneous rocks are associated with the alteration mineral assemblages at both

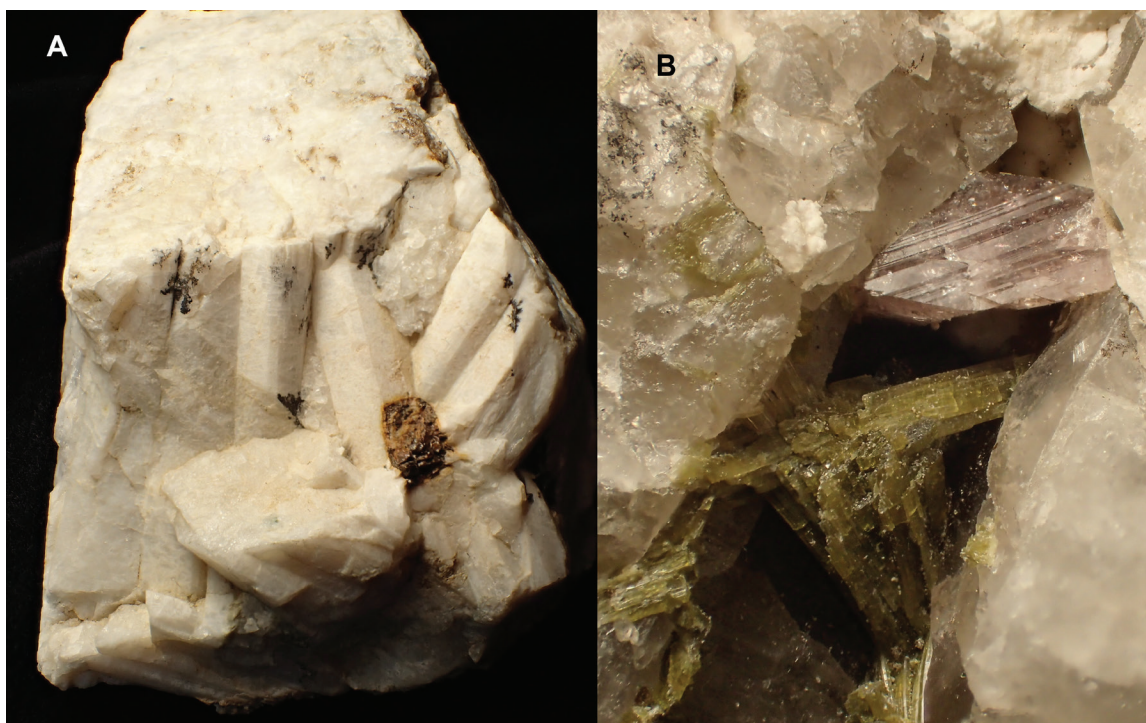


Figure 3. (A) Scapolite (meionite) from skarn along Delmoe Road (fig. 1, location 2), with patches of stilbite. Specimen 6 cm wide. (B) Lavender axinite from railroad cut (fig. 1, location 3), 5.5 mm crystal, with green epidote.

References Cited

- Deer, W.A., Howie, R.A., and Zussman, J., (eds.), 1997, *Rock-Forming Minerals: Disilicates and Ring Silicates*, Volume 1B: The Geological Society, London.
- Hamilton, W., and Myers, W. B., 1974, Nature of the Boulder batholith of Montana: *Geological Society of America Bulletin*, v. 85, p. 365–378.
- Klepper, M.R., Weeks, R.A., and Ruppel, E.T., 1957, *Geology of the southern Elkhorn Mountains, Jefferson and Broadwater Counties, Montana*: U.S. Geological Survey Professional Paper 292, 82 p.
- Knudsen, P., 2011, Vignettes of four Montana mineral localities: 32nd Annual New Mexico Mineral Symposium and 3rd Annual Mining Artifact Collectors Association Symposium, November 12-13, 2011, Socorro, NM.
- Olson, N.H., Sepp, M.D., Dilles, J.H., Mankins, N.E., Blessing, J.M., and Scarberry, K.C., 2017, *Geologic Map of the Mount Thompson 7.5' quadrangle, southwest Montana*: Montana Bureau of Mines and Geology EDMAP-11.
- Olson, N.H., Dilles, J.H., Kallio, I.M., Horton, T.R., and Scarberry, K.C., 2016, *Geologic Map of the Ratio Mountain 7.5' quadrangle, southwest Montana*: Montana Bureau of Mines and Geology EDMAP-10.
- Prostka, H.J., 1963, *Geologic map of the Dry Mountain quadrangle, Montana*: USGS Bull. 121-F, 1:24,000 scale.
- Reuss, R., 1976, Pipestone mine, Bald Mountain, Boulder batholith, Jefferson County, Montana USA: *Mineralogical Record*, Jan./Feb.
- Smedes, H.W., Klepper, M.R., and Tilling, R.I., 1988, *Preliminary map of plutonic units of the Batholith, Southwestern Montana*: USGS Open-File Report 88-283, 1:200,000 scale.



Geologist Dick Gibson. Photo by A. Roth, MBMG.



Geologists at the Map Chat at the Butte Brewing Company in uptown Butte, MT. Photo by A. Roth, MBMG.

Mineralogy, Fluid Inclusion, and S-Isotope Data for the Heddleston Porphyry Cu-Mo Deposit, Montana

B. Schubert and Cristopher H. Gammons*

Department of Geological Engineering, Montana Tech, Butte, Montana

**Corresponding author, cgammons@mtech.edu*

Abstract

The Heddleston porphyry Cu-Mo deposit is located in Lewis and Clark County, Montana, near the headwaters of the Blackfoot River. It is immediately west of the historic Mike Horse mine, an important producer of Pb-Zn from polymetallic veins and lodes. The Heddleston property was explored extensively by the Anaconda Company in the 1960s and 1970s, but was never mined. Specimens of polished drill core from the deposit are archived in the Anaconda Research Collection at Montana Tech campus. The purpose of this project was to use the archived samples to examine the geochemistry and mineralogy of the Heddleston and Mike Horse deposits using modern methods of ore deposit research, including portable X-ray fluorescence (pXRF), short-wave infrared (SWIR) mineral analysis, fluid inclusion studies, scanning electron microscopy (SEM), and sulfur isotope analysis.

The Heddleston porphyry deposit is centered on the Eocene Mike Horse stock, a quartz monzonite body that intruded mid-Proterozoic Spokane Formation argillite, and a thick (200 to 500 ft) Precambrian diorite sill. Drill core used for this study was from a hole (DH 265-161) completed to a depth of at least 1,200 ft near the center of the district, but just outside the mapped limit of the Number 3 Tunnel ore body. Several generations of quartz veins are present, including early quartz–chalcopyrite–pyrite veins that show narrow potassic alteration envelopes, unaltered quartz–molybdenite veins, and quartz–pyrite–chalcopyrite veins with phyllic alteration. Some of the late-stage veins contain galena, sphalerite, and Ag-bearing tetrahedrite–tennantite. Based on SWIR data, the prevalent alteration minerals in the porphyry host rock are hydrothermal muscovite (sericite), K-illite, kaolinite, and halloysite. Most of the kaolinite is well crystalline (i.e., kaolinite WX) and probably hypogene, while the poorly crystalline kaolinite (kaolinite PX) may have formed during weathering. Fluid inclusions from quartz–molybdenite and quartz–pyrite veins homogenized between 300 and 450°C and have liquid/vapor ratios that vary considerably. Many inclusions contain halite daughter minerals, with sylvite and/or chalcopyrite daughter minerals also sometimes present. This information suggests that boiling of a primary magmatic fluid occurred in the temperature range of 350 to 450°C, resulting in a metal-rich, hypersaline brine. Stable isotopes of S ($\delta^{34}\text{S}$) in pyrite range from 3.5 to 5.2‰, and overlap with values for pyrite, sphalerite, and galena in two samples from Mike Horse and $\delta^{34}\text{S}$ data for hypogene sulfides in the world-class Butte porphyry-lode deposit. This suggests that the two porphyry systems inherited sulfur from a common source. However, the Heddleston deposit differs considerably from Butte due to its smaller size, younger age (Eocene vs. late Cretaceous), host rocks (Precambrian metasediments vs. Butte Granite), shallower depth of emplacement, and lack of copper-rich “Main Stage” veins.

Introduction

The Heddleston porphyry Cu-Mo deposit is located 33 miles northwest of Helena in Lewis and Clark County, Montana (fig. 1). The deposit lies within the Great Falls Tectonic Zone (Miller and others, 1973) near the northern edge of the Lewis and Clark Line, a NNW–SSE-trending structural lineament that separates gently folded and weakly metamorphosed sedimentary rock to the north from highly deformed sediments intruded by granitic plutons and batholiths to the south (Vuke and others, 2009). Country rock in the Heddleston district consists of argillite of the mid-Proterozoic Spokane Formation that has been intruded by a thick, shallow-dipping diorite sill of presumed late Proterozoic age (fig. 2). These rocks are cut by a number of Eocene quartz monzonite porphyry stocks and dikes mapped collectively as the Mike Horse stock by Vuke (2014).

Polymetallic lode mining in the Heddleston district began in 1889 at the Mike Horse, Paymaster, Car-

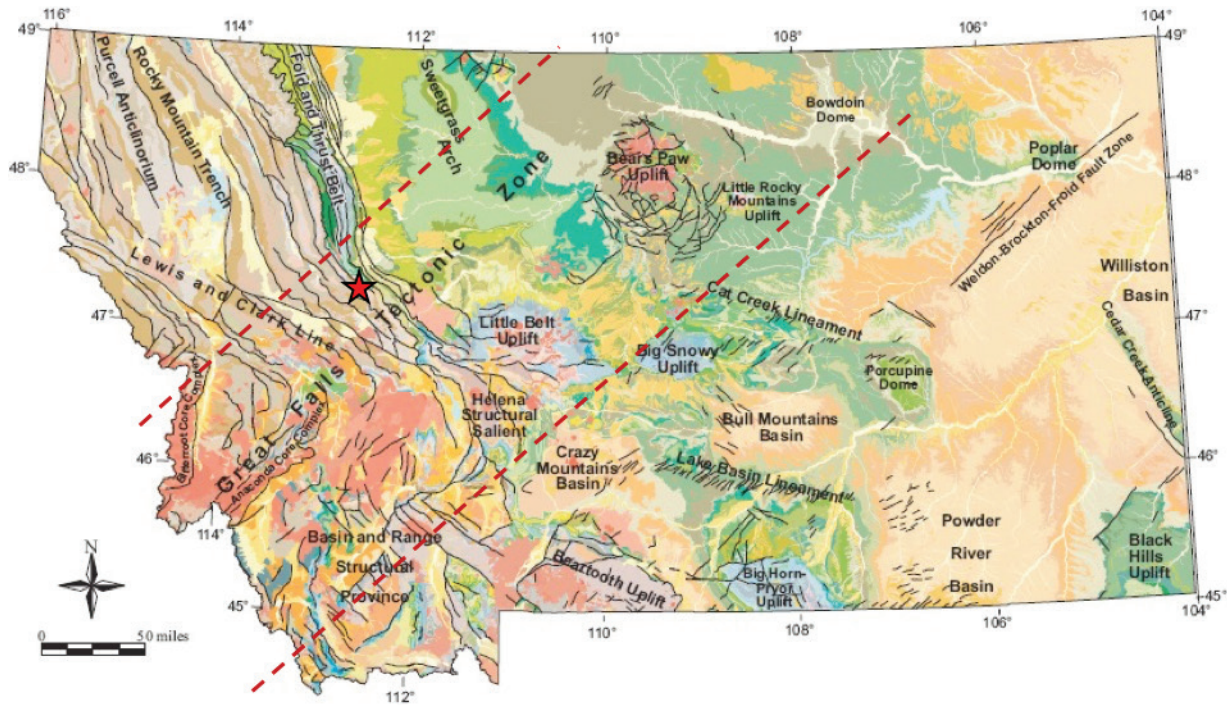
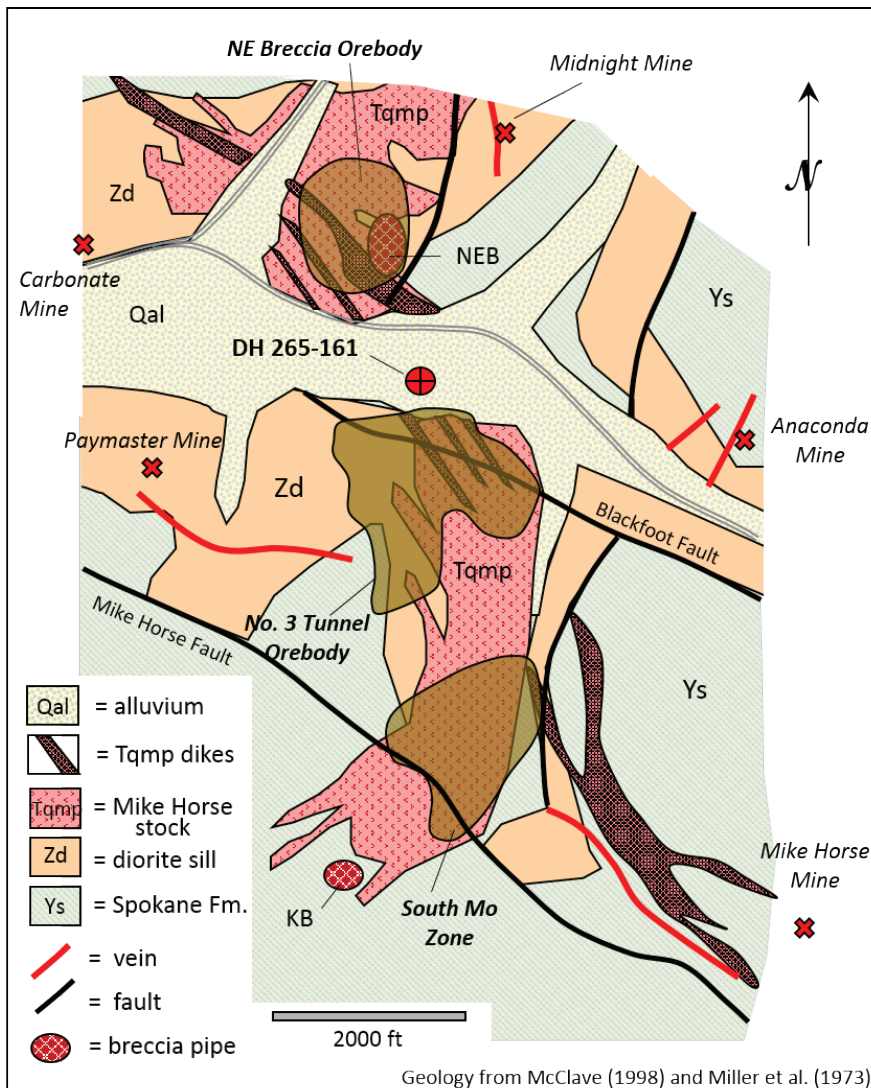


Figure 1. Regional geologic setting of the Heddlestone District (shown with red star). The brown dashed lines show the approximate boundaries of the Great Falls Tectonic Zone. Modified from Vuke and others (2009).



bonate, Anaconda, and Midnight mines (fig. 2). The Mike Horse mine, the largest in the district, produced roughly \$24 million of lead, zinc, silver, and gold, through 1955 (McClave, 1998). The Anaconda Company, and later ASARCO, explored the Heddlestone porphyry copper deposit a few miles west of the Mike Horse mine from 1962 through 1972. Recent estimates reported a mineable reserve at Heddlestone of 93 million tons of ore at a grade of 0.48% Cu using a 0.3% cutoff (McClave, 1998), which makes the Heddlestone deposit the second largest known porphyry copper deposit in Montana.

A synthesis of information published by Miller and others (1973) and McClave (1998) shows that the Heddlestone district displays several overlapping styles of mineralization. Early “protore” produced disseminated chalcopyrite in the Precambrian diorite

Figure 2. Map of the geology of the Heddlestone District, showing the location of historic mines and three zones of economically important mineralization on the Heddlestone property (from McClave, 1998 and Miller and others, 1973). NEB, North-east breccia body; KB, Kleinschmidt breccia pipe; DH, Drill Hole.

sill and Eocene intrusions and secondary K-feldspar and biotite. The protore is cut by Cu- and Mo-bearing vein swarms and stockworks, with individual veins that range from a few millimeters to a few centimeters in width. Quartz–molybdenite veins are typically unaltered, while quartz–pyrite and quartz–pyrite–chalcopyrite veins have phyllic alteration envelopes. Miller and others (1973) reported a K-Ar date of 44.5 Ma for hydrothermal muscovite (sericite) of this stage. Two bodies of intrusive breccia, the Northeast Breccia and the smaller Kleinschmidt Breccia, have been mapped (NEB and KB in fig. 2). These breccias contain varying-sized clasts of argillite, diorite, and quartz monzonite porphyry in a fine, aplitic groundmass. The clasts are mineralized, with good grades of copper and/or molybdenum ore locally. Late-stage polymetallic veins and lodes surround the main Mike Horse stock, and were targets of early mining in the district. These lodes exhibit significant width and strike length, and are enriched in Pb, Zn, Ag, and sometimes Au, as opposed to Cu and Mo, which are restricted to the porphyry ore body. Supergene enrichments of chalcocite (\pm covellite) replacing or coating pre-existing sulfides are superimposed on earlier stages of mineralization. Rather than forming a continuous “blanket” of secondary chalcocite, the supergene enrichment zone varies in thickness and in grade. The best chalcocite ore formed near pre-existing structures, such as faults and vein swarms.

Anaconda geologists identified three areas of potential for a bulk-tonnage mine (McClave, 1998). From north to south (fig. 2), these are the “NE Breccia orebody,” the “Number 3 Tunnel” orebody, and the “South Mo zone.” The NE Breccia orebody includes the NE Breccia pipe and contains both Cu and Mo mineralization. The No. 3 Tunnel orebody was the main target of the Anaconda Co., and is defined by an extensive, shallow (<1,000 ft), chalcocite enrichment zone that contains copper-rich protore. The South Mo zone has not been completely explored but it consists of a higher concentration of quartz–molybdenite veins at depth with good ore grades (e.g., 0.04 to 0.1% Mo) locally.

Schubert (2017) recently completed a preliminary fluid inclusion and stable isotope investigation of Heddleston, using samples archived in the Anaconda Research Collection at Montana Tech. Aside from the conference papers of Miller and others (1973) and McClave (1998), there are no other publications related to the Heddleston porphyry deposit. This paper highlights important findings detailed by Schubert (2017).

Methods

The drill core studied during this project came from Anaconda drill hole 265-161, which is indexed as specimen #7501 in the Anaconda collection on the Montana Tech campus in Butte. This particular drill core was selected due to its location just outside of the main Number 3 Tunnel orebody area (fig. 2), and because it consisted of nearly 100 polished core specimens (most around 3 in. to 8 in. in length) obtained from depths that ranged from 66 ft to 1,296 ft. In addition, several hand samples from the Mike Horse mine were available in the Anaconda collection.

The specimens were examined for ore and alteration mineralogy using a combination of methods, including X-ray fluorescence (using a Niton pXRF instrument), SWIR spectroscopy (using a Terraspec Halo instrument), reflected and transmitted light microscopy, and scanning electron microscopy (SEM-EDS). Fluid inclusion heating runs were performed on doubly polished thick sections using a USGS-style stage with a 32X objective lens. Very few freezing runs were performed due to the small diameter of most of the inclusions. Sulfide minerals were separated by hand using a binocular microscope and the separates then sent to the University of Nevada-Reno for S-isotope analysis. S-isotope values are reported in per mil (‰) relative to the Vienna Canon Diablo Troilite standard (VCDT). Analytical precision for $\delta^{34}\text{S}$ is estimated at ± 0.1 ‰. More details about instrumentation and procedures are described in Schubert (2017).

Results

Petrography

Drill hole 265-161 penetrated mostly porphyritic igneous rock of the Mike Horse stock (fig. 3). The porphyry contains conspicuous, coarse (up to 1-in diameter) phenocrysts of feldspar, and lesser biotite and quartz, in a gray to dark gray, aphanitic groundmass. In general, hydrothermal alteration in the drill core is weak, except near cross-cutting veins. Quartz–molybdenite veins have little or no alteration, and tend to cut the core at a high

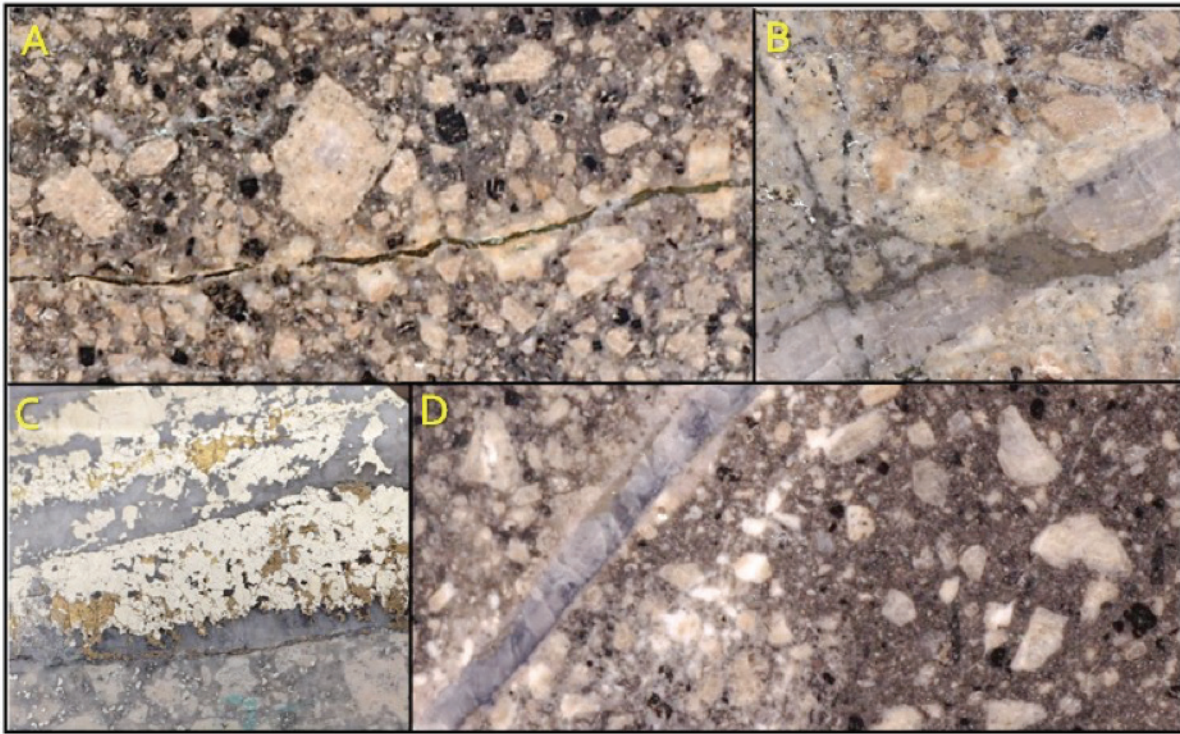


Figure 3. Photographs of drill core from Heddleston. Height of all photos is approximately 2 in. (A) Fresh porphyry cut by narrow chalcopyrite vein with potassic alteration; (B) Several generations of veins cutting porphyry, with supergene chalcocite; (C) Quartz-pyrite-chalcopyrite vein with weak phyllic alteration; (D) Quartz-pyrite vein with phyllic alteration later broken and filled with quartz-molybdenite vein.

angle, indicating a predominantly shallow vein dip. In contrast, most quartz-pyrite and quartz-pyrite-chalcopyrite veins have sericitic alteration envelopes and a steep dip that parallels the long axis of the core. Over 100 core specimens were analyzed by SWIR using the Terraspec Halo instrument. Alteration minerals identified by the Halo include (in descending order of abundance): muscovite, K-illite, halloysite, Mg-illite, montmorillonite, kaolinite-WX (well crystalline), rectorite, kaolinite-PX (poorly crystalline), pyrophyllite, and phengite. There are no obvious trends in alteration mineralogy or Terraspec scaler values with depth in the core. Pyrophyllite was found in fewer than 10% of the samples examined, indicating the possible presence of localized advanced argillic alteration. Kaolinite WX, Mg-illite, rectorite, and phengite probably formed from high-temperature argillic alteration, while kaolinite PX most likely formed during weathering.

Most polished slabs from Heddleston have a simple ore mineralogy that consists of pyrite, chalcopyrite, and molybdenite. Bornite was not recognized, consistent with observations by Miller and others (1973) and McClave (1998). Molybdenite always occurs in quartz veins, whereas chalcopyrite is disseminated throughout the country rock and sometimes in quartz-pyrite veins. Core samples show only trace supergene chalcocite, probably because drill hole 265-161 was completed in a valley bottom, and outside of the main zone of supergene enrichment in the No. 3 Tunnel orebody (fig. 2). A late polymetallic vein from a depth of 865 ft contains Ag-bearing tetrahedrite, galena, and sphalerite (fig. 4A). All Mike Horse samples are rich in pyrite, sphalerite, and galena, with lesser amounts of chalcopyrite and tetrahedrite-tennantite (fahlore), in a dolomite-quartz gangue (fig. 4B). Some pyrite grains contain small rounded inclusions of pyrrhotite. Based on SEM-EDS analysis, sphalerite from Heddleston and Mike Horse has 2.1 to 3.3 wt% Fe, and 0.5 to 0.8 wt% Fe, respectively (details in Schubert, 2017). Table 1 gives the EDS chemical analyses and computed chemical formulas for six fahlore grains from Heddleston and one grain from Mike Horse. Fahlores from both deposits were elevated in zinc, and showed a positive correlation between Ag and Sb. In general, the similar mineralogy observed for the Mike Horse vein and the late polymetallic vein at Heddleston suggests they formed at more or less the same time, and under similar conditions.

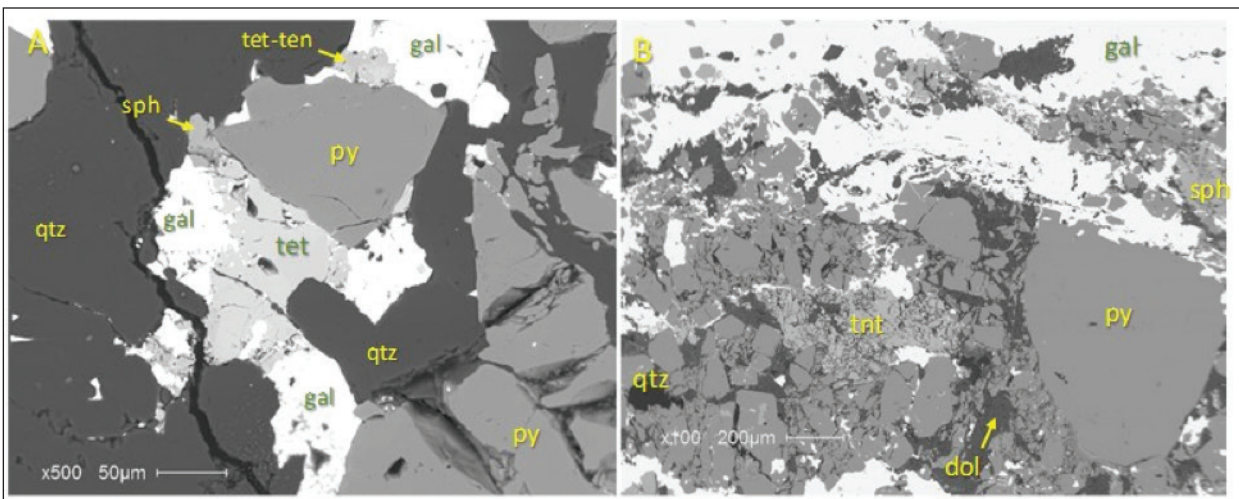


Figure 4. SEM-BSE photographs. (A) Late vein with polymetallic sulfide assemblage from Heddeleston (865' depth); (B) Sulfide-rich vein from Mike Horse mine. Abbreviations: py, pyrite; tet, tetrahedrite; tnt, tennantite; gal, galena; sph, sphalerite; qtz, quartz; dol, dolomite.

Table 1. SEM-EDS data for tetrahedrite-tennantite and calculated formulas.

	S	Ag	Sb	Fe	Cu	Zn	As	Mineral/Formula
Sample from Heddeleston (7501-865)								
1	Wt%	22.9	3.8	24.0	2.2	35.2	6.6	Zincian tetrahedrite
	At%	41.8	2.1	11.8	2.4	33.3	6.0	$(\text{Cu}_{9.4}\text{Ag}_{0.6})(\text{Zn}_{1.4}\text{Fe}_{0.6})(\text{Sb}_{3.3}\text{As}_{0.7})\text{S}_{13}$
2	Wt%	23.6	3.9	24.7	0.7	35.6	7.0	Zincian tetrahedrite
	At%	46.2	2.3	12.8	0.8	35.2	6.7	$(\text{Cu}_{9.4}\text{Ag}_{0.6})(\text{Zn}_{1.8}\text{Fe}_{0.2})(\text{Sb}_{3.2}\text{As}_{0.8})\text{S}_{13}$
3	Wt%	23.6	3.8	25.2	1.3	35.3	7.7	Zincian tetrahedrite
	At%	42.9	2.1	12.1	1.3	32.4	6.8	$(\text{Cu}_{9.4}\text{Ag}_{0.6})(\text{Zn}_{1.7}\text{Fe}_{0.3})(\text{Sb}_{3.3}\text{As}_{0.7})\text{S}_{13}$
4	Wt%	26.3	0.7	7.0	1.1	42.1	8.4	Zincian tennantite
	At%	43.5	0.3	3.1	1.0	35.1	6.8	$(\text{Cu}_{9.9}\text{Ag}_{0.1})(\text{Zn}_{1.7}\text{Fe}_{0.3})(\text{As}_{3.1}\text{Sb}_{0.9})\text{S}_{13}$
5	Wt%	26.4	1.1	12.7	5.3	31.4	14.5	Zincian tennantite
	At%	44.2	0.6	5.6	5.1	26.5	11.9	$(\text{Cu}_{9.8}\text{Ag}_{0.2})(\text{Zn}_{1.4}\text{Fe}_{0.6})(\text{As}_{2.1}\text{Sb}_{1.9})\text{S}_{13}$
6	Wt%	31.6	1.9	13.1	13.7	27.4	5.9	Tetrahedrite
	At%	50.2	0.9	5.5	12.5	22.0	4.6	$(\text{Cu}_{9.6}\text{Ag}_{0.4})(\text{Zn}_{0.5}\text{Fe}_{1.5})(\text{Sb}_{2.2}\text{As}_{1.8})\text{S}_{13}$
Sample from Mike Horse (MH 1774)								
7	Wt%	25.5	0.0	1.5	1.3	34.7	8.8	Zincian tennantite
	At%	41.8	0.0	1.5	1.3	34.7	8.8	$\text{Cu}_{10}(\text{Zn}_{1.7}\text{Fe}_{0.3})(\text{As}_{3.6}\text{Sb}_{0.4})\text{S}_{13}$

Fluid Inclusions

Fluid inclusions were examined from centimeter-scale quartz veins from several different depths in the drill hole 265-161 core collection: however, no suitable material for fluid inclusions was found in the samples from Mike Horse. The shape, size, and phase-ratios displayed by each inclusion of interest was noted. Although numerous, most inclusions were small ($< 10 \mu\text{m}$ in diameter). The ratio of bubble volume to total volume at room temperature was estimated using charts in Roedder (1984) and recorded as “bubble volume percent.” Thus, an inclusion with a central vapor bubble occupying 50% of the total volume of the inclusion would be referred to as “B50” (e.g., Rusk and others, 2008). Most inclusions with bubble volumes $> B60$ showed total homogenization to the vapor phase, whereas inclusions $< B60$ homogenized to liquid. A fair number of inclusions have one tiny opaque crystal, believed to be chalcopyrite based on its octahedral shape and failure to dissolve on heating. A distinct population of B10 to B20 inclusions had large daughter crystals of halite, and some showed a second, smaller salt crystal believed to be sylvite (KCl) (fig. 5). Coexisting vapor-rich and liquid-rich inclusions tended to homogenize in the same range of temperature for the same sample, consistent with the idea that the fluids were boiling when the quartz veins formed. The hypersaline inclusions with salt daughter minerals and small bubble volumes represent the degassed brine phase.

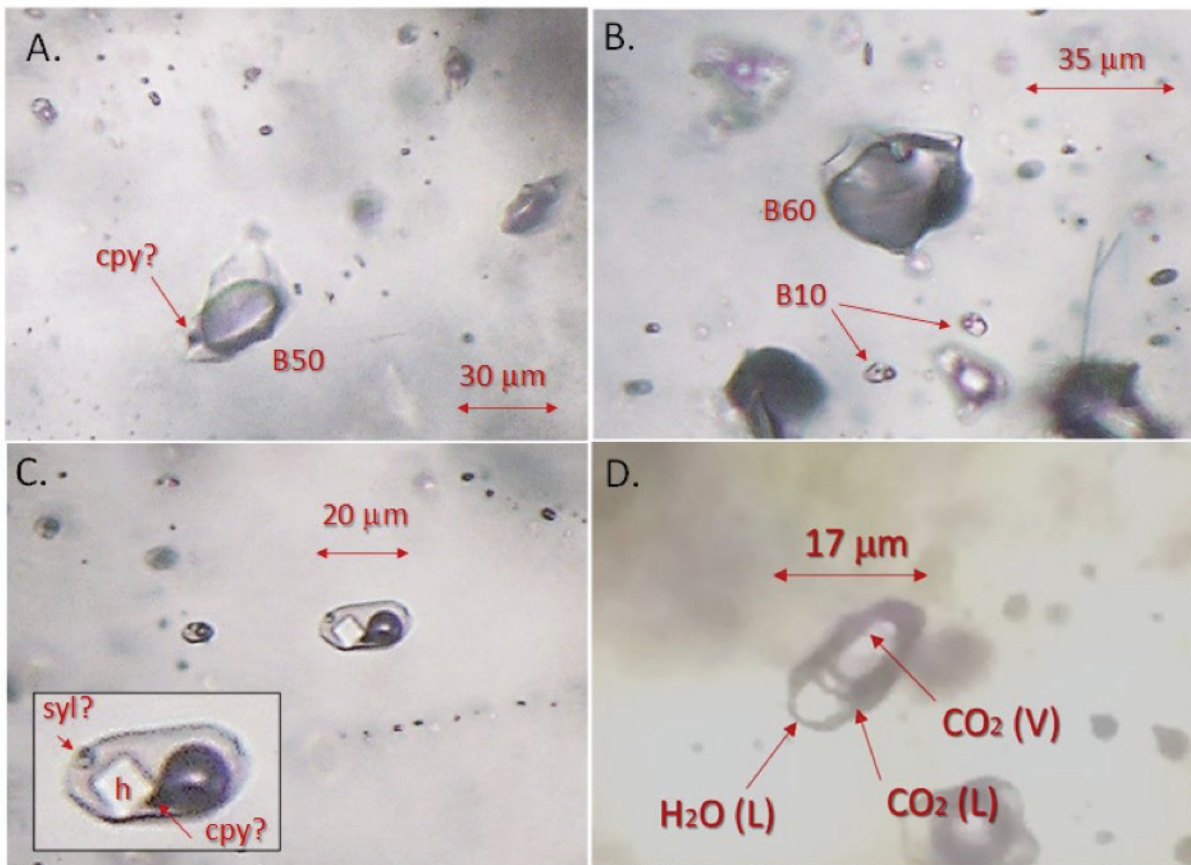


Figure 5. Fluid inclusions from a quartz–molybdenite vein from Heddleston at a depth of 322 ft. (A) Large B50 fluid inclusion with small opaque (chalcopyrite?) daughter; (B) large B60 inclusion near two small B10 inclusions with salt daughter minerals (pointed out by arrows); (C) two B10 inclusions identical in composition and shape, with multiple daughter minerals identified as halite (h), chalcopyrite (cpy), and sylvite (syl); (D) CO₂-rich inclusion show a rim of liquid CO₂ at a temperature near 0°C.

Homogenization temperatures recorded in this study ranged from 170°C to 438°C, and most inclusions homogenized between 300°C and 400°C (fig. 6). The average L-V homogenization temperatures for all liquid-rich and vapor-rich inclusions in this study were $331 \pm 44^\circ\text{C}$ and $337 \pm 58^\circ\text{C}$, respectively (errors denote 1 standard deviation). A small number of inclusions remained un-homogenized at 450°C, the upper temperature limit of the equipment used in this study. Inclusions with halite daughter minerals showed NaCl dissolution between 128°C and 396°C, corresponding to salt concentrations in the range of 37 to 42 wt% NaCl, or roughly 12 times saltier than seawater. Two inclusions with a second daughter crystal of sylvite showed KCl dissolution at 35°C to 36°C. Based on the temperature dependence of the solubility of KCl [taken from <http://chemicals.etacude.com/p/more/kcl.html>], this corresponds to a total concentration of roughly 38 wt% KCl. In other words, the inclusions that contained two salt daughter minerals had similar concentrations (wt%) of NaCl and KCl when the inclusions were trapped.

Because of the small size of most of the fluid inclusions in this study, only a few freezing runs were attempted. Two inclusions large enough to use were found at a depth of 515 ft in the drill core. Ice melting temperatures were close to -16.7°C for both inclusions, and a ring of liquid CO₂ formed around the central CO₂-rich vapor bubbles on freezing (fig. 5D). The two CO₂ phases homogenized at $+8.3^\circ\text{C}$ to CO₂(v). This means that there were no “double-bubbles” at room temperature. It’s possible that more CO₂-rich inclusions would have been found from other samples if more freezing runs had been performed in this study.

Sulfur Isotopes

Seven pyrite samples from Heddleston and five sulfide separates from Mike Horse were submitted for stable S-isotope analysis. The Heddleston samples came from depths of 83 ft to 783 ft in the core. There is a relatively narrow range in $\delta^{34}\text{S}$ for pyrite from Heddleston (avg. $4.4 \pm 0.6\%$) with no significant change with depth (table

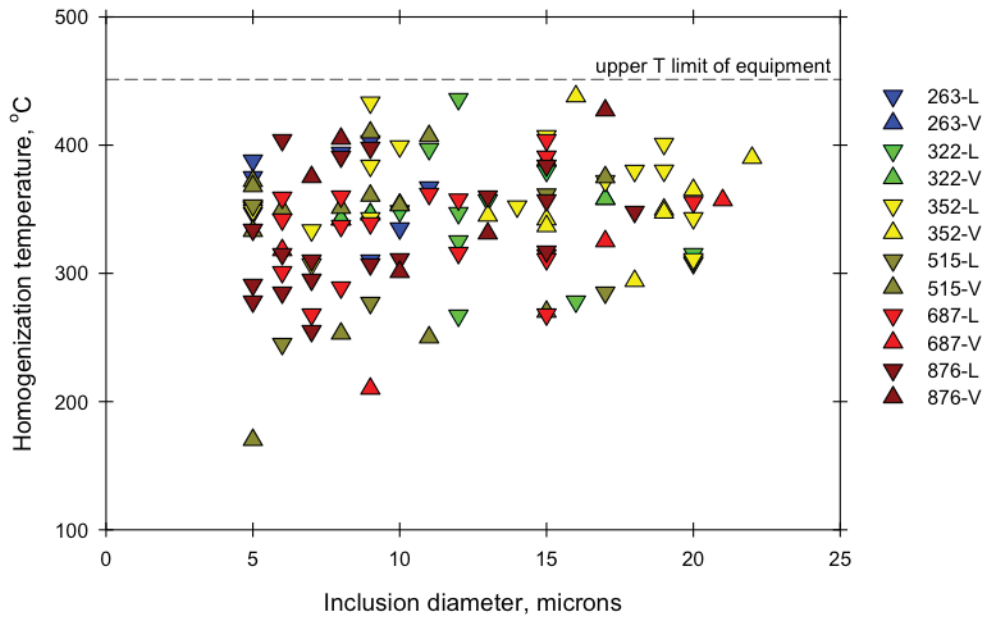


Figure 6. Homogenization temperature vs. inclusion diameter in fluid inclusions from different depths (in feet) of the Heddleston deposit. Final homogenization to liquid (L) or vapor (V).

2). Similar $\delta^{34}\text{S}$ values exist for pyrite, galena, and sphalerite from the Mike Horse mine ($\text{avg. } 3.5 \pm 0.8\text{‰}$). An attempt was made to compute a temperature based on the S-isotope composition of coexisting sphalerite and galena for sample #1494. The measured separation of 1.6‰ between the two minerals corresponds to a temperature of roughly 390°C (using fractionation factors of Czamanske and Rye, 1974). Given a $\pm 0.1\text{‰}$ analytical error, the uncertainty in this estimate is roughly $\pm 50^\circ\text{C}$. Although more samples are needed to make a definitive estimate, the stable isotope results suggest that the Mike Horse vein formed at a relatively high temperature that overlaps with that of the Heddleston deposit.

Table 2. Sulfur isotope data for Heddleston and Mike Horse.

Heddleston			
AMC#	Mineral	Depth (ft)	$\delta^{34}\text{S}$, ‰
7501	Pyrite	83	3.9
7501	Pyrite	169	4.6
7501	Pyrite	221	3.5
7501	Pyrite	344	4.4
7501	Pyrite	547	4.4
7501	Pyrite	602.5	5.2
7501	Pyrite	783	4.7
Mike Horse mine			
6455-5	Pyrite		3.3
6455-6	Pyrite		2.8
6455-7	Pyrite		3.0
1494	Sphalerite		4.9
1494	Galena		3.3

Discussion

Source of Sulfur and Copper

In their review of S-isotope systematics of Butte, Field and others (2005) argued that much of the sulfur, and possibly much of the metal in the pre-main stage porphyry Cu-Mo mineralization, was assimilated from metasediments of the Mesoproterozoic Belt Supergroup. This same idea may apply to Heddleston. A simplified geologic map shows areas of stratabound enrichment of copper in Belt strata in a region that extends 40 km northwest from the Heddleston district (fig. 7). According to Earhart and others (1981), three different styles of mineralization are found: (1) enrichments of copper in “greenbeds,” i.e., strongly reduced horizons surrounded by predominantly red-bed, or oxidized horizons; (2) copper in “greybeds” of the Spokane and Empire Formations; and (3) polymetallic, Cu-Pb-Zn-Ag mineralization in carbonate rocks of the basal Helena Formation. Areas in red in figure 7 are known to contain Cu-sulfides and other minerals of economic importance. Although no large mines exist in the area, there has been some recorded production and also sporadic exploration drilling. The fact that the Heddleston porphyry Cu-Mo deposit is surrounded by stratiform mineralization supports the idea that it may have inherited some metal and S from the Belt.

Data summarized in figure 8 show that sulfides from Heddleston (this study), from nearby sediment-hosted deposits in the Helena Formation at Cotter Basin (Byer, 1987), and from Butte (Field and others, 2005) all have a similar range in $\delta^{34}\text{S}$ values. Sulfide minerals from Cotter Basin (a mix of pyrite, chalcopyrite, and bornite) have an average $\delta^{34}\text{S}$ value of 4.1 ± 1.4 ‰, which is very close to the average for pyrite from Heddleston (4.4 ± 0.6 ‰). Because of numerous large thrust faults in this part of the Front Range (fig. 7), it’s likely that the Belt section is repeated beneath the Heddleston area, further increasing the odds that the Mike Horse stock, and associated hydrothermal fluids, assimilated Belt rocks on their path to the surface.

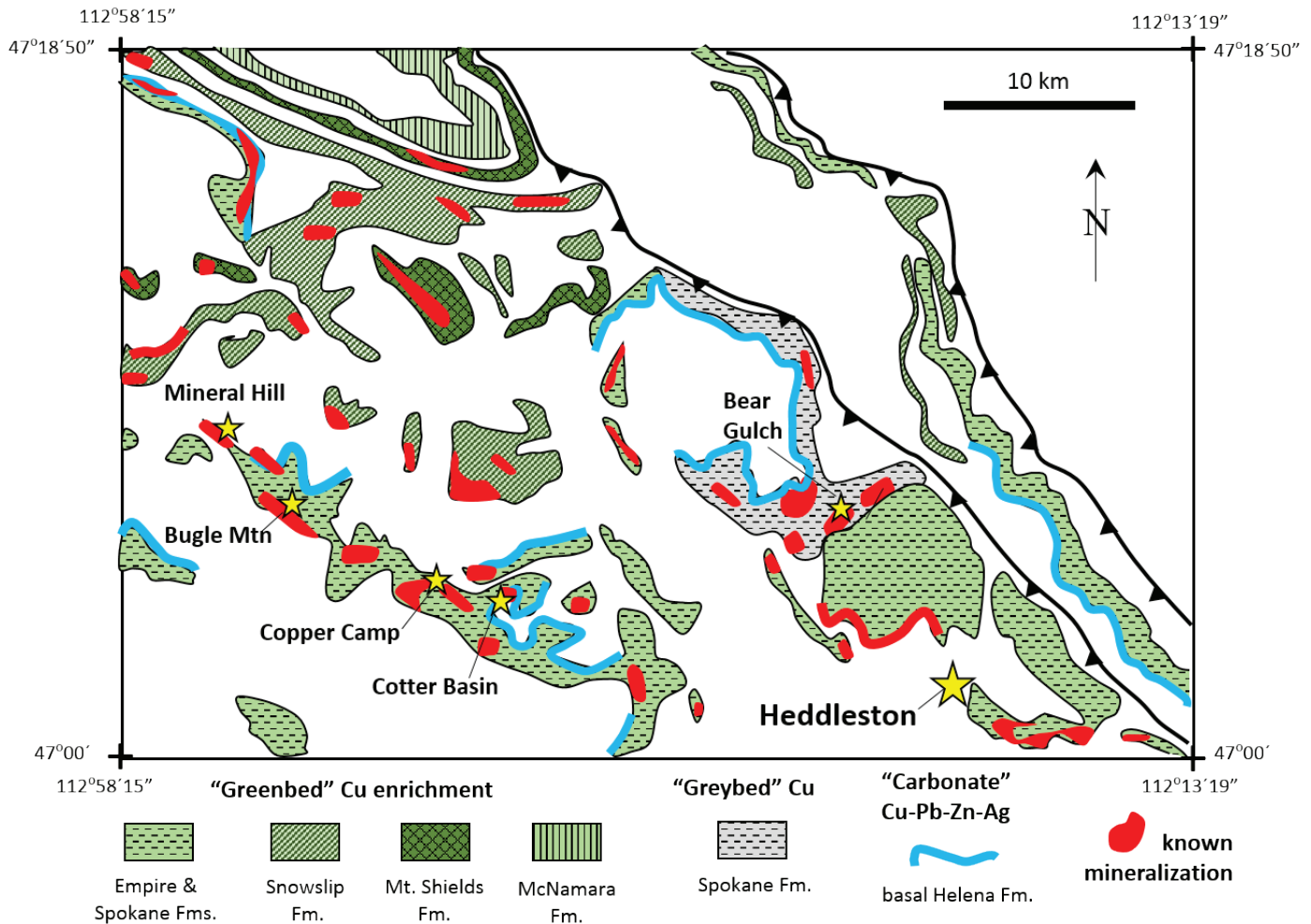


Figure 7. Map showing areas of stratiform copper and polymetallic mineralization in the Belt sedimentary rocks in a region extending from Heddleston to the northwest. Redrafted from Earhart and others (1981) and Byer (1987).

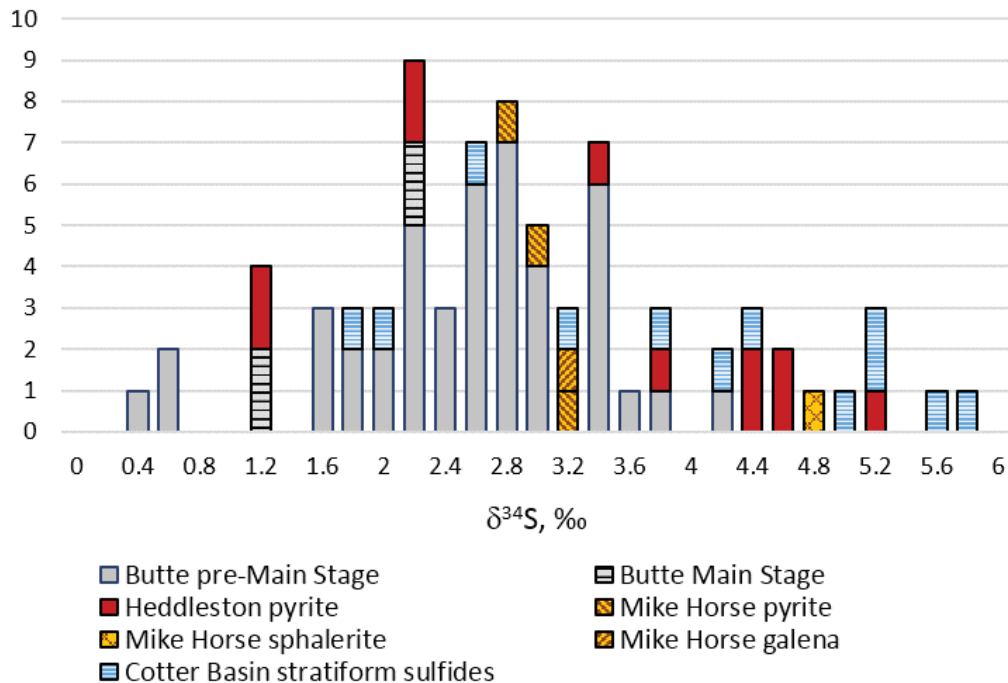


Figure 8. Sulfur isotope compositions of pyrite from Butte Main Stage veins and pre-Main Stage veins (from Field and others, 2005), sulfide minerals from stratabound mineralization at Cotter Basin (Byer, 1987), and pyrite, sphalerite, and galena from Heddleston and Mike Horse (this study).

Comparison of Heddleston and Butte

Because Butte is such a huge porphyry deposit and it is located less than 50 linear miles from Heddleston, it is worth making some comparisons between the two porphyry systems. The following is a list of some similarities:

- Both deposits lie within the Great Falls Tectonic Zone, and are part of a northeast–southwest-trending belt of porphyry Cu-Mo and porphyry Mo deposits that runs from south-central Idaho to north-central Montana.
- Both deposits are large porphyry Cu-Mo systems. Although McClave (1998) quotes 70 M tons of mineable reserves at Heddleston, the USGS reported a total resource of 302 M tons at 0.36% Cu, 0.005% Mo, 0.053 g/ton Au, and 5.2 g/ton Ag (Singer and others, 2005). This larger resource is still much less than the total production and reserves at Butte, estimated by the USGS as 5000 M tons at 0.67% Cu and 0.028% Mo (Singer and others, 2005).
- Both deposits contain a significant volume of ore that has been enriched by supergene processes. At Butte, supergene chalcocite mineralization was important in the Berkeley open pit (McClave, 1973). At Heddleston, secondary chalcocite also plays a role in the definition of the No. 3 Tunnel ore reserve (Miller and others, 1973; McClave, 1998).
- Both deposits contain late, polymetallic veins rich in Pb-Zn-Ag. At Butte, the veins are actually lodes, and were referred to as the Main Stage. At Heddleston the polymetallic veins are named after the historic mines that surround the central ore body: Mike Horse, Paymaster, Carbonate, Midnight, and Anaconda.
- The S-isotope composition of pyrite from Heddleston overlaps with $\delta^{34}\text{S}$ data for pyrite from Butte (fig. 8). At Heddleston, there is little difference between the $\delta^{34}\text{S}$ of porphyry-style pyrite vs. pyrite, galena, and sphalerite in late polymetallic veins from Mike Horse. The same relationship exists for pre-Main Stage vs. Main Stage mineralization at Butte (Field and others, 2005).
- Heddleston and Butte are both linked to major environmental problems related to acid mine drainage and metal contamination in streams. The problems at Butte include the acidic Berkeley pit lake and the piles of contaminated mine waste that swept down the upper Clark Fork River during floods. Although at a smaller

scale, similar problems related to contamination of the upper Blackfoot River exist in the Heddleston district, including failure of the Mike Horse tailings dam in 1975.

Main differences between Butte and Heddleston:

- Porphyry Cu-Mo mineralization at Butte is late Cretaceous in age (64.5 Ma, Lund and others, 2002), whereas Heddleston is Eocene in age (44.5 Ma, Miller and others, 1973). The 20-million-year separation in ages means that differences in tectonic, structural, and magmatic processes may have occurred when the two deposits formed.
- The main host rock at Butte is Boulder Batholith granite (76.9 ± 0.8 Ma, du Bray and others, 2009). Although there are some porphyry dikes at Butte that are believed to be the same age as pre-Main Stage mineralization, they are relatively small. In contrast, Heddleston has a large, well-exposed porphyry stock (the Mike Horse stock) in the center of the district and similar-aged dikes cut surrounding country rocks. Unlike Butte, ore at Heddleston is also developed in the Belt-aged Spokane Formation and a Precambrian mafic sill.
- The late Main Stage veins and lodes of Butte were abundant in the central part of the ore body and were rich in copper minerals. Towards the outer parts of Butte, Main Stage lodes shifted to Pb-Zn-Ag-rich. In contrast, at Heddleston, there appears to be a lack of large, Cu-rich veins and lodes in the central part of the district. In DH 265-161, late polymetallic veins are thin, and are rich in galena, sphalerite, and tetrahedrite. Larger Pb-Zn-Ag veins and lodes surround the deposit (for example, Mike Horse), but they are few and small in dimension compared with Butte.
- The porphyry-style mineralization at Butte is thought to have formed at depths of 6 to 9 km (Rusk and others, 2008), which makes Butte one of the deepest porphyry Cu-Mo deposits known world-wide. Rusk and others (2008) found very few examples of hypersaline fluid inclusions with large halite daughter minerals and concluded that the magmatic fluids at Butte rarely boiled, due in part to their great depth of formation. In contrast, fluid inclusions from Heddleston show abundant evidence of boiling, both from numerous hypersaline, salt-bearing inclusions, and the co-existence of liquid-rich and vapor-rich inclusions that homogenized near the same temperature range. These observations suggest that the Heddleston deposit formed at shallower depth than Butte.

In summary, despite certain similarities between the Butte porphyry and the Heddleston porphyry deposits, there are significant differences between them, rendering comparisons between the two systems problematic and questionable.

Acknowledgments

This research was made possible by grants to the first author from the Society for Mining, Metallurgy & Exploration (SME), the Montana Tobacco Root Geological Society (TRGS), Anadarko, and financial aid from Montana Tech. We thank Dr. Simon Poulson of University of Nevada-Reno for the S-isotope analyses, and Gary Wyss of the Center for Advanced Mineral Processing (CAMP) at Montana Tech for his help with the SEM-EDS work.

References Cited

- du Bray, E.A., Lund, K., Tilling, R.I., Denning, P.D., and DeWitt, E., 2009, Geochemical database for the Boulder batholith and its satellitic plutons, southwest Montana. U.S. Geological Survey, Digital Data Series 454.
- Byer, G., 1987, The geology and geochemistry of the Cotter Basin stratabound + vein copper-silver deposit, Helena Formation, Lincoln, Lewis and Clark County, Montana. M.S. thesis, Univ. of Montana, Missoula, MT.
- Czamanske, G.K., and Rye, R.O., 1974, Experimentally-determined sulfur isotope fractionations between sphalerite and galena in the temperature range 600°C to 275°C. *Economic Geology*, v. 69, p. 17-25.
- Earhart, R. L., Mudge, M. R., Whipple, J. W., and Connor, J. J., 1981, Mineral resources of the Choteau 1 x 2 quadrangle, Montana: U.S. Geological Survey, Miscellaneous Field Studies Map MF-858-A.

- Field, C.W., Zhang, L., Dilles, J.H., Rye, R.O, and Reed, M.H., 2005, Sulfur and oxygen isotopic record in sulfate and sulfide minerals of early, deep, pre-Main Stage porphyry Cu-Mo and late Main Stage base-metal mineral deposits, Butte, District, Montana. *Chemical Geology*, v. 215, p. 61-93.
- Lund, K., Aleinikoff, J.N., Kunk, M.J., Unruh, D.M., Zeihen, G.D., Hodges, W.C., du Bray, E.A., and O'Neill, J.M., 2002, SHRIMP U-Pb and $40\text{Ar}/39\text{Ar}$ age constraints for relating plutonism and mineralization in the Boulder Batholith region, Montana. *Economic Geology* v. 97(2), p. 241-267.
- McClave, M.A., 1973, Control and distribution of supergene enrichment in the Berkeley Pit, Butte district, Montana. Chapter K in *Guidebook for the Butte Field Meeting of Society of Economic Geologists*, Butte, MT, August, 1973.
- McClave M.A., 1998, The Heddleston porphyry copper-molybdenum deposit – An update. *Northwest Geology*, v. 28, p. 91-100.
- Miller, R. N., Shea, E. P., Goddard Jr, C. C., Potter, C. W., and Brox, G. B., 1973, Geology of the Heddleston copper-molybdenum deposit in Lewis and Clark County, Montana: Pacific Northwest Metals and Minerals Conference, Coeur d'Alene, Idaho, AIME Proceedings (pp. 1-33).
- Roedder, E., 1984, Fluid Inclusions. Mineralogical Society of America, *Reviews in Mineralogy*, v. 12, 646 pp.
- Rusk, B. G., Reed, M. H., and Dilles, J. H., 2008, Fluid inclusion evidence for magmatic-hydrothermal fluid evolution in the porphyry copper-molybdenum deposit at Butte, Montana. *Economic Geology*, v. 103(2), p. 307-334.
- Schubert, B., 2017, Mineralogy and geochemistry of the Heddleston porphyry Cu-Mo deposit, Montana. http://digitalcommons.mtech.edu/grad_rsch/114.
- Singer, D. A., Berger, V. I., and Moring, B. C., 2005, Porphyry copper deposits of the world: database, map, and grade and tonnage models. U.S. Geological Survey, Open File Report, 1060(9).
- Vuke, S. M., 2014, Preliminary geologic map of the Dearborn River 30' x 60' quadrangle. Montana Bureau of Mines and Geology, Open-File Report 649.
- Vuke, S. M., Porter, K.W., Lonn, J.D., and Lopez, D.A., 2009, Geologic map of Montana field notebook. Montana Bureau of Mines and Geology, Geologic Map 62-E, 59 p.



Conference participants head underground to look at the Madison Au-Cu-Ag skarn at Silver Star, MT. Photo by A. Roth, MBMG.



Montana Tech geology professor Dr. Chris Gammons gives the geologic overview at the Madison Au-Cu-Ag skarn at Silver Star, MT. Photo by A. Roth, MBMG.

Ringings Rocks, Montana: A Modern Gas Diapir?

John W. Gabelman

Introduction—The Sea of Ringing Rocks

The Ringing Rocks (fig. 1A) Felsenmeer (German: “sea of rock”) is a barren pile of chaotically jumbled loose rocks (fig. 1B) that are exposed in the hills north of Pipestone, Montana. The Ringing Rocks occur within the mafic monzonite rim zone of the eponymous pluton (fig. 2) (Protska, 1966; Butler, 1983; R. Berg, written commun., 2017), noted for its circular plan section and therefore pipe-like geometry (figs. 1B, 2). Review of the mechanism of their well-known tintinnabulation is deferred to the complete version of this report. This summary addresses only the geologic origin of the Ringing Rocks Felsenmeer.

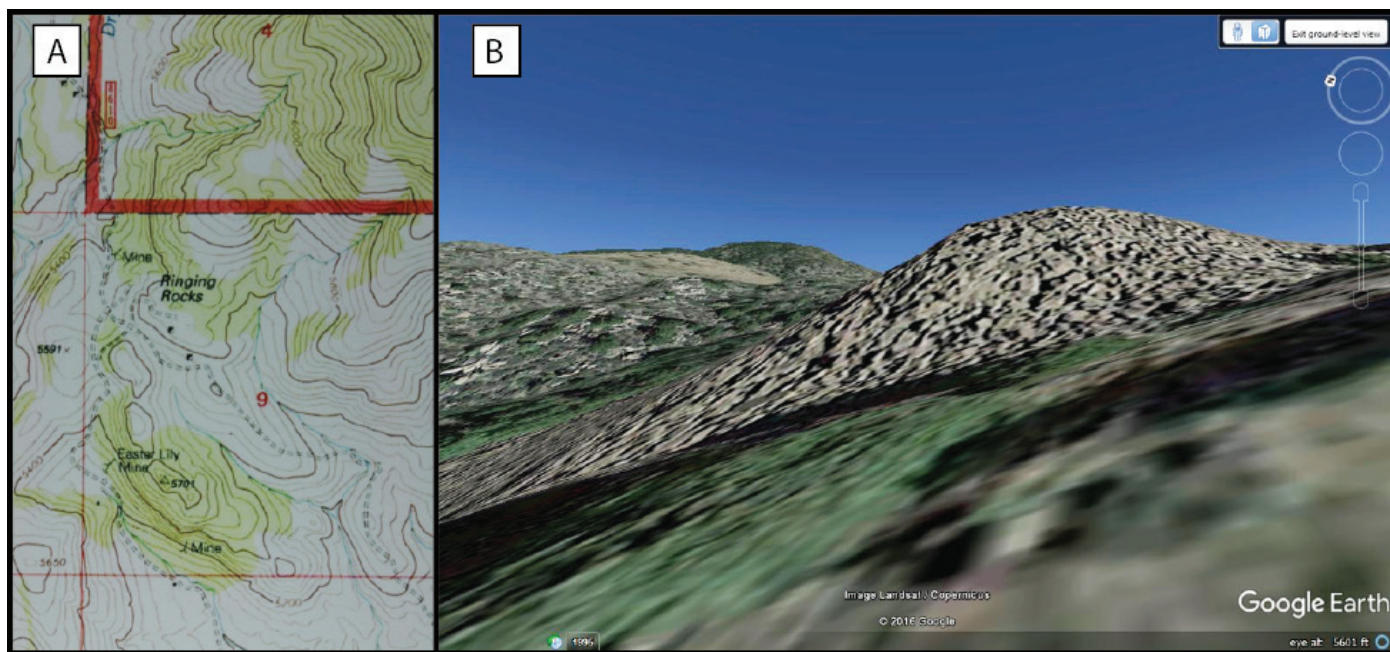


Figure 1. (A) Topography of the Ringing Rocks and Easter-Lily plutons located at NW, NW, 9, T. 2 N., R. 5 W., Jefferson County; Dry Mt. USGS 1:24,000 topographic quadrangle. (B) Slant view across the Ringing Rocks to the hills of the Ringing Rocks pluton core north, emphasizing its topographic isolation. The pile is a smooth double dome (the second hidden).

The Ringing Rocks form a crude trapezoid in plan, elongated northwestward, about 100 m long by 90 m wide with sides that face about 50 degrees off the cardinal directions. The body of Ringing Rocks has about 25 m of topographic relief. The rock field is draped over the north edge of a small, nearly flat bench in the main Dry Mountain ridge (fig. 1A), with the greatest portion stretching northwest down the slope. It is arched, with two main and three minor local protrusions (summits) in the field (fig. 1B). The main and highest summit is in the southwest portion of the rock field, just above the parking lot.

The trapezoid of jumbled rocks (fig. 3A) is a unique feature of the entire rim band of the mafic monzonite pluton (fig. 2). Outcrops outside the trapezoid are normally closely jointed with blocks similarly oriented. Thus, the Ringing Rocks and their origins appear to be independent of the pluton, although the respective genetic processes may be distantly related by reactivation.

The Ringing Rocks are composed entirely of individual blocks (figs. 1B, 3) that obviously once constituted a singular rock body. All blocks in the pile consist of fragmental joint blocks that are prismatic and angular. The outwardly smooth surface is wrinkled into local summits and swales. Vestiges of an original stack of jointed blocks (fig. 4A) demonstrate that the Ringing Rocks were fragmented from an originally jointed, solid rock body.

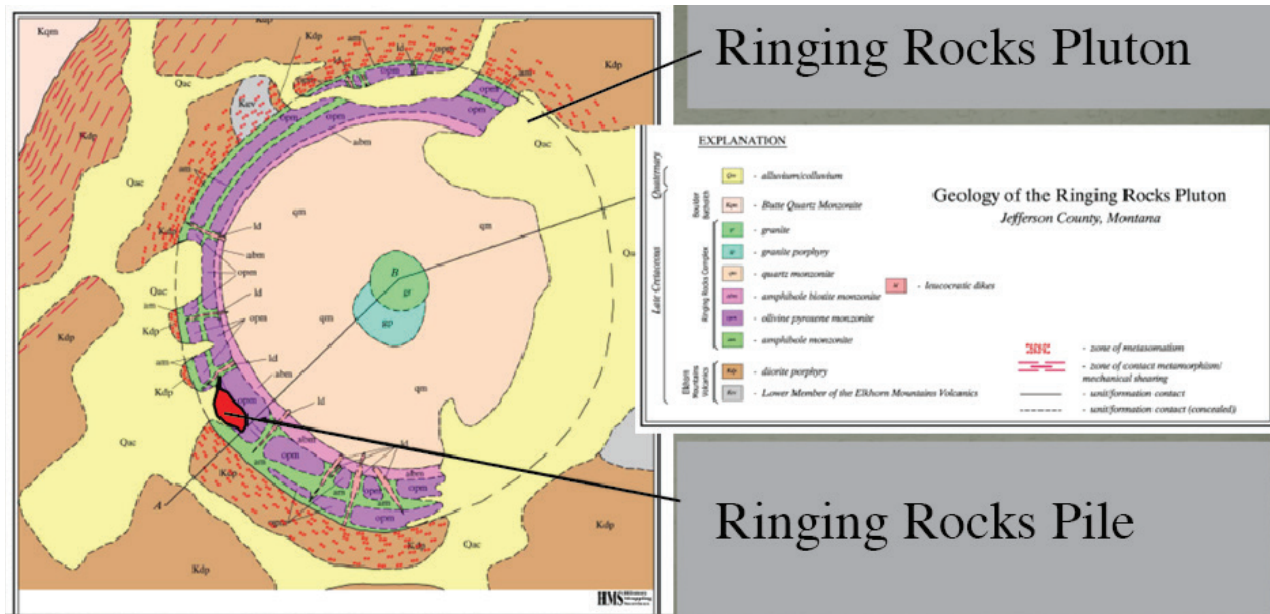


Figure 2. Geology of the Ringing Rocks Pluton modified from R. Berg, written commun. (2017). The Ringing Rocks occur in the southwestern part of the mafic monzonite band shown in red.



Figure 3. Images of the Ringing Rocks. (A) Google Earth view southwestward down and across the Ringing Rocks. Shadows emphasize positions, size, and relative elevations of three major and two minor interior summits, as well as the roughness and chaotic disposition of blocks. Emphasizes gradients from near-coherent to more chaotic block orientation, radiant from pile margin and local summits. Seemingly rectilinear margins correlate with prominent fracture-joint directions. (B) View north from the parking lot across steep slope of the Ringing Rocks. Photo 5016, by Rose Marie Mason. (C) Sharp edges and corners of rhombohedral and tetrahedral blocks toward the interior of the Ringing Rocks, at Locality RR-104. Many blocks are hardly displaced from near-outcrop, expressed by planarity dipping to the right. (D) Cubic and tetrahedral blocks on south margin of the Ringing Rocks. Photo 5009 by Rose Marie Mason.

The Current Investigation

The Ringing Rocks and environs were photographed and sampled to distinguish them from the rest of the Ringing Rocks Pluton and from the external country rock (fig. 2). A circumferential examination of the pile boundary defined a transition zone 2–5 meters wide and 1–3 meters in relief, rather than a sharp contact (compare figs. 3 and 4). The transition zone (fig. 3A) separates regimes that exhibit distinct local topography and structure. Although prominent morphologically, the transition zone is obscure petrologically, as mafic monzonite occurs on both sides of the zone.

The surface of the mafic monzonite country rock outside the transitional boundary is expressed as isolated scattered sharp outcrops a few square meters in area from <1 m to 4 m relief. Outside of the transition zone scattered outcrops rise abruptly from a smoothly undulating floor of forest- and humus-covered eluvium. This floor and (the) island outcrops are typically strongly weathered with veneers a few centimeters thick and extensively covered with pale green lichens. Most typical and significant is the exfoliation rounding (50-60%) of all edges and corners, commonly leaving near-spherical boulders and outcrop projections.

Well-expressed joint patterns in large outcrops of the Boulder Batholith (Homestake Pass) and associated plutons (Ramsay) exhibit similar regional patterns of straight joints that tightly enclose similarly oriented rectangular to cubic blocks. These outcrops are adopted as a standard for undisturbed strongly jointed coherent outcrops of massive igneous rocks in the immediate region. Three general stages in the disorientation and destruction of coherent outcrops by normal weathering and erosion are observed within the Boulder Batholith. During stage one, blocks become separated, shift outward, and are raised by frost heaving, freezing/



Figure 4. Images of the Ringing Rocks Transition Zone. (A) Panorama 11, Locality 119. View SW along the transition zone. (B) (4-11-17-89; 7775.) Chaotically loosened and rotated blocks in the Ringing Rocks at the west margin at Locality 128 in the circumferential survey. View across the transition zone. Coherent outcrop of the pluton core in background. (C) Boulder-strewn apron in the transition zone marginal to the Ringing Rocks. Exfoliation rounding, assisted by chemical oxidation of feldspars to clay, is an important accompaniment to all these stages. Corners are rounded, then edges, accompanied by reduction in block size, and finally spheres result. The great difference in the degree of exfoliation inside and outside the Ringing Rocks Pile is critical in interpreting the chronology of events.

wedging, and crack expansion. This looser collection of blocks retains its basic position and orientation. During stage two, advanced separation and loosening of the pile occurs. Gravity pulls blocks downhill where they lean outward and slide with their bases still relatively anchored. Stage three blocks are isolated and exhibit various orientations, but are anchored in eluvium or soil, or rest on the outcrop.

Ringings Rocks and Their Matrix

Morphology and wasting features at the Ringings Rocks are unique with respect to weathered and eroded rock observed in the surrounding Boulder Batholith. The interior of the Ringings Rocks is structurally chaotic and characterized by rotated blocks with large intervening spaces. It is composed entirely of joint blocks, liberated, rotated, collapsed, and exhibiting little trace of their original pattern. The rock still appears fresh, and edges and corners remain sharp and only weakly rounded by incipient exfoliation. Mafic monzonite blocks within the Ringings Rocks and its transition zone (fig. 5B) exhibit relict joint patterns that differ radically from those in the host mafic monzonite band (fig. 2), which suggests that lithology is not a factor in controlling joint patterns. This leaves genetic mechanisms and reactions to the consistent destructive process as causes of differences in rock morphology and wasting features.

Pore space in the Ringings Rocks holds 15–20% air. The blocks are never cemented together by a rock or mineral matrix and the block pile is essentially self-suspended. Soil and water- or wind-deposited material is not evident. So, the suspension requirement for tintinnabulation prevails throughout. The surfaces of blocks are weathered with a tan-brown paint, and uniform chemical alteration skin only several millimeters thick. The rocks beneath the surface blocks are essentially pristine, and minimally altered and weathered. The environment of bare angular rock, deep crevices, and lack of fine debris is detrimental to vegetation. Lichens on block surfaces are absent and there is no evidence that vegetation ever existed on the Ringings Rocks, or in the voids between blocks. Fracturing and formation of the pile appears to be the last significant event in its history.

Disposition of Blocks at the Ringings Rocks

Blocks in the Ringings Rocks are dominantly chaotic and rotated, as illustrated by large-scale images (fig. 3A) and local side views (fig. 3C). Blocks tend to be rhombohedral (fig. 3C), cubic (fig. 3B), or tetrahedral (figs. 3C,3D) joint blocks damaged to varying degrees and fractured into smaller rhombs, cubes, or tetrahedrons. Angular slivers that have broken off the blocks are common. Block width is rather consistent, which is a distinctive feature of the Ringings Rocks. Blocks vary from 0.5 m to 2.5 m wide and are about 1.5 m wide on average. A few blocks are up to 3 m wide and fragments smaller than boulder size are rare.

Edges and corners are angular to sharp (figs. 3B–3D) in the interior and modestly (3-5%) rounded toward the block field margins. A total of 60–65% of the blocks are in point contact at 3 to 8 points (fig. 5A). The blocks are differentially rotated so they contact dominantly at corners (fig. 4B), less commonly at edges (figs. 3B, 3D), and rarely at surfaces. Adjacent blocks approach common orientation toward the interior summits and toward the edges (fig. 5B). Yet all are in neighbor-contact. Thus, a range of block suspension is demonstrated.



Figure 5. (A) (BN5013.) Barbara Nye posing by slightly foliated, strongly rotated blocks with large intervening spaces in the Ringings Rocks margin at the parking lot. Most blocks are in point-contact. (B) Slant view west–southwest across the Ringings Rocks composed entirely of loose, rotated joint blocks. Note isolated satellite piles at left. Core of the Ringings Rocks pluton lower right.

Structure of the Ringing Rocks

Google Earth images (figs. 3A, 5B), magnified and rotated to effect low-level oblique observation (about 1: 7,500), offer details of shapes and modifications to groups of blocks within the Ringing Rocks. Although joint block orientations are typically outwardly chaotic (fig. 3B), traces of an original coherence are apparent in groups of blocks that are barely or moderately moved or rotated. In lateral view, summit blocks appear more rhombic and tightly packed whereas slope blocks define a loose aggregate of disrupted mutilated joint blocks, like a loosened expanded shatter-work with an air matrix. Five interior summits are enhanced by shadows in side-illumination (fig. 3A). The relative orientations of the summit blocks allow interpretation of the texture and structure of the Ringing Rocks (fig. 6A). A 30-m-wide border zone contains blocks that retain enough parallelism to define mega-joint lines parallel to the borders (fig. 6B).

Shadow lines define block parallelism and are partially concentric around the five interior summits. These features illustrate a gradient of disruptive deformation increasing inward, divisible into subgradients radiating from the five summits, which may represent uplift centers. Lines of shadows or illuminated block faces define long lineaments partially or completely crossing the whole field, and some align with lineaments in the enclosing late Cretaceous Elkhorn Mountains tuffs. These observations suggest that regional structures, or fault systems, may control localization and differential uplift (fig. 6B) in and around the Ringing Rocks.

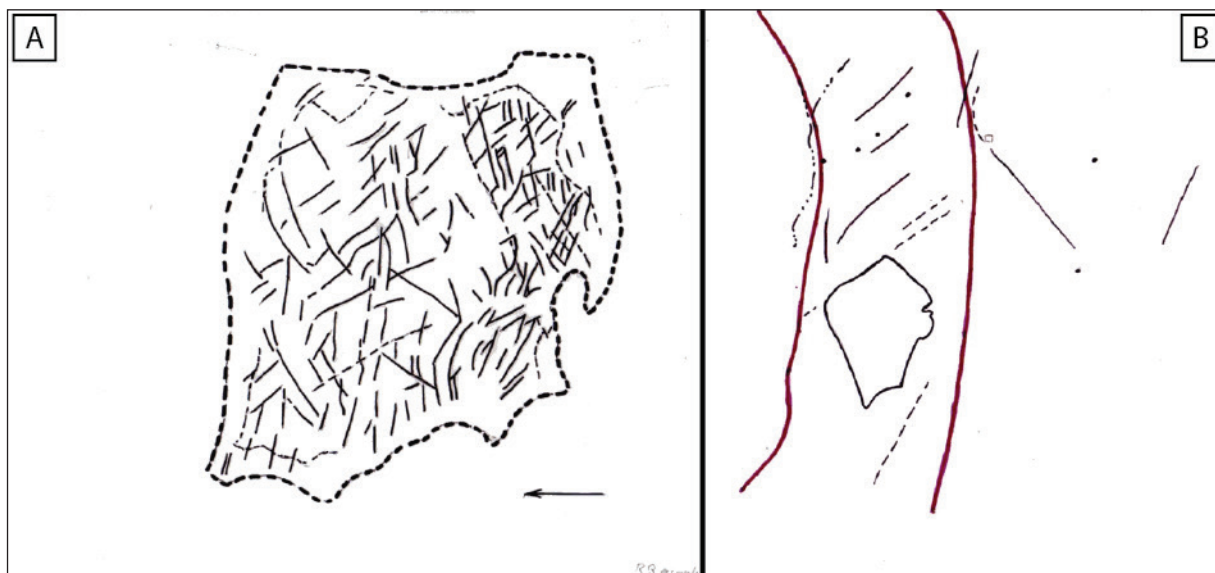


Figure 6. (A) Lineaments and curves interpreted from Image Gogglescale 29 compose a pattern of disturbed joints. (B) Overlay for Image Gogglescale19, showing the position of the Ringing Rocks in the local mafic monzonite rim, and suggesting structural joint control over Ringing Rocks emplacement.

Discussion

The Source Dilemma

The Ringing Rocks, or anything like it, is a unique feature in the area (fig. 1A). Possible source rocks include late Cretaceous quartz monzonite of the Boulder Batholith, diorite porphyry of the Elkhorn Mountains Volcanics, and mafic monzonite of the Ringing Rocks pluton (fig. 2). Mafic monzonite of the Ringing Rocks pluton is the only body of that rock in the region. The entire pile of Ringing Rocks, within the range of observation, lies within the mafic monzonite band. The mafic monzonite of the normal band appears megascopically different around the edges of the Ringing Rocks, but the matrix of the pluton must be mineralogically similar enough to the Ringing Rocks to retain the classification by former investigators.

Accepting the petrology of former investigators, the principal chemical difference between the Ringing Rocks and the mafic monzonite (pluton) [band] that contains them (fig. 2) may be the degree of supergene atmospheric weathering, the Ringing Rocks being unusually fresher, and therefore younger. The Ringing Rocks and

their pluton are petrographically unique in the large enclosing area. If the Ringing Rocks were derived as debris from a higher source, such as a landslide or talus field, they should relate to an identifiable source within the topography capable of providing it. In the absence of such, the Ringing Rocks body can have been derived only from the band in which it occurs and must be essentially in-place.

Depth and Age of Formation

The Pile seems to be coherent, intact, and hardly eroded. The shattered body could extend to the depth where strain exceeds the strength of the rock. The 25 m of total relief of the Ringing Rocks can be considered a cross-section through a deeper body. But the amount of vertical rise is indicated to be small. I infer the vertical displacement to have been at most only tens of meters. The relative amounts and distribution of exfoliation in the marginal zone suggest a diapir that rose through an already strongly exfoliated surface, pushing up completely angular rocks.

Hydrothermal mineralization occurred in the region during late Cretaceous pluton emplacement (Olson and others, 2016). Quartz–tourmaline (schorlite)–gold mineralization was superimposed on the pluton and environs. This mineralization was of high temperature and was solidly emplaced in most open spaces near large controlling fractures. Presumably all space available to the ore fluids at the time of invasion, within reasonable reach of trunk channels, was filled. No evidence of mineralization is found in or adjacent to the Ringing Rocks although prospect pits and shallow shafts lie within 200 m of them. The absence of even vestiges of this mineralization in the highly porous Ringing Rocks demonstrates that pore spaces were not available at the time of mineralization, and that the Ringing Rocks formed much later than the plutons and related mineral deposits.

The Ringing Rocks are so independently superimposed on their like-named pluton that it constitutes an independent process and environment more typical of shallow or surficial depths, which have no evident surface source. Occurrence of the Ringing Rocks within the rim of the pluton (fig. 2) implies a close chronological association between the feeding channels of each. If the Ringing Rocks formed at approximately the same time as the pluton, they expectedly must have extended much higher with a substantial upper part removed by erosion. However, physiography implies little or minimal erosion and a young, even modern age for the Ringing Rocks. The chaos of the pile interrupts and is imposed on the strongly exfoliated outcrops of the enclosure, and is developing its own thin weathering rinds and slight exfoliation anew. This suggests that the Ringing Rocks are no older than the time required to develop the new rinds and exfoliation.

The Space Dilemma and Mechanism of Formation

Although the geometry, orientation, and porosity of the Ringing Rocks are typical and indicative of collapse, the anomalous amount of space still contradicts the normal gradient of decreasing space and requires another formation mechanism. The most logical is uplift preceding collapse. This would create room for fragmentation into blocks, block separation, and rotation. Collapse to create rotation and chaos followed the interruption or cessation of uplift. As cavity filling is inevitable, the degree and depth extent of open mega-porosity are a measure of the age of the porosity. Given expected flooding of porosity and availability of wind-blown particles and run-off eluvium, porosity should be partly filled, especially if the original surface was higher and reduced by erosion. Thus, the open-cavity system in the Ringing Rocks must extend deeper than their surface enclosure. This depth remains unknown, but is considered significant.

After shape, independence, chaotic orientation, and freshness of the blocks, the next most distinctive and critical genetic feature of the pile is the uniquely large amount of space between blocks. Such porosity is illogical at depth as lithostatic pressure would squeeze intergranular pore spaces closed. Logically, a significant portion of this space should be filled and therefore, the extent, geometry, and volume of the cavity system must be critical indicators of the formative process. The 15–20% air porosity at the Ringing Rocks presents the enigma of creating that space. A logical source for creating such space, into which the blocks could collapse, is the rise of magmatic or juvenile space-creating agents (fluids/gases). Atmospheric gasses must have their subterranean spaces structurally or chemically prepared for them, whereas volcanic and juvenile gases can create their own.

An outcrop-shattering and -destruction force is needed to produce the Ringing Rocks, much stronger than

that which produced the enclosing rolling landscape. The anomaly of the youthful Pile with no surface source in mature surroundings implies that it had to be created *in situ*. Transgressive Pipe structures, including or excluding igneous material mixed and finely comminuted, result from rapid extremely forceful (explosive) drilling, to produce cylindrical or approximate structures. Diatremes (Greek: “through rapid piercing”) are fast and violent whereas diapirs (exemplified by salt and gypsum domes) are slow and gentle.

Shapes begin as multiple-straight-sided poly-outlines for diapirs and/or circular outlines for diatremes. The degree of cylindricity is attributed to the pressure and velocity of the gas or other driving agent. The most likely, virtually only, agents capable of such drive are liquids or gases, volcanic, non-volcanic juvenile, or from tectonic compression. Solids are involved essentially as grinding tools liberated from walls. The Ringing Rocks mass is evidenced to be more a diapir by the lack of shattering beyond the expanded-rotated joint-block stage, and by the textural cohesiveness of the pattern of blocks. The force and velocity of movement were low enough to prevent evolution from a trapezoidal shatter pattern to cylindrical shape, but enough to distort the trapezoid. A compromise is a diapir faster than a salt dome. Nine parameters interpreted for the driving force are: slow, gradational, vertical, shallow, weak, young, irregular distribution, small displacement, and single event.

Conclusion

The isolation and point suspension of the blocks must be the critical cause of their melodiousness. Each block is effectively hanging, and able to respond to impact by resonant standing waves, like a bell. The Ringing Rocks cut the mafic monzonite rim band of the late Cretaceous Ringing Rocks stock that is both host, and source, to the rock field. The strong freshness of all blocks opposes any significant chemical alteration or oxidation of the mafic monzonite. Thus, the Ringing Rocks must have formed recently in geological terms, and certainly after Pleistocene alpine glaciation of the region.

Although chronologically divorced from it, coincidence of the Ringing Rocks within the Ringing Rocks pluton suggests a connection of feeding channels, perhaps reopening of a filled magmas passage. An entire isolated hill of positive relief was selectively intensely shattered by vertically focused deformation. The rise was moderate and gradual, more as an arch illustrated by surficial joint-surface orientations constituting a marker horizon. It left such uniquely large porosity that collapse after significant rise was required. Absence of intrusive magmatic and hydrothermal products within the porosity relegates the invading agent to gas and the structure a diapir. Excellent preservation of gross physiography, structure, and texture, plus minimal weathering and reduction, support a near-modern age.

Acknowledgments

I am grateful to Dick Berg for his inspiration, introduction to the project, and continuing evaluation, editing and encouragement; to Peggy Delaney for encouragement and guidance; to Joan Gabelman for severe filial editing; and to Kaleb Scarberry for sensible consolidation and editing.

References Cited

- Butler, Barbara A., 1983, Petrology and geochemistry of the Ringing Rocks pluton, Jefferson County, MT: Missoula, Mont., University of Montana, Master's thesis
- Olson, N.H., Dilles, J.H., Kallio, I.M., Horton, T.R., and Scarberry, K.C., 2016, Geologic Map of the Ratio Mountain 7.5' quadrangle, southwest Montana: Montana Bureau of Mines and Geology EDMAP-10.
- Prostka, H.J., 1966, Igneous geology of the Dry Mountain Quadrangle, Jefferson County, Montana, *in* Contributions to General Geology, U.S. Geological Survey Bulletin 1221-F.



John (center) and Joan (left) Gabelman enjoy lunch during the Madison Au-Cu-Ag skarn field trip at Silver Star, MT. Photo by D. Herman, MBMG.



Joan (left center) and John (right center) Gabelman talk with students at the poster session.

Timing of Pluton Emplacement and Mineralization of the Boulder Batholith

Stanley L. Korzeb and Kaleb C. Scarberry

Montana Bureau of Mines and Geology

A variety of mineral deposit types occur within the Boulder batholith, including epithermal veins, breccia pipes, copper porphyries, skarns, limestone replacements, and disseminated gold deposits. Mining districts and plutons discussed in this report are shown in figure 1. New and existing radiometric ages are used to describe five mineralizing events that occurred during emplacement of the batholith.

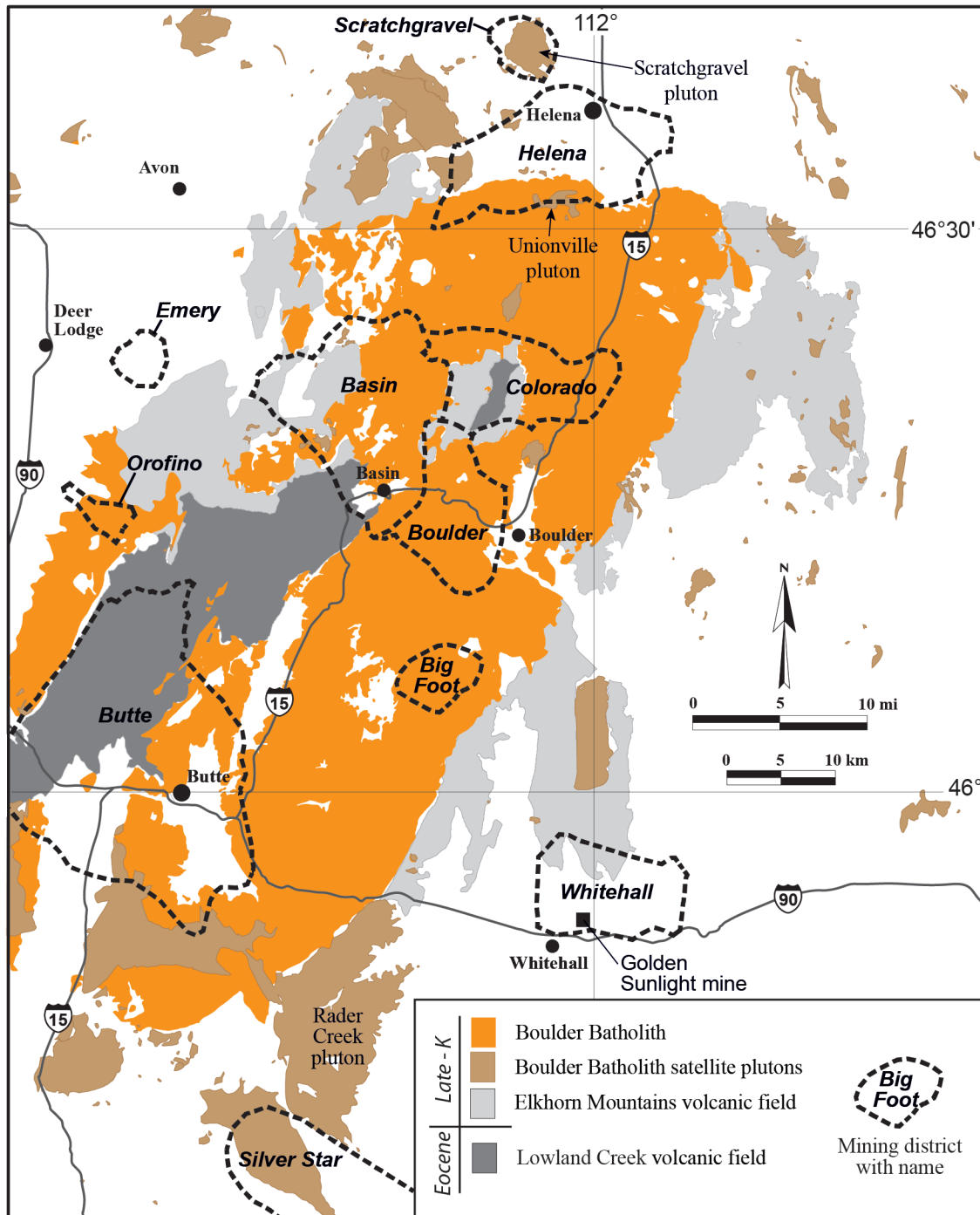


Figure 1. Late Cretaceous–Eocene magma systems and mining districts.

Age of the Magma Systems

The Boulder batholith was emplaced in two stages: an early stage from 83 Ma to 77 Ma and a late stage from 75 to 77 Ma that produced the Butte granite (fig. 2A), the main mass of the batholith (Lund and others, 2002; summary in Olson and others, 2017). Northwest-striking high-angle faults exerted control on the distribution of early stage plutons. The early stage plutons are northwest elongate, cut low-angle thrust faults and sill complexes, and host northwest-striking hydrothermal vein systems. Late-stage intrusions are northeast-elongate and formed in a regional pull-apart structure (Berger and others, 2011).



Figure 2. (A) Hand sample of Butte granite. (B) Middle EMV rhyolite ignimbrite. (C) Late eruptive LCV lava flows and tuffs.

Formation of the Elkhorn Mountains Volcanic field (EMV) was co-magmatic with early stage batholith pluton emplacement, beginning at about 85 Ma and continuing until about 77 Ma (summary in Olson and others, 2017; M. Schmitz, written commun.).

The EMV sequence consists of lower, middle, and upper members. The lower EMV consists primarily of andesitic–rhyodacite lavas, pyroclastic units, and volcanogenic sediments. The middle EMV is dominated by large-volume rhyolite ignimbrite (fig. 2B) eruptions and represents one of the largest ignimbrite provinces known on Earth (Smith, 1960; Smedes, 1966; Klepper and others, 1974). Middle member eruptions formed calderas (e.g., Scarberry, 2016). Bentonite deposits in eastern Montana shales (Knechtel and Patterson, 1956) are, in part, remnants of these explosive eruptions. Olson and others (2016) describe intra-caldera deposits on the east flank of the Boulder batholith and report radiometric ages that range from about 85 Ma to 83 Ma. Zircon ages of 77.4 and 78.5 Ma (M. Schmitz, written commun.) were obtained from intra-caldera middle member rhyolite ignimbrites east of Deer Lodge (Scarberry, 2016). The upper EMV consists of reworked volcanoclastic detritus eroded from primary volcanic accumulations (Becraft and others, 1963).

Following eruption of the EMV, late stage Butte granite intruded the volcanic field (Klepper and others, 1957, 1971). The northeast-trending Butte granite is 90 km long and 50 km wide and volumetrically the dominant pluton of the Boulder batholith (Berger and others, 2011; du Bray and others, 2012). U/Pb zircon ages for the Butte granite range from 76.7 ± 0.5 to 74.7 ± 0.6 Ma, and petrologic data suggest that it consists of compositionally distinct intrusions formed during two magmatic episodes (du Bray and others, 2012).

Following emplacement of the Butte granite, 66 Ma plutons intruded the Boulder batholith region. A 66 Ma quartz monzonite intrusion at Boulder Baldy and the 66.5 Ma quartz porphyry dike in the Continental Pit suggest that 66 Ma plutons may be more common than originally thought, and served as regionally important sources of mineralizing fluids in the Boulder batholith region (Lund and others, 2002). These plutons and related mineral deposits suggest these systems served as regionally important mineralizing sources (Lund and others, 2002).

After a magmatic hiatus of about 10 million years, the Eocene Lowland Creek Volcanic field (LCV) erupted into northeast-striking half grabens that traversed the Boulder Batholith between about 53 Ma and 49 Ma (Smedes, 1962; Dudàs and others, 2010). The LCV overlies mid-Proterozoic, Permian, and Cretaceous sedimentary rocks along the west edge of the Eocene graben. Smedes (1962) divided the LCV into six laterally discontinuous units that formed during two eruptive cycles. The first eruptive cycle produced volcanoclastic deposits, tuffs, and tuff breccia. The latter eruptive cycle produced lava flows (fig. 2C) and tuffs (Dudàs and others,

2010). Foster (1987) suggested that the last eruptive cycle resulted from caldera-forming eruptions.

Age of the Mineral Systems

Skarn deposits on the margins of the Boulder batholith are related to intrusion of early stage plutons and are among the oldest mineralizing events. The skarns formed in reactive formations from heat and fluids generated from adjacent satellite plutons. Because skarn deposits form during igneous intrusions, the age of local intrusions may provide a nice proxy for the age of district-wide skarn mineralization (table 1).

Table 1. Published ages for plutons with related skarn mineralization along their contacts with carbonate rocks.

Pluton/Mining District	Age	Reference
Scratchgravel/Scratchgravel Hills	86 ± 4 Ma	McClernan, 1983
Rader Creek/Silver Star	80.7 ± 0.8 Ma	du Bray and others, 2012
Unionville/Helena	78.2 ± 0.5 Ma	du Bray and others, 2012

Note. The Scratchgravel pluton was dated using the K-Ar method on hornblende, whereas the other pluton dates are from the U-Pb method on zircon.

The Rader Creek granodiorite at 80.7 ± 0.8 Ma (Du Bray and others, 2012) reacted with Mississippian through Devonian carbonates (Robb, 2016) to produce skarn mineralization in the Silver Star district; if the skarn developed when the intrusion was emplaced, the age of the skarn should be similar. The Scratchgravel pluton (table 1) is thought to be an early stage Boulder batholith pluton (McClernan, 1983). Skarn mineralization in Belt Supergroup carbonaceous shale (Empire Formation) formed along the margin of the pluton (McClernan, 1983). The Unionville pluton (table 1) is a granodiorite in the Helena district at the northern edge of the Boulder batholith. Skarn deposits formed marginal to the pluton in Mississippian Madison limestone (McClernan, 1983). Skarn deposits throughout the Helena district may be similar in age to the Unionville pluton.

Their age and proximity to caldera deposits suggest that mineral veins formed along both the eastern and western flanks of the Boulder batholith during the latest stages of EMV middle member volcanism. Mineralization at the Golden Sunlight mine occurred coincident with EMV volcanism at about 77 Ma and within the Emery mining district at about 77.9 Ma (table 2). The Golden Sunlight mine exploits an Au-Ag breccia pipe with an age (76.9 Ma) that correlates with Elkhorn Mountain Volcanic (78–76 Ma), suggesting the breccia pipe formed during Elkhorn Mountain volcanism. The breccia pipe formed from emplacement of alkali-calcic rhyolite and subsequent collapse of the Belt Supergroup wall rock and rhyolite (De Witt and others, 1996). Deep epithermal to mesothermal veins in the Emery mining district are located near the margin of a middle member caldera (Korzeb and others, 2018) that formed in lower member andesite lava flows (Scarberry, 2016). Hydrothermal systems related to epithermal vein development often occur near caldera margins, and are driven by late stage intrusion, resurgent doming, and cooling of the caldera (Simmons and others, 2005).

Aplite dikes and epithermal mineral veins hosted by the Butte granite likely formed at the same time. The epithermal veins vary in age from about 74 Ma to 75 Ma (table 2), and they formed after the granite had solidified and fractured (du Bray and others, 2012). Zircon in aplite, also hosted by Butte granite, yielded an age of 74.5 ± 0.6 Ma (this study), similar in age to the epithermal veins. Epithermal veins hosted by the Butte granite suggest a hydrothermal system was established near the close of late stage Boulder batholith magmatism. Porphyry intrusions associated with the Boulder batholith magma system have ages of about 64 Ma to 66 Ma (Lund and others, 2002; Rusk and Reed, 2008). At Butte, a world-class Cu-Mo porphyry system and related epithermal veins (summary in Houston and Dilles, 2013) developed following emplacement of the Butte granite. The Cu-Mo porphyry mined now at the Continental Pit formed at 63.6 Ma (table 2). After the Butte granite intrusion solidified, a number of small plutons followed.

The last major volcanic event in the Boulder batholith was the eruption of the LCV (52.9–48.6 Ma; Dudàs and others, 2010). Epithermal veins and a diatreme have ages (50–45.26 Ma) that correlate with the Lowland

Table 2. Published and new ages for district/mine mineral deposits and the geologic events they are associated with.

District/Mine	Age	Magma System	Reference
Whitehall/Golden Sunlight	76.9 ± 0.5 Ma	Elkhorn Mtn. Vlc. field	De Witt and others, 1996
Emery/Hidden Hand	77.9 ± 0.20 Ma	Elkhorn Mtn. Vlc. field	Korzeb and others, 2018
Big Foot/State	75.12 ± 0.25 Ma	Late-stage (Butte pluton)	Olson and others, 2016
Big Foot/Ajax	73.81 ± 0.12 Ma	Late-stage (Butte pluton)	Olson and others, 2016
Basin/Eva May	74.4 ± 0.3 Ma	Late-stage (Butte pluton)	Lund and others, 2002
Boulder/Hope-Bullion	74.4 ± 1.2 Ma	Late-stage (Butte pluton)	Lund and others, 2002
Butte/Continental Pit	63.6 ± 0.2 Ma	post-Butte pluton	Lund and others, 2002
Oro Fino/Banker	45.26 ± 0.11 Ma	Lowland Crk. Vlc. field	This study
Colorado/Montana Tunnels	50 Ma	Lowland Crk. Vlc. field	Sillitoe and others, 1985
Oro Fino	74.5 ± 0.6 Ma	Aplite dike	This study

Note. Ages were determined using the ^{40}Ar - ^{39}Ar method on muscovite (sericite) from altered host rocks. The Golden Sunlight Mine age was determined using the ^{40}Ar - ^{39}Ar method on biotite from lamprophyre dike rock. Note: error for Montana Tunnels age was not reported by Sillitoe and others (1985).

Creek volcanic ages. The volcanic sequence erupted from calderas along a half graben trending northeasterly across the west side of the Butte granite pluton. Epithermal veins and a mar volcano related to caldera development formed in conjunction with the eruption of the volcanic sequence. The diatreme at Montana Tunnels (50 Ma) is described by Sillitoe and others (1985) to be emplaced during a hydrovolcanic event at the close of Lowland Creek volcanism.

Epithermal veins in the Oro Fino district (45.26 Ma) occupy northeast and north-south-trending fractures in the Butte granite. When the graben formed, fractures developed in the host granite along the graben margin. Ages for the epithermal veins (table 2) imply a hydrothermal system was established near the close of Lowland Creek volcanism and caldera development. This hydrothermal system vented through fractures in the adjacent granite, forming epithermal veins with an age that correlate with LCV ages.

Conclusion

Near the close of magmatic events, mineralizing systems are often initiated that develop mineral resources. Magmatic events that supplied the heat and fluids that drive hydrothermal systems will have ages that correlate with mineralizing event ages, demonstrating the two events are linked. This paper connects resource-bearing mineralizing systems to episodes of magmatic activity in the Boulder batholith. We identify the following periods of magma-related ore formation:

1. Satellite pluton intrusion between about 86 Ma and 78 Ma that developed Au-Cu skarns.
2. Caldera resurgence related to EMV ignimbrite-forming eruptions between about 78 Ma and 77 Ma and development of Au-Ag and base-metal, low-sulfidation epithermal veins and Au-Ag breccia pipes.
3. Butte granite emplacement between about 76 Ma and 74 Ma developed Au-Ag base metal low-sulfidation epithermal veins and pegmatites at the close of the magmatic event.
4. Late stage satellite plutons emplaced about 64 Ma and 66 Ma developed porphyry Cu-Mo deposits and epithermal veins.
5. Caldera resurgence related to LCV eruptions about 53 Ma and 49 Ma developed low-sulfidation Au-Ag base metal veins and breccia pipes.

References

- Becraft, G.E., Pinckney, D.M., and Rosenblum, S., 1963, Geology and mineral deposits of the Jefferson City Quadrangle, Jefferson and Lewis and Clark Counties, Montana: U.S. Geological Survey Professional Paper 428, 101 p.
- Berger, B.R., Hildenbrand, T.G., and O'Neill, J.M., 2011, Control of Precambrian basement deformation zones on emplacement of the Laramide Boulder batholith and Butte mining district, Montana, United States: U.S. Geological Survey Scientific Investigations Report 2011-5016, 29 p.
- De Witt, E., Foord, E.E., Zartman, R.E., Pearson, R.C., and Foster, F., 1996, Chronology of late Cretaceous igneous and hydrothermal events at the Golden Sunlight gold-silver breccia pipe, southwestern Montana: U.S. Geological Survey Bulletin 2155, 48 p.
- du Bray, E.A., Aleinikoff, J.N., and Lund, K., 2012, Synthesis of petrographic, geochemical, and isotopic data for the Boulder batholith, southwest Montana: U.S. Geological Survey, Professional Paper 1793, 39 p.
- Dudàs, F.O., Ispolatov, V.O., Harlan, S.S., and Snee, L.W., 2010, $^{40}\text{Ar}/^{39}\text{Ar}$ geochronology and geochemical reconnaissance of the Eocene Lowland Creek volcanic field, west-central Montana: *Journal of Geology*, v. 118, p. 295–304.
- Foster, F., 1987, Epithermal precious metal systems associated with an Eocene cauldron: Lowland Creek volcanic field, southwestern, Montana, in Berg, R.B., and Breuninger R.H., eds., *Guidebook of the Helena area, west-central Montana*: Montana Bureau of Mines and Geology Special Publication 95, p. 53–54.
- Houston, R.A., and Dilles, J.H., 2013, Structural geologic evolution of the Butte district, Montana: *Economic Geology*, v. 108, p. 1397–1424.
- Klepper, M.R., Robinson, G.D., and Smedes, H.W., 1974, Nature of the Boulder batholith of Montana—Discussion: *Geological Society of America Bulletin*, v. 85, p. 1953–1960.
- Klepper, M.R., Ruppel, E.T., Freeman, V.L., and Weeks, R.A., 1971, Geology and mineral deposits, east flank of the Elkhorn Mountains, Broadwater County, Montana: U.S. Geological Survey Professional Paper 665, 66 p.
- Klepper, M.R., Weeks, R.A., and Ruppel, E.T. 1957, Geology of the southern Elkhorn Mountains, Jefferson and Broadwater Counties, Montana: U.S. Geological Survey Professional Paper 292, 82 p.
- Knechtel, M.M., and Patterson, S.H., 1956, Bentonite deposits in marine Cretaceous Formations, Hardin District, Montana and Wyoming: U.S. Geological Survey Bulletin 1023, 116 p.
- Korzeb, S.L., Scarberry, K.C., and Zimmerman, J.L., 2018, Interpretations and genesis of Cretaceous age veins and exploration potential for the Emery mining district, Powell County, Montana: *Montana Bureau of Mines and Geology Bulletin* 137, 51 p.
- Lund, K., Aleinikoff, J.N., Kunk, M.J., Unruh, D.M., Zeihen, G.D., Hodges, W.C., du Bray, E.A., and O'Neill, M.O., 2002, SHRIMP U-Pb and $^{40}\text{Ar}/^{39}\text{Ar}$ constraints for relating plutonism and mineralization in the Boulder batholith region, Montana: *Economic Geology* v. 97, p. 241–267.
- McClernan, H.G., 1983, Metallic mineral deposits of Lewis and Clark County, Montana: *Montana Bureau of Mines and Geology Memoir* 52, 72 p.
- Olson, N.H., Sepp, M.D., Dilles, J.H., Mankins, N.E., Blessing, J.M., and Scarberry, K.C., 2017, Geologic map of the Mount Thompson 7.5' quadrangle, southwest, Montana: *Montana Bureau of Mines and Geology EDMAP-11*.
- Robb, W., 2016, Madison project located in Madison County, Montana: unpublished 43-101 Technical Report prepared for Carolina Capital Corp., 64 p.
- Rusk, B.G., and Reed, M.H., 2008, Fluid inclusion evidence for magmatic-hydrothermal fluid evolution in the porphyry copper-molybdenum deposit at Butte, Montana: *Economic Geology* v. 103, p. 307–334.

- Scarberry, K.C., 2016, Geologic map of the Sugarloaf Mountain 7.5' quadrangle, Deer Lodge, Jefferson, and Powell Counties, MT: Montana Bureau of Mines and Geology Open-File Report 674, 1:24,000 scale.
- Sillitoe, R.H., Graubeger, G.L., and Elliott, J.E., 1985, A diatreme-hosted gold deposit at Montana Tunnels, Montana: *Economic Geology* v. 80, p. 1707–1721.
- Simmons, S.F., White, N.C., and John, D.A., 2005, Geologic characteristics of epithermal precious and base metal deposits, *in* Hedenquist, J.W., Thompson, J.F.H., Goldfarb, R.J., and Richards, J.P., eds., *Economic Geology one hundredth anniversary volume: Society of Economic Geologists*, p. 485–522.
- Smedes, H.W., 1962, Lowland Creek Volcanics, an upper Oligocene formation near Butte, Montana: *Journal of Geology*, v. 70, p. 255–266.
- Smith, R.L., 1960, Ash flows: *Geological Society of America Bulletin*, v. 71, p. 795–842.
-



MBMG's Economic Geologist Stan Korzeb (left) at the Madison Au-Cu-Ag skarn at Silver Star, MT. Photo by K. Scarberry, MBMG.

The Black Butte Copper Deposits, Central Montana: Their Geology and Development

Jerry A. Zieg

Stratabound pyritic zones in shale of the Newland Formation within the lower Belt Supergroup contain important copper deposits near Black Butte, Meagher County, Montana (fig. 1). These unusual sediment-hosted copper deposits formed in a deep water hot springs sedimentary exhalative setting along the northern margin of the Middle Proterozoic ‘Belt’ sea. The copper deposits occur in part of an extensive synsedimentary hydrothermal field which covered an area of at least 15 miles by 5 miles, and hydrothermal activity persisted during deposition of at least 1 kilometer of Newland shale and carbonate. The hydrothermal activity introduced large volumes of iron and smaller volumes of copper, cobalt, lead, zinc, silver, gold, barium, and strontium into basin muds. Widespread sulfide concentrations at some stratigraphic levels show evidence of increased syndepositional slumping of local sedimentary units, suggesting a tie between increased hydrothermal activity and major faulting events that accommodate basin subsidence. Sulfide zones occur at the base of the Newland Formation and persist up stratigraphic section for approximately 3,500 feet into its upper part. Hydrothermal activity appears focused at the interplay between an east–west-trending basin margin fault zone and a northeast-trending structural zone coincident with the Great Falls Tectonic Zone.

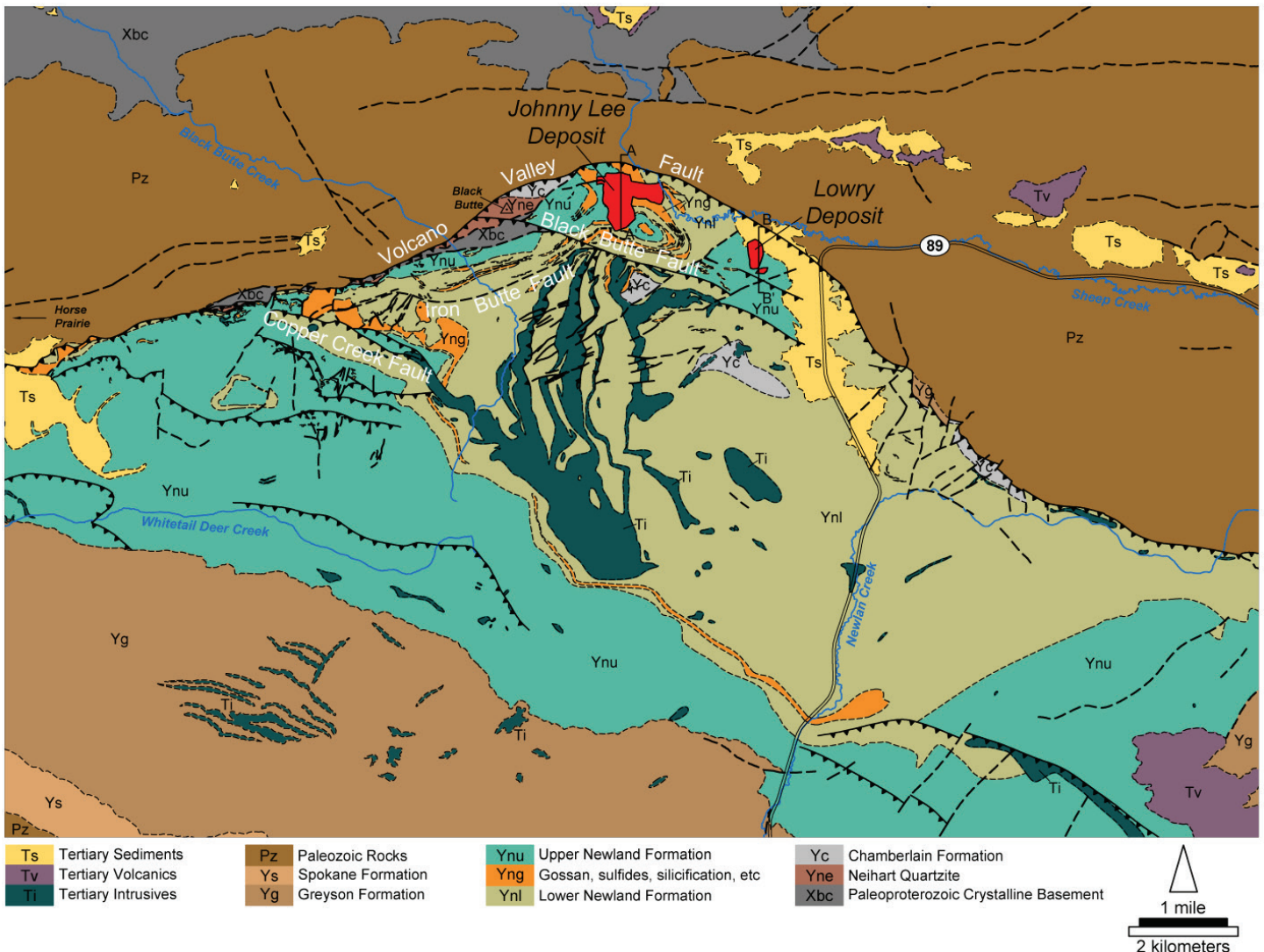


Figure 1. Geologic map of the Black Butte Copper Project area, Meagher County, Montana.

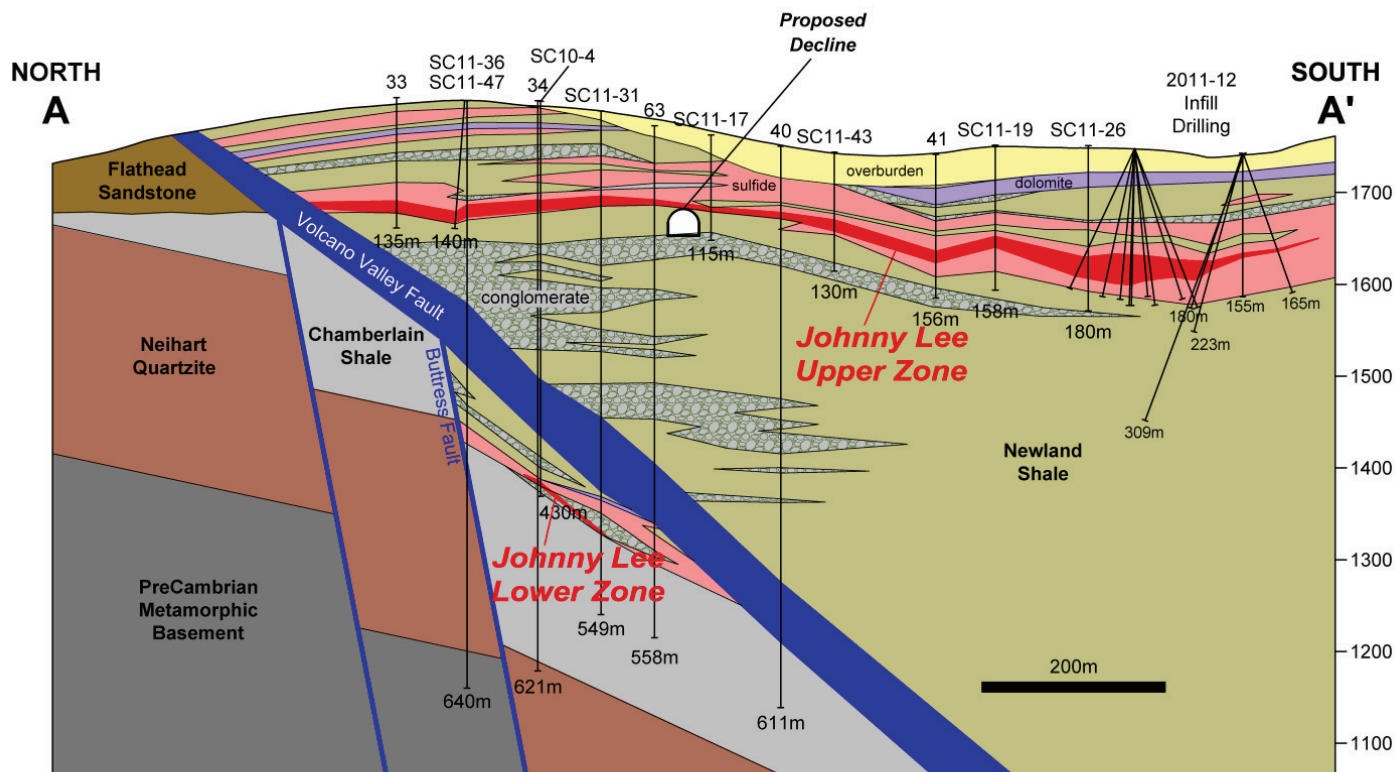


Figure 2. Geologic cross section through the Johnny Lee deposit, Black Butte Copper Project, Meagher County, Montana.

Cominco American Inc. and new joint venture partner BHP Ltd. discovered the Johnny Lee copper deposit (fig. 2) in 1985 after Cominco had completed 9 years of exploration in the district. After Cominco defined the initial resource, entirely on private lands, they abandoned the property in 1995. Tintina began drilling in 2010 and has outlined an indicated and measured resource of 1.18 billion pounds of copper and 35.6 million pounds of cobalt in 15.7 million tonnes grading 3.4% copper and 0.1% cobalt. The copper resource consists of three separate zones of mineralization: the upper and lower zones of the Johnny Lee deposit, and the Lowry deposit (fig. 3). The Johnny Lee deposit copper resource consists of 11.6 million tonnes grading 3.6% copper, with its upper zone grading 2.8% Cu and its lower zone grading 6.4% Cu. The copper resource consists of primarily chalcopyrite, with small amounts of tennantite, bornite, and chalcocite, in a bedded pyrite host rock. Barite is a significant component of the resource, and a geological resource of 19 million tonnes with 50% barite overlies and overlaps with the Johnny Lee upper copper zone resource. The entire Johnny Lee upper sulfide zone, including the copper and barite zones, contains 106 million tonnes of 29% pyrite. The Lowry deposit lies approximately 1 mile east of the Johnny Lee deposit and consists of an indicated resource of 4.1 million tonnes grading 2.9% Cu.

Tintina is planning an underground cut-and-fill mining operation for the Johnny Lee deposit, and will utilize a 5,000-foot access ramp to keep all surface activities well away from Sheep Creek. The anticipated mining and milling of 3,300 tonnes per day will result in production of about 400 tonnes of copper concentrate per day. About 45% of the mill tailings will return underground as paste backfill, and the remainder will slurry as a lightly cemented paste into a double-lined surface storage impoundment where it will air dry and harden. All waste rock will also occupy the central tailings impoundment. All water encountered onsite will receive reverse osmosis water treatment and will return to the groundwater system via underground infiltration galleries, buried below frost zone, in areas with high bedrock percolation rates. No water will be discharged into surface waters. Reclamation includes covering the hard, dry cemented mass of surface tailings with a liner that will be welded to the lower double liner to totally encapsulate the tails, after which they are buried. The cemented tailings facility, after reclamation, becomes 75 acres of pasture land. Tintina's mining and reclamation plan is designed to surpass all water non-degradation standards and statutory levels for water quality and volume and

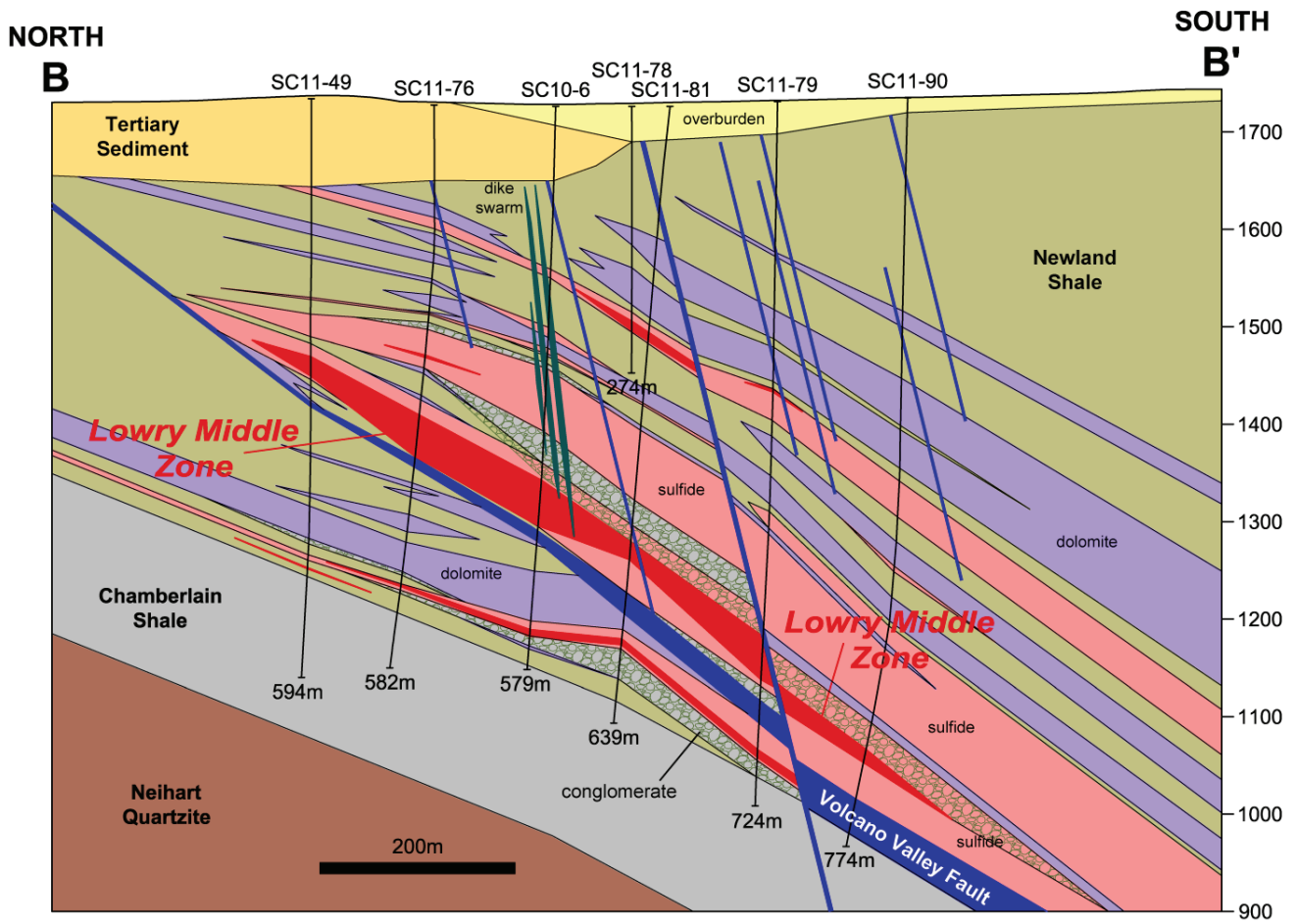


Figure 3. Geologic cross section through the Lowry deposit, Black Butte Copper Project, Meagher County, Montana.

to have no adverse effects on water quality or quantity. Upon reclamation, 100% of the mine property surface area will return to its historic use of cattle grazing. In December 2015, Tintina submitted to the Montana Department of Environmental Quality (DEQ) an application for a mine operating permit for the Johnny Lee deposit. On August 14, 2017, the DEQ declared Tintina’s permit application ‘complete and compliant.’ Following this, the DEQ will issue a draft mine operating permit and will begin a year-long Environmental Impact Study (EIS), after which they can issue a final mine operating permit.



Hedenbergite ($\text{CaFeSi}_2\text{O}_6$) crystals on the underground walls at the Madison Au-Cu-Ag skarn at Silver Star, MT. Photo by A. Roth, MBMG.



Chalcantite ($\text{CuSO}_4 \cdot 5\text{H}_2\text{O}$) crystals on the underground walls at the Madison Au-Cu-Ag skarn at Silver Star, MT. Photo by A. Roth, MBMG.

Petrology and Mineralogy of the Mount Rosa Complex, El Paso County, Colorado

Philip M. Persson

Colorado School of Mines, Fort Collins, Colorado

The ~1.08 Ga Pikes Peak Batholith is a type example of anorogenic (A)-type granite and host to numerous late-stage sodic and potassic plutons, including the Mount Rosa Complex (MRC) (fig. 1), composed of early peraluminous and later peralkaline rocks. The MRC is located ~15 km west of Colorado Springs in Central Colorado. The MRC is composed of Pikes Peak biotite granite, fayalite-bearing quartz syenite granitic dikes, Mount Rosa Na-Fe amphibole granite, mafic dikes that range from diabase to diorite, and numerous rare earth element (REE) and other high field strength element (HFSE; e.g. Th, Zr, Nb) rich Niobium–Yttrium–Fluorine (NYF)-type pegmatites. Field work, petrography, SEM-based methods, whole-rock geochemistry, and electron probe micro-analysis (EPMA) of micas were performed on all rock units to determine their textural, mineralogical, and geochemical characteristics. These data are used to trace the magmatic evolution of the MRC and better understand HFSE enrichment processes within the MRC.

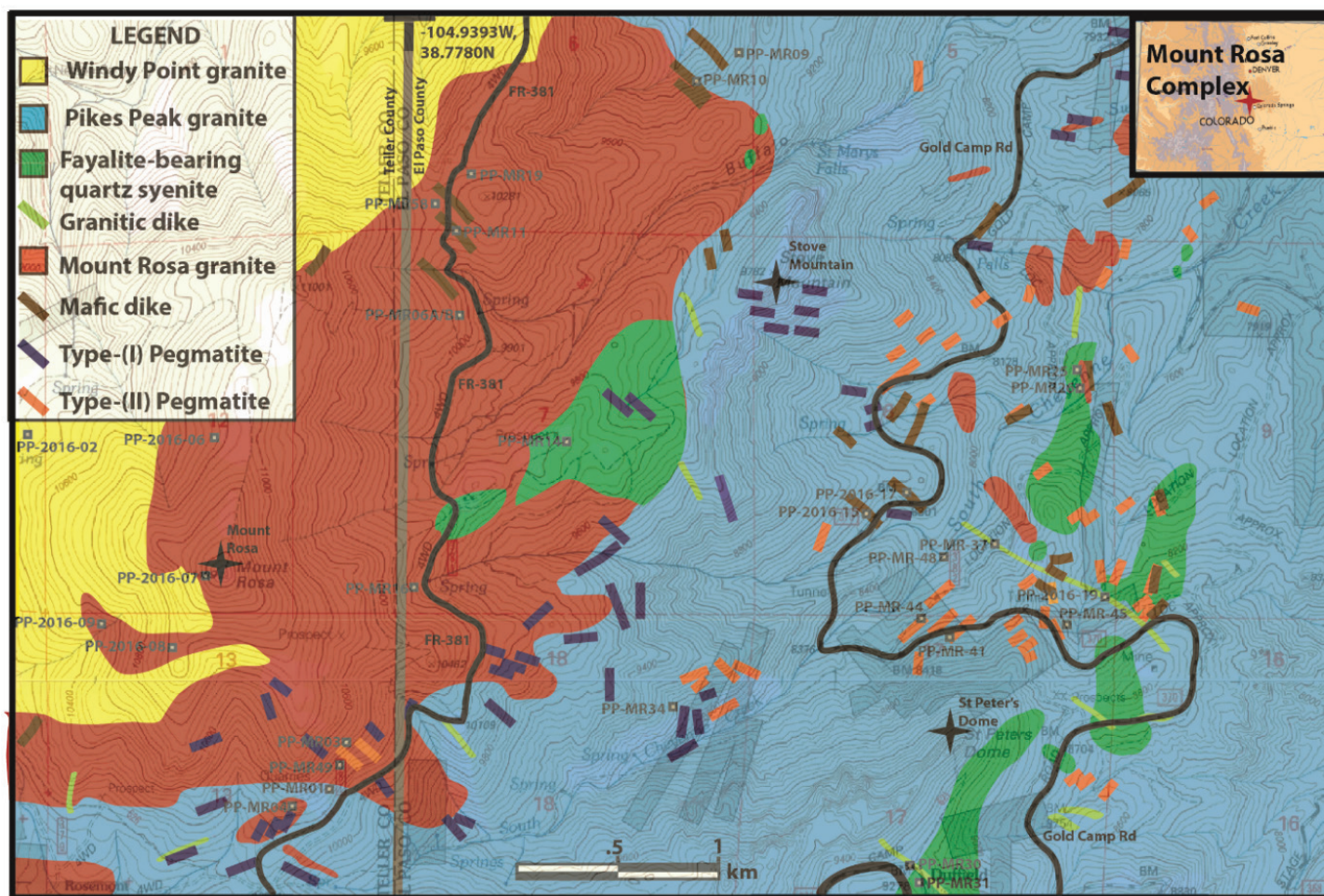


Figure 1. Geologic map of the Mount Rosa Complex (mapping by Gross, 1962, Keller and others, 2005, and Persson, 2014–2016).

Early plutons, such as the Pikes Peak biotite granite and fayalite-bearing quartz syenite, are peraluminous and contain annite–siderophyllite micas with high Fe/(Fe + Mg) ratios (fig. 2). These plutons show relatively minor enrichments in REE and other HFSE compared to primitive mantle. Later peraluminous granitic dikes, which form a crude radial geometry around the inferred intrusive center, contain Al-rich siderophyllite mica (fig. 2), and are relatively depleted in HFSE. Sill-like bodies, blobs, and dikes of the peralkaline Mount Rosa Na-Fe amphibole granite are mineralogically and texturally variable. The amphibole granites have large pegma-

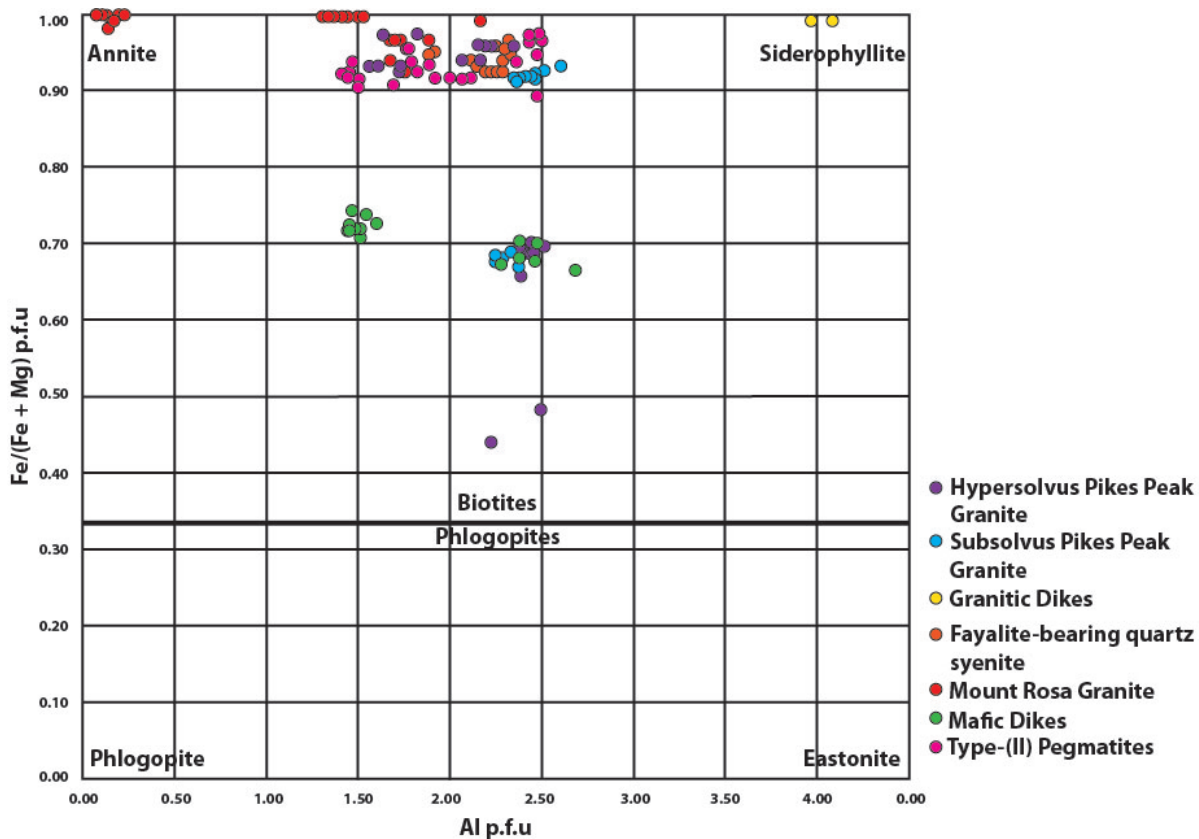


Figure 2. Compositional variation in analyzed MRC biotites after Deer and others (1962).

titic areas and coarse and fine-grained enclaves. End-member annite (fig. 2) is enriched in Na, K, and F, and the Mount Rosa granite is enriched in REE and other HFSE compared to primitive mantle and older rock units.

Biotite in mafic dikes is Mg-rich compared with biotite from other MRC rocks (fig. 2). These mafic dikes show strong whole-rock enrichment in REE, Zr, and other HFSE. While Type-(I) pegmatites are mineralogically simple with irregular contacts, Type-(II) pegmatites are mineralogically complex and have sharp intrusive contacts. Samples from a transect across an 80-cm-thick, zoned Type-(II) pegmatite show low F + Cl contents in biotite near the contact zone (0.30 a.p.f.u. Cl + F), and increasing concentration of F + Cl in micas towards the core. Biotite from the wall zone is geochemically similar to the Mount Rosa granite and contains 2.5 a.p.f.u. F + Cl. Polyolithionite–trilithionite from the core zone is associated with cryolite (Na_3AlF_6) pods, fluorite, and arfvedsonite pseudomorphs and has extremely high concentrations of F + Cl (up to 7.0 a.p.f.u.)

Early units such as the Pikes Peak granite, fayalite-bearing quartz syenite, and granitic dikes have similar parental melts to the Pikes Peak Batholith. However, the Mount Rosa granite, with its peralkaline chemistry and textural and mineralogical heterogeneity, may have formed from separation of a late immiscible peralkaline melt during magmatic evolution of the MRC. Mafic dikes have characteristics of the early peraluminous units (Pikes Peak granite and quartz syenite), such as P and Ba enrichments and mineralogy. The mafic dikes also share qualities of later peralkaline units (Mount Rosa granite, Type-(II) pegmatites), such as enrichment in Zr and REE, an abundant fluorite and albite content, and a less clear petrologic relationship to the parental melts of the Pikes Peak and Mount Rosa granites. Pegmatites are interpreted as the final melts after the Mount Rosa Na-Fe amphibole granite crystallized.

Three major alteration events were observed at the MRC: (I) early albitization that is most intense around the Mount Rosa granite; (II) an acidic aegirization/hematization stage that replaced Na-Fe amphibole with aegirine, and mafic silicates with Fe oxides; and (III) hydrothermal Ca-F metasomatism that altered magmatic minerals through Ca-F replacement (fig. 3). In this final stage, incompatible elements were likely re-mobilized by late F-rich fluids that precipitated REE fluorocarbonates minerals and hydrothermal zircon in Type-(II) pegmatites.

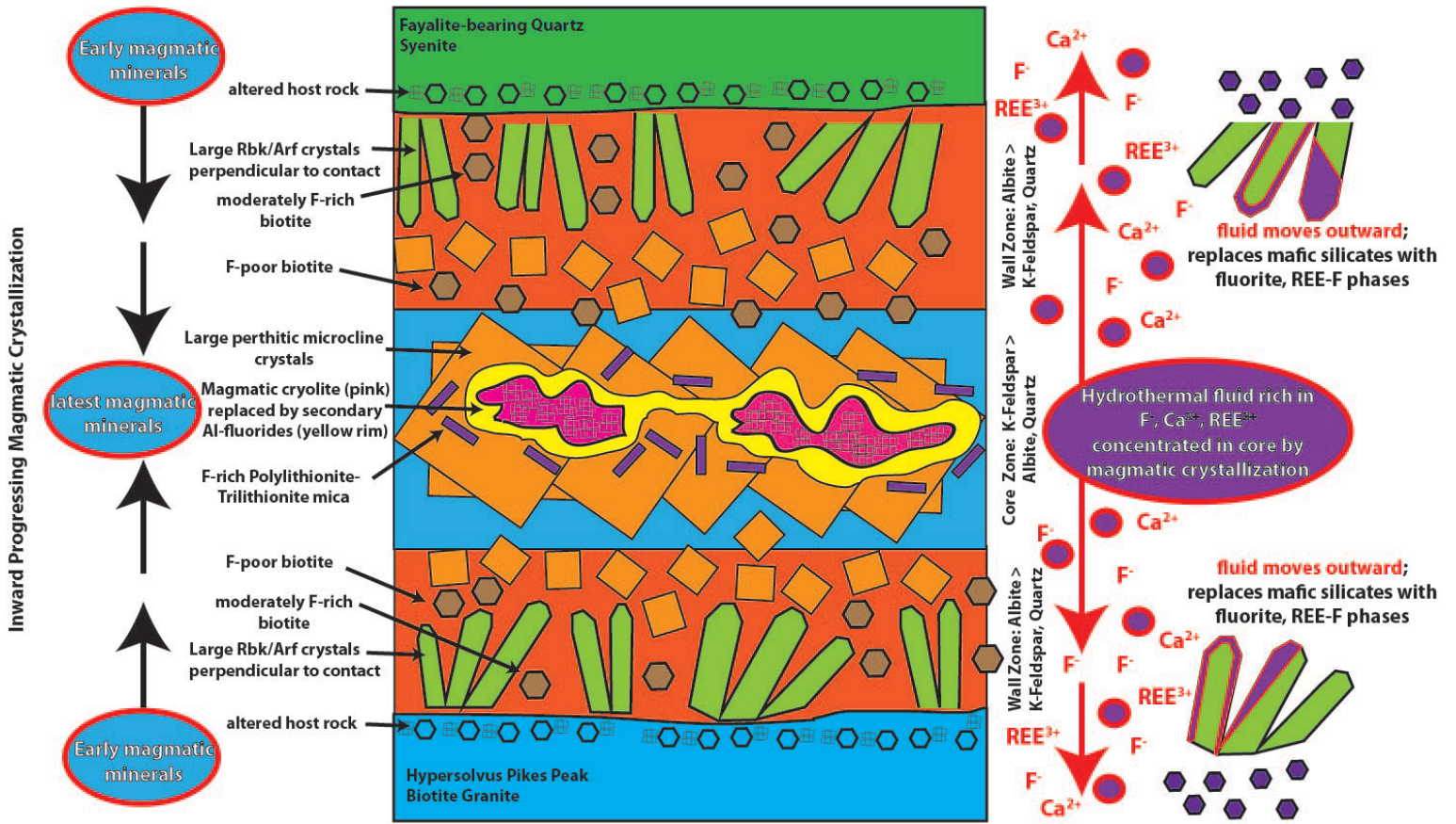
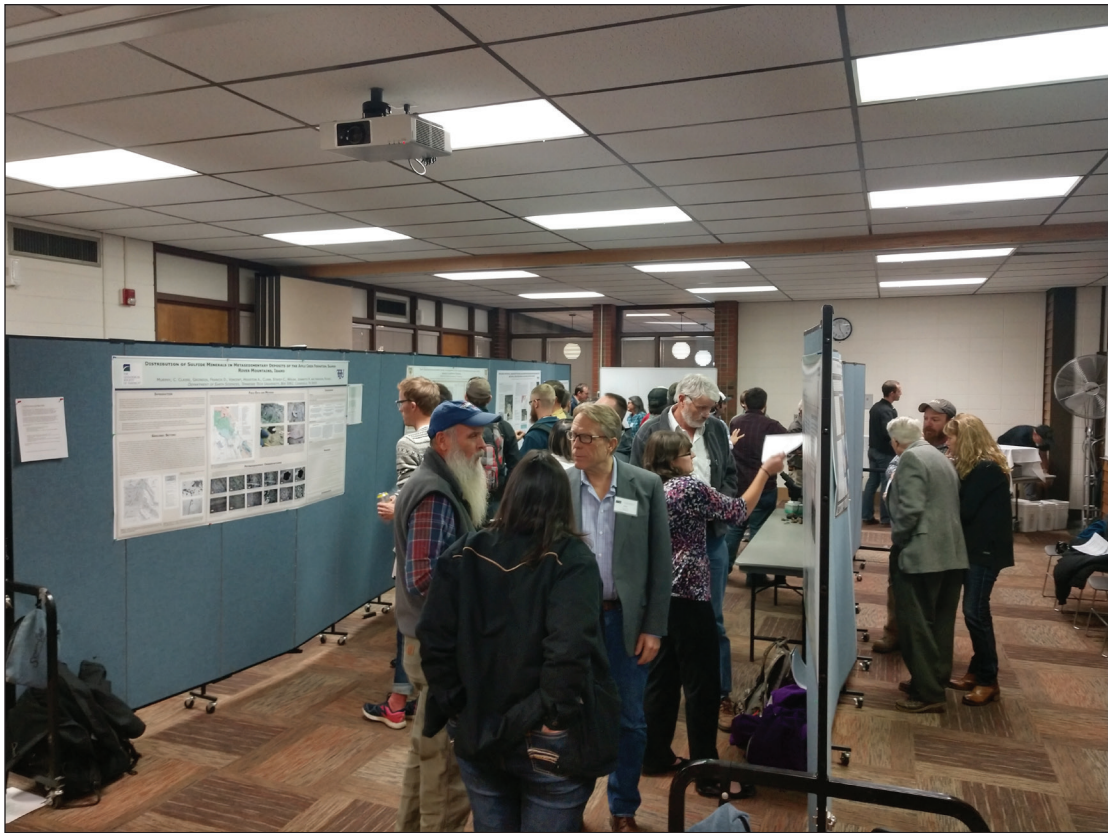


Figure 3. Schematic cartoon of Type-(II) pegmatite crystallization and mineralogy.



Conference participants at the student poster session. Photo by A. Roth, MBMG

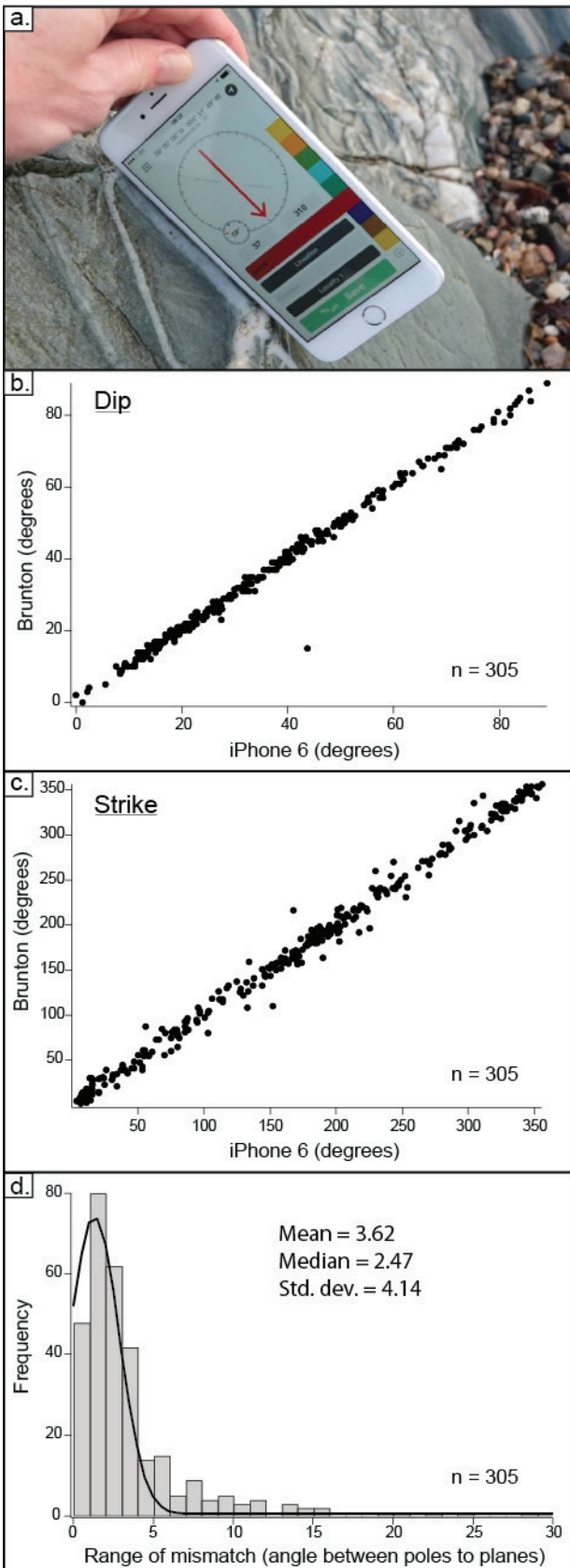


Colorado School of Mines M.S. graduate Philip Persson (right center) at the Golden Sunlight Mine north of Whitehall, MT. Photo by A. Roth, MBMG.

Using Your Smartphone for Field Work

Jesse G. Mosolf

Montana Bureau of Mines and Geology



Mobile devices have become nearly ubiquitous, and an increasing number of geoscientists use smartphones to collect field data. Smartphone applications (apps) have emerged for iOS, Android, and Windows platforms that make it easier than ever to navigate and collect field data. This abstract provides documentation of some current smartphone hardware and apps that may be useful to the field scientist.

Smartphones truly are all-in-one devices. They are equipped with an internal GPS receiver, a high-resolution camera, cellular phone, inclinometer, compass, and an easy-to-use touch screen. GPS accuracy with a smartphone is usually less than 4 m, but submeter resolution is possible when it is paired with an external Bluetooth GPS receiver (e.g., Bad Elf GNSS Surveyor). Smartphone cases that protect against adverse field conditions are available and some contain a compact external battery that increases power capacity between charges. Smartphones can be charged easily using either the 12V outlet in a field vehicle, or a packable solar panel (e.g., Goal Zero Venture 30) if working off-grid during multi-day field excursions.

Smartphone GPS apps share similarities with software interfaces on dedicated handheld GPS devices; however, apps like Gaia and Avenza Maps generally have more features and are easier to use. The Gaia app can download topographic basemaps and satellite imagery for navigation outside of wireless networks, and can record waypoints, create routes, and geotag photographs. The Avenza Maps app reads geospatial PDF, GeoPDF, and GeoTIFF maps that are exported from ArcGIS or web-mapping services (e.g., CalTopo). These features allow the operator to view their location on a georeferenced map of choice (e.g., a previously published geologic map), record GPS tracks, and add place marks. Cadastral information can be viewed and queried using the onX Hunt app, aiding the navigation of public lands checker boarded with private lands.

Apps such as Collector for ArcGIS, and Fieldmove Clino by Midland Valley, are tailored for collecting field data. Collector can visualize, collect, query, and edit GIS datasets (points, lines, areas, and related data). The user can design and implement custom data collection forms, making Collector

Figure 1. (A) Gathering structural data in the field using an iPhone equipped with Field Move Clino. Photo courtesy of Midland Valley. (B and C) Dip and strike measured by a Brunton Geo versus an iPhone 6 for 305 unique planes. (D) Histogram of the angular mismatch of poles to planes between phone and pocket transit for each of the paired measurements shown in (B) and (C).

a useful tool for a wide range of field applications. Fieldmove Clino is specifically designed for field geology and uses the smartphone's internal GPS, inclinometer, and compass to rapidly acquire point, line, and plane data. While structure data collected using Fieldmove Clino on Android devices has been reported to be inaccurate (Novakova and Pavlis, 2017), over 300 plane measurements collected with Fieldmove Clino on an iPhone 6 reported here are nearly indistinguishable from those collected using a Brunton pocket transit (fig. 1). This result corroborates recent findings by Allmendinger and others (2017) who suggested that Apple iOS devices are suitable for the collecting field data. Fieldmove Clino also boasts digital mapping capabilities that are useful for mapping features readily viewed in remotely sensed imagery. Data collected in Fieldmove Clino are easy to export into ArcGIS and Move desktop, and can also be exported as kmz files to view in Google Earth. GIS data and geospatial files used by various smartphone apps can be organized and managed in the Dropbox app, permitting the user to access saved basemaps and geodatabases, and to regularly back up field data when in range of the wireless network.

Smartphones equipped with the apps discussed above and many others, too numerous to review here, greatly improve work efficiency and productivity in the field, and will likely become a staple in the future geoscientist's field kit.

References

- Allmendinger, R.W., Siron, C.R., Scott, C.P., 2017, Structural data collection with mobile devices: Accuracy, redundancy, and best practices: *Journal of Structural Geology*, v. 102, p. 98–112.
- Novakova, L., Pavlis, T.L., 2017, Assessment of the precision of smart phones and tablets for measurement of planar orientations: A case study: *Journal of Structural Geology*, v. 97, p. 93–103.



MBMG field geologist Jesse Mosolf. Photo by A. Roth, MBMG.

Nature of the Mineralization and Alteration Mapped at the Clementine Porphyry Copper Prospect in the Northern Pioneer Mountains of Southwest Montana

George H. Brimhall* and Bruce D. Marsh

Clementine Exploration LLC, Wise River, Montana

**Speaker, Principal Geologist and Managing Member*

A regional genetic model for the origin of linear belts of porphyry Cu-Mo deposits, including the giant deposits at Butte, Montana, Bingham Canyon, Utah, and a spectrum of smaller geochemically varied intrusion-related (Au, Ag, Cu, W, and Mo) deposits, occurring southwest of Butte within the Pioneer Mountains, led to the discovery of a new zone of alteration and mineralization at the Clementine prospect. Southwest of Butte, a linear belt of historic mining districts with a regular spacing of about 7 km extends through the Pioneer Mountains from Beal Mountain on the north and Bannack on the south end. These ore deposits, including the Quartz Hill, Cannivan Gulch, Hecla, Argenta, and Bannack Districts, many of which are localized within dome structures, occur along a single north-south-trending regional anticlinal hinge of the frontal (easternmost) anticline of the Cordilleran fold and thrust belt of Sevier (Late Cretaceous) age. Regional interpretation, combined with new geological mapping, integrates structural, magmatic, and hydrothermal processes into a set of numerical process-based models consistent with an idealized east-west cross section published by Kalakay and others (2001). Taken altogether, these observations address problems associated with syncompressional pluton emplacement centered on the need to make room for magma in environments where crustal shortening, not extension, occurs on a regional scale. Finite element modeling (Nemcok and Henk, 2006) of an analogous fold-and-thrust belt explored for oil in the Western Carpathians Mountains of Romania showed the existence of an overall mean stress decrease inside the thrust sheet anticlines. Our interpretation asserts that in southwest Montana similar thrust sheet anticlines were also the loci of magma ascent, mineralization, and alteration processes in syncompressional environments at the top of frontal thrust ramps where “releasing steps” at ramp tops served as initial points of emplacement, subsequent pluton growth, and exceptional levels of chemical differentiation within underlying laccoliths. Besides facilitating magma ascent, these localized lower pressure zones may also provide a mechanism for raising the probability of inducing magmatic water saturation, driving magmatic-hydrothermal mineralization, and thus explaining the ubiquitous mineralization and alteration of many of the plutons in the Butte-Pioneer Mineral Belt as defined by Brimhall and Marsh (2014).

Besides the commonality of magmatic water saturation in the ore-forming plutons, we also propose here a mechanism that explains the regular spacing of mining districts, a theme that has been fundamental in focusing our fieldwork leading to geological discoveries at Clementine. From aerially extensive buoyant ribbon-like layers presumably existing at depth along thrust fault flats, our calculations show diapiric ascent occurring at a regular spacing determined by Rayleigh-Taylor gravitational fluid (magmatic) instabilities. Ascent of magma up along thrust ramps into the anticlinal hinge zone supplies an additional component of hydrostatic head that pushes the melt up-dip, which feeds the diapir more easily, allowing it to rise more quickly from the source and hence escaping solidification. In the absence of diapiric ascent, magmas would otherwise tend to rapidly cool and crystallize essentially in place, lacking enough thermal inertia to remain liquid in the form of a dike or sill.

Using our regional exploration model with both its regional structural and magma self-organizational aspects, we recognized a gap between the Beal Mountain and Quartz Hill Districts. Consequently, we focused our fieldwork on the former Divide District, which had no prior history of metal production but occurs at a suggestive spacing with an associated anticlinal fold. While mapping in densely forested areas using digital mapping methods (Brimhall and Vanegas, 2001; Brimhall and others, 2002, 2006) within a nappe window into the Lewis Over-Thrust, Clementine Exploration LLC discovered a mineralized syntectonic frontal thrust fault-bend anticline surrounded by an orbicular alteration pattern similar to alteration in the contact aureole at Carr Fork, Bingham, Utah, described by Atkinson and Einaudi (1978), with the exception that instead of actinolite lining the orbicules, Clementine has chlorite and muscovite, at least on the surface (fig. 1A). At Clementine, this

orbicular chlorite-muscovite wall rock alteration with minor disseminated chalcopyrite, pyrrhotite, and ilmenite on the eastern edge of the zone, occurs within the Cretaceous Kootenai and Blackleaf Formations and is the outermost manifestation of discernable hydrothermal activity and chemical metasomatism related to mineralization processes farther inside the Clementine anticline. On the west side of the anticline, the orbicular zone extends northeastward more than 3 km and on the east side, 2 km away, it extends at least 2.3 km northeastward, but the exposure there is considerably worse and removed by a granitic pluton intruding the sedimentary section along the entire east side of the anticline. On the east side of the anticline, the orbicular zone has linings of biotite and muscovite rather than chlorite and muscovite, which we interpret as either a metamorphic overprint by the adjacent granite pluton to the east or additional heat supplied by that pluton that raised the local temperature (figs. 1B, 1C). On the western edge of this orbicular zone, minor chalcopyrite, pyrrhotite, and ilmenite occur as a mirror image of the same zonation across the Clementine anticline on the western flank of the fold axis. The importance of the size of the orbicular alteration zone in the context of exploration is important in at least two ways: (1) the extensive aerial alteration footprint indicates that the magmatic-hydrothermal system inside the anticline may be large, possibly very large, and (2) a potential exists for copper skarn mineralization as at Carr Fork.

While we believe that Butte, Bingham Canyon–Carr Fork, and Clementine all formed as part of the Sevier thrust and fold structure, important differences exist locally in relation to district scale structure and differential interaction with reactive wall rocks. We see a spectrum of petrologic effects with Butte at one end with the homogeneous Butte Granite wall rock and Clementine on the other, dominated by differential reaction with Paleozoic through Cretaceous sediments formed on a Passive Tectonic margin. At Butte, the early high temperature pre-Mainstage wall rock alteration is biotitization of igneous hornblende and replacement of sphene by rutile and anhydrite (Roberts, 1973). Once the east–west-striking porphyry dikes intruded the Butte granite, a dense fracture network developed and free convective flow circulated within the fractured volume of rock affected by biotitization of hornblende. In contrast, fluid flow at Clementine was confined by both the syntectonic frontal thrust fault-bend anticline in the foot wall of the Grasshopper Thrust plate and the overlying hanging wall Missoula Group Belt series sediments.

We think that this confined flow led to superheating of the aqueous fluids. The hydrothermal system and underlying magmatic heat source were capped by impermeable rock such that the solutions could not establish a large regional network and undergo pervasive systematic cooling as happened at Butte. We view the axially symmetric orbicular alteration zones, beyond the next inner zone of vein/fracture fillings, as representing an advancing reaction front for supersaturated solutions expressed as orbicular growths just outside of an advancing skarn zone, where the main reactive carbonate members were encountered. The orb zone represents the outer reaches of the Reaction Front of the ‘Supersaturated’ solution, and now represents the arrested develop-



Figure 1. (A) Orbicular wall rock alteration consisting of chlorite and muscovite-lined orbs up to about 1-inch diameter also containing sparse disseminations of chalcopyrite, pyrrhotite, and ilmenite. Sample from the west side of the Clementine anticline along the Indian Creek Road. (B) Orbicular wall rock alteration consisting of muscovite and biotite-lined orbs up to about 0.5-inch diameter. Brown circles are oxidation effects where ferrous iron contained in pyrrhotite, ilmenite, and chalcopyrite escaped from the primary mineral hosts, diffused a short distance where it was fixed by oxidation in a ferric mineral state. Sample from the east side of the Clementine anticline north of US Forest Service Road 8486 near where a large granitic body intrudes the entire east flank of the Clementine anticline and may be responsible for either a higher ambient temperature of orbicular wall rock alteration or alternatively, later thermal metamorphism of a chlorite-muscovite assemblage in orbicules to a muscovite-biotite assemblage. (C) Vein-type wall rock alteration. Veinlets of biotite and muscovite appear to stream away from clotted mineral centers.

ment of the outward migration of the front, or, alternatively, it represents the point where the outward migrating fluid lost its ‘supersaturation’ or highly reactive condition. At Carr Fork (Atkinson and Einaudi, 1978), an Early Stage of contact metasomatism produced: diopside in quartzite and in interbedded, thin silty limestone beds; wollastonite, with minor idocrase (vesuvianite) and garnet, in thick cherry limestone; and a trace amount of sulfides. Actinolite alteration of diopside in quartzite and garnetization of wollastonite-bearing marble represent the beginning of Main Stage mineralization and are time equivalent with biotite-orthoclase alteration of igneous rocks. At Clementine, while we have not yet recognized wollastonite, we have mapped extensive strike lengths of disseminated Fe- sulfides associated with the orbicular zone near the adjacent outer skarn front, making the mappable genetic parallels with Carr Fork fairly close.

At Clementine, the orbicular alteration zone surrounds a hornfels zone with a large elliptical breccia complex more than 2 km long, north to south and 0.5 km wide east to west, cross cutting the axial plane of the regional anticline where Madison limestone is exposed. Positioned exactly at the apex of the doubly plunging anticline is a set of mineralized vein gossans extending over a strike length of 0.6 km cutting the breccia and also consisting of breccia fragments with a mineralized matrix. The iron content of the vein gossans varies between 2 and 35 weight percent. We interpret the gossans as oxidized equivalents of primary vein sulfide assemblages. Multi-element assays show a regional zoning pattern in the vein system discovered. Nearest the Madison limestone on the north end, the existing metal suite consists of tungsten, antimony, gallium, germanium, and rhenium, whereas away from the Madison and towards an exposed pluton on the south end, the metal suite is distinctly different and consists of: copper, silver, gold, molybdenum, zinc, lead, and tellurium. Arsenic occurs throughout the vein system, implying that copper sulfides at depth may be analogous to Butte where tennantite occurs in the Intermediate Mainstage Zone and enargite in the Central Zone where a higher sulfidation stage existed with advanced argillic alteration. The porphyry–copper geochemical signature clearly indicates that the Clementine prospect is NOT a Stibnite Idaho Yellow Pine type gold deposit nor a Beal Mountain sediment-hosted gold system. Instead, we interpret the zoned vein gossan geochemistry as most likely representing the upper reaches of a porphyry–copper deposit influenced chemically on its margins by reactive carbonate wall rocks, much like a Cordilleran polymetallic deposit of the South American Andes.

Finally, discovery this summer of maroon hematite, “live” limonite in the copper, silver, gold, molybdenum, zinc, lead, and tellurium vein zone helps considerably in target definition and effective use of field time. Using an Olympus “Delta” hand-held XRF unit, we could acquire semi-quantitative chemical data far in advance of assays, thus adapting our mapping strategy in real-time. The mineralization we seek, then, is a deep, large underground copper metalloid mining target without the environmental burden of handling and emplacement of voluminous waste rock necessary in open pit mining dictated by high stripping ratios. Conversely, an underground mine specifically developed to minimize the environmental foot print could meet the challenge of a modern 21st Century underground mine in Montana, deserving of a social license for mining with production of copper and critical metalloid semi-conductor byproducts that could help support a sustainable energy future.

References

- Atkinson, W., and Einaudi, M.T., 1978, Skarn formation and mineralization in the contact aureole at Carr Fork, Bingham, Utah: *Economic Geology*, v. 75, p. 1326–1365.
- Brimhall, G.H., and Vanegas, A., 2001, Removing science workflow barriers to adoption of digital geological mapping by using the GeoMapper Universal program and Visual User Interface, *in* D.R. Soller, ed., *Digital mapping techniques’01—Workshop proceedings: U.S. Geological Survey Open File Report 01-223*, p. 103-114, <http://pubs.usgs.gov/of/2001/of01-223/brimhall.html>.
- Brimhall, G.H., Vanegas, A., and Lerch, D., 2002, GeoMapper Program for paperless field mapping with seamless map production in ESRI ArcMap and GeoLogger for drill-hole data capture: Applications in geology, astronomy, environmental remediation and raised relief models, *in* D.R. Soller, ed., *Digital mapping techniques’02—Workshop Proceedings: U.S. Geological Survey Open File Report 02-370*, p. 141–151, <http://pubs.usgs.gov/of/2002/of02-370/brimhall.html>

- Brimhall, G.H, Dilles, J., and Proffett, J., 2006, The role of geological mapping in mineral exploration in wealth creation in the minerals industry, Special Publication 12, Anniversary Publications of the Society of Economic Geologists, p. 221–241.
- Kalakay, T., John, B.E., and Lageson, D.R., 2001, Fault-controlled pluton emplacement in the Sevier fold-and-thrust belt of southwest Montana, USA: *Journal of Structural Geology*, v. 23, p. 1151–1165.
- Nemcok, M., and Henk, A., 2006, Oil reservoirs in foreland basins charged by thrust belt source rocks; insights from numerical stress modelling and geometric balancing in the west Carpathians: *Geological Society Special Publications*, v. 253, p. 415–428.
- Roberts, S.A., 1973, Pervasive early alteration in the Butte district, Montana, *in* Guidebook for the Butte field meeting, Society of Economic Geologists, p. HH-1–HH-8.



Clementine Exploration Manager George Brimhall. Photo by A. Roth, MBMG.

Experiments on the Hydrothermal Solubility of Gold and Iron, and the Origin of Iron–Oxide–Copper–Gold (IOCG) Deposits

Christopher H. Gammons* and Nick Allin

Department of Geological Engineering, Montana Tech, Butte, Montana

**Corresponding author*

Iron–oxide–copper–gold (IOCG) deposits are a newly recognized, yet poorly understood, class of hydrothermal mineral deposits. The giant Olympic Dam deposit of South Australia is the type example and one of the largest ore deposits in the world. Other examples include Candelaria, Chile and several smaller deposits in the Cordillera of the US and Canada. By definition, IOCG deposits are iron oxide rich (hematite, magnetite, or both) with elevated gold and copper. The Olympic Dam deposit is also uranium rich. Copper typically occurs in the form of bornite or chalcopyrite, but other common sulfide minerals, such as pyrite, are usually scarce or absent. IOCG deposits are commonly brecciated, with a hydrothermal Fe-oxide matrix and a near absence of quartz veining. Ore fluids were highly saline brines with either a magmatic or basinal origin, and temperature of formation estimates range from 250°C to 450°C.

There have been few experimental studies on the high temperature solubility of hematite, which is one of the main impediments to understanding the origin of IOCG deposits. The authors are currently measuring hematite and gold solubility, and the stability of aqueous Fe(III)-chloride complexes, in acidic brines at 150 to 300°C (NSF Grant No. 1624420). Experiments conducted at Montana Tech use sealed quartz tubes and small stainless steel pressure vessels. Preliminary findings include the following: (1) the dominant form of dissolved Fe(III) in acidic brines at $T > 200^\circ\text{C}$ is FeCl_4^- ; (2) the dominant form of dissolved Fe(II) in the same conditions is $\text{FeCl}_2(\text{aq})$; (3) the solubility of hematite as FeCl_4^- increases rapidly as temperature rises above 200°C, as salinity increases, and as pH drops below 5; (4) the solubility of gold is high (> 10 ppm) near the dissolved $\text{FeCl}_4^-/\text{FeCl}_2$ redox boundary.

We propose that some IOCG deposits form when basinal brines are heated by shallow intrusions yet maintain a high oxidation state in equilibrium with hematite. Hematite is especially abundant in mid- to late Proterozoic terrestrial clastic sediments, which formed when Earth's atmosphere was oxygenated but land plants had not yet evolved. A hydrothermal fluid containing dissolved FeCl_4^- would be unusually oxidized and capable of dissolving other redox sensitive metals, such as gold, copper, and uranium. Metal precipitation would result from a temperature decrease, fluid mixing, a pH increase, or an increase in the concentration of hydrogen sulfide (e.g., by thermochemical sulfate reduction) to precipitate chalcopyrite and bornite.

Although no IOCG deposits are known to exist in Montana, a band of hydrothermal U-Th-REE \pm Au \pm fluorite deposits associated with specular hematite exists in the Bitterroot, Sapphire and Beaverhead Mountain ranges. These deposits share certain characteristics with IOCG deposits, but are notably lacking in copper.



Montana Tech Geologic Engineering M.S. graduates Jenna Kaplan (left), Sara Edinberg (center), and Kyle Eastman (right) look at rocks in the Boulder batholith near Boulder, MT. Photo by D. Herman, MBMG.



MBMG field geologist Kaleb Scarberry shares his thoughts about Boulder batholith magmatism near Boulder, MT. Photo by D. Herman, MBMG.

Exploration at the Madison Au-Cu-Ag Skarn, Silver Star, Montana

Jenna M. Kaplan

*Project Geologist, Broadway Gold Mining Ltd., P.O. Box 18, Silver Star, Montana,
JKaplan@MTech.edu*

Abstract

The Madison Mine is an Au-Cu-Ag skarn that formed at the contact of the Rader Creek granodiorite with Mississippian Madison limestone on the southeastern margin of the Highland Mountains in Silver Star, Montana (fig. 1). Mineralization occurred at the intersection of two major structural zones, the Great Falls Tectonic Zone and the Southwest Montana Transverse Zone (Perry Line). The structures are primary controls on two porphyry, skarn and gold mineralizing events that affected southwestern Montana: (1) Cretaceous (e.g., Butte, Golden Sunlight); and (2) Eocene (e.g., New World, Emigrant; Berger and others, 2011). Compelling drill targets, believed to relate to a large-scale porphyry system, have been identified at the mine based on new observations of surface geology and geophysics.

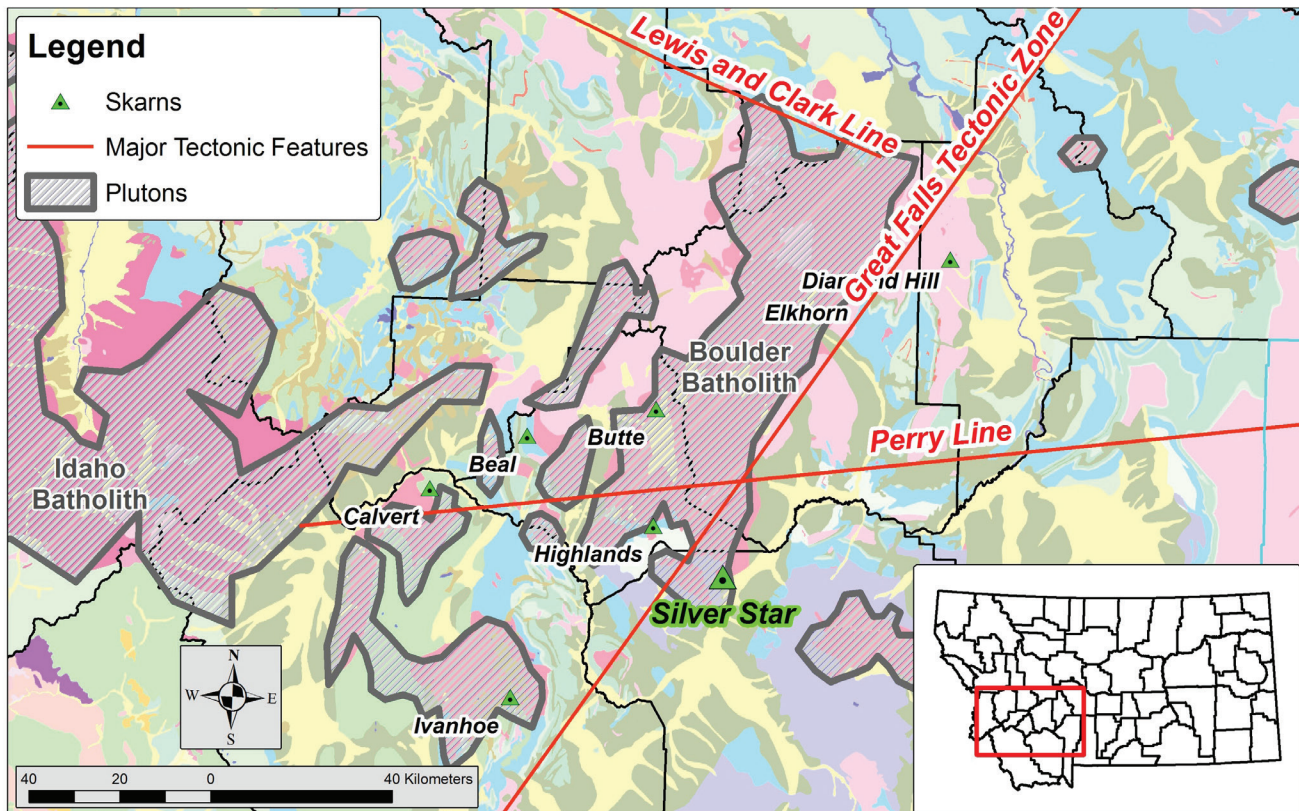


Figure 1. Regional geology and the intersection between the Great Falls Tectonic Zone and the Perry Line (Childs Geoscience, written commun., 2017).

Introduction

Geologic Setting / Skarn Mineralogy / Conditions of Mineralization

Local and regional faulting appears to have played a key role in localizing mineralization at the mine (fig. 2). Although the Au-Cu-Ag skarn developed along the intrusive contact between the late Cretaceous Rader Creek pluton and Mississippian carbonates, faults like the Silver Star Fault, a major thrust fault that places Precambrian metasedimentary rocks over younger Mississippian–Devonian sedimentary rocks, may also contain mineralization (fig. 2). Gold-bearing jasperoid occurs in addition to Au-Cu-Ag skarn mineralization at the Madison deposit (fig. 3). The primary skarn sulfide minerals are pyrrhotite, pyrite, chalcopyrite, and minor bornite. Gold occurs as electrum grains in the primary sulfides as well as in calc-silicate minerals.

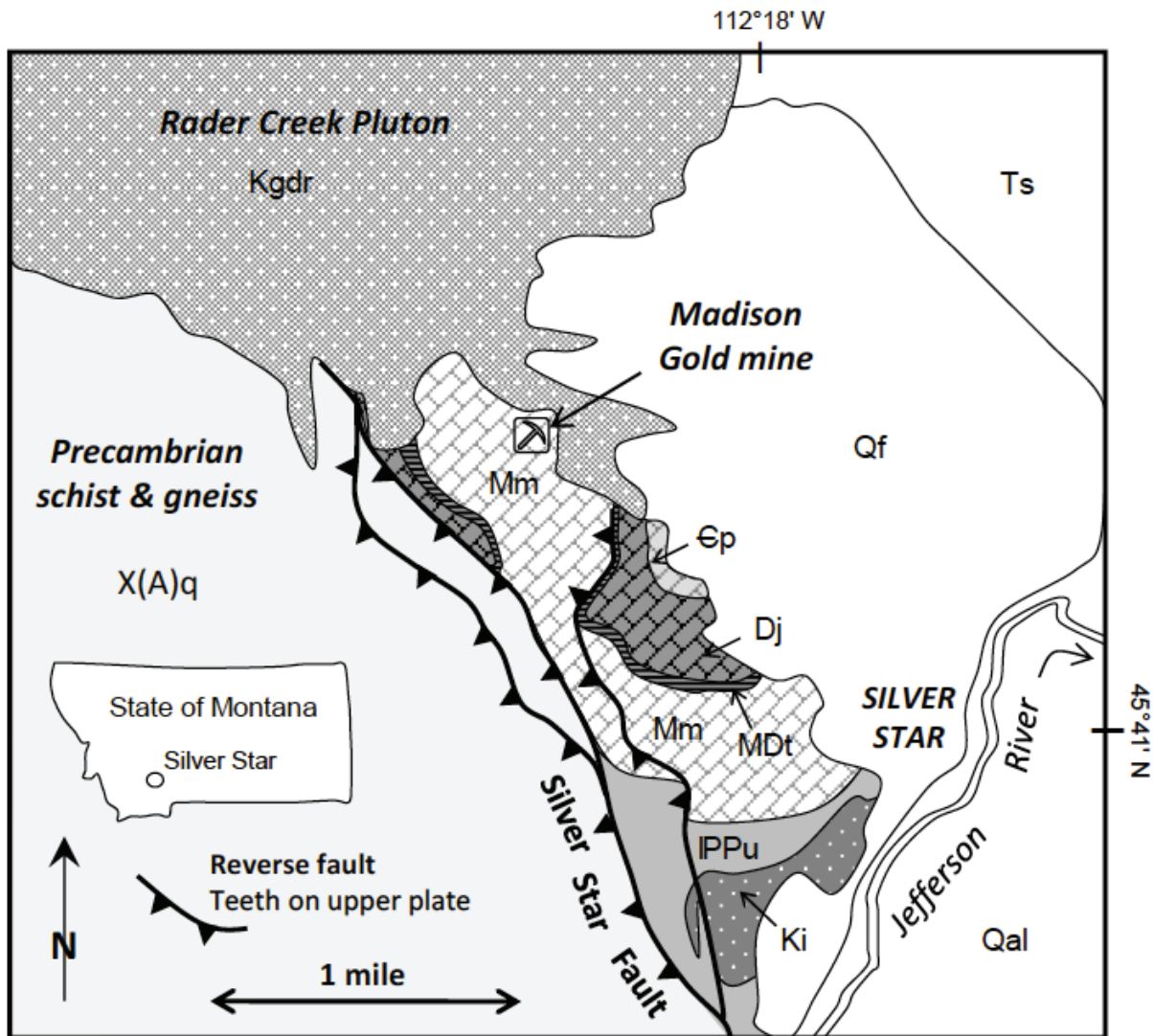


Figure 2. Generalized geologic map of Broadway Gold's claim area. Map abbreviations: X(A)q, Archean gneiss, schist, and amphibolite; Ep, Cambrian Pilgrim Fm.; Dj, Devonian Jefferson Fm.; MDt, Devonian–Mississippian Three Forks Shale; Mm, Mississippian Madison Group; IPPu, Pennsylvanian and Permian metasediments; Kgdr, Rader Creek granodiorite; Ki, smaller Cretaceous intrusions; Ts, Tertiary sediments; Qf, Quaternary alluvial fans; Qal, Quaternary alluvium (Sotendahl and Gammons, 2012).

Mineralization occurred over a wide range of temperatures (Sotendahl and Gammons, 2012). Sulfur isotope data from the skarn supports a magmatic source of S and high temperature of formation. As temperatures cooled, the skarn gangue minerals shifted from an anhydrous assemblage consisting primarily of garnet and diopside–hedenbergite, to a more hydrous assemblage consisting of phlogopite, amphibole, and chlorite. Early pyrrhotite was replaced by pyrite, which was followed by hypogene oxidation (fig. 4) that caused intense oxidation of the skarn protore to form a subcylindrical body of high-grade Au-bearing goethitic jasperoid. During this oxidation, Cu-bearing sulfides were destroyed, releasing Cu-rich fluids that replaced pyrite to form high-grade chalcocite pods.

Current Work

Exploration Drilling

The first stage of the current exploration project confirmed ore reserves from several twinned holes that were drilled the 1980s and 1990s, and defined the size and boundaries of the Au-bearing jasperoid and massive sulfide bodies more precisely (fig. 5). The next phase of drilling began in the fall of 2017 and will focus on intersections between jasper and massive sulfide (fig. 6). This phase will follow up on electromagnetic conductors, induced polarization targets, surface mapping, and soil survey anomalies and will investigate the northwest contact between the Rader Creek pluton with Mississippian limestones as a potential Cu-porphyry target (fig. 7).

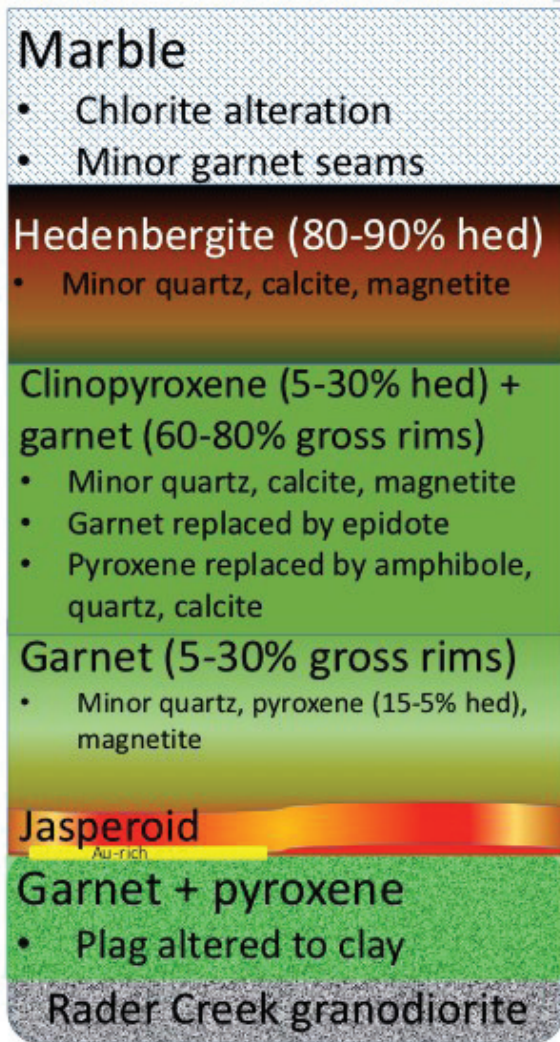


Figure 3. A model of the Madison deposit based after Foote (1986). Hed, hedenbergite; gross, grossular (J. Zimmerman, written commun., 2017).

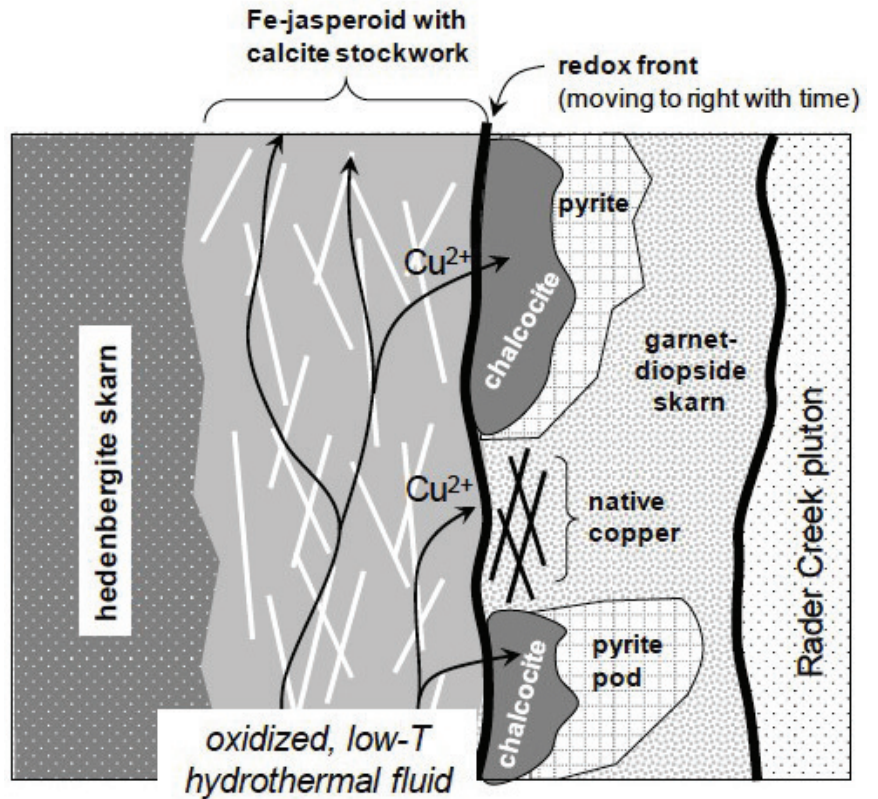


Figure 4. Schematic diagram of hypogene oxidation at the mine site after Sotendahl and Gammons (2012).

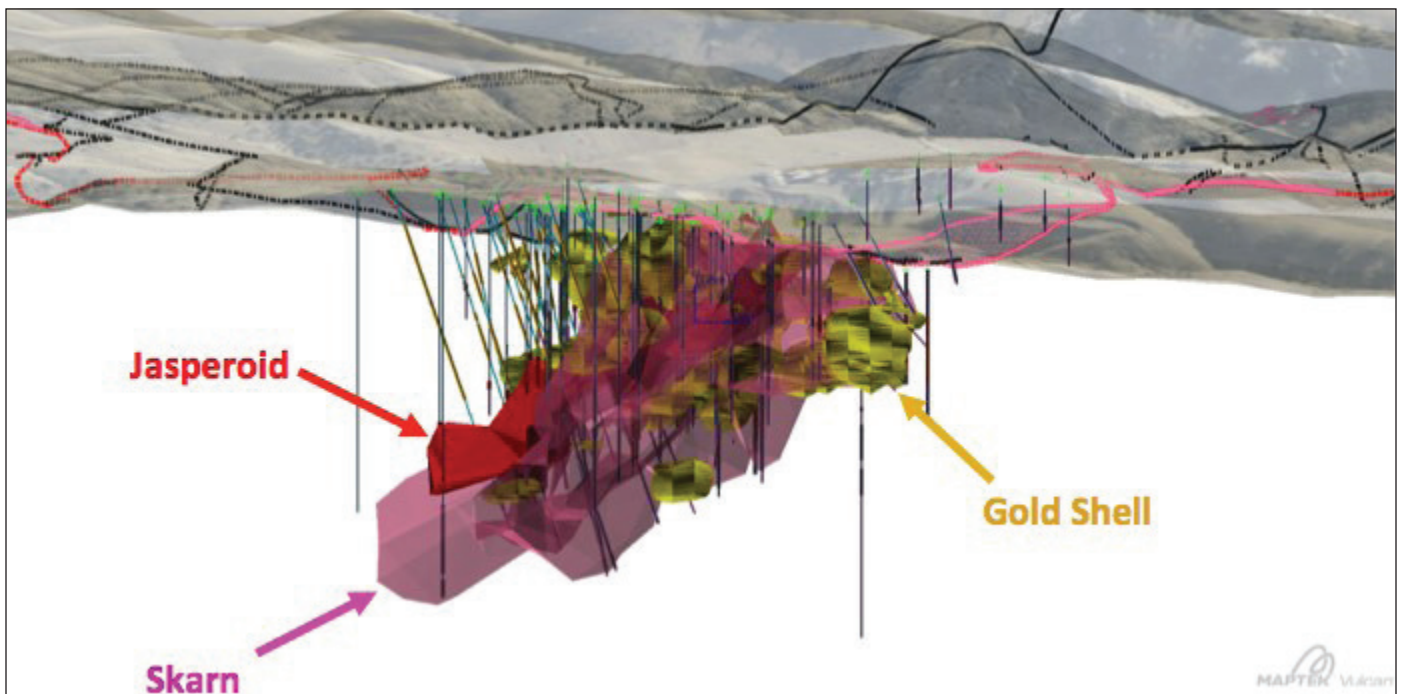


Figure 5. 3D model created from first phase of surface drilling depicting the Au-bearing jasperoid and skarn (Childs Geoscience, written-commun., 2017).

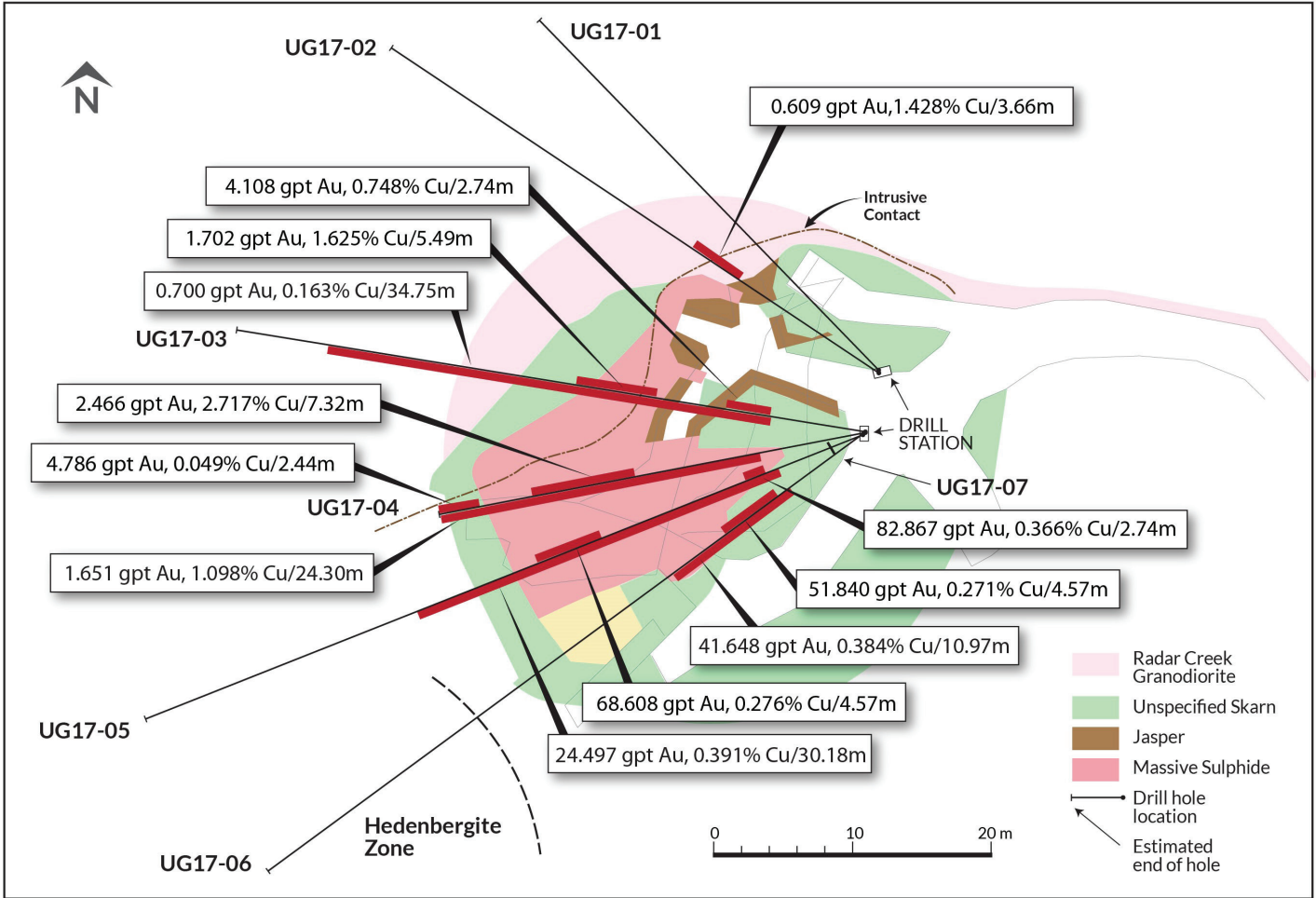


Figure 6. Underground drill fan with drilling highlights. Massive sulfide consistently contains high gold grades along with gold continuation with the skarn body (J. Kaplan, written commun., 2017).

Acknowledgments

A special thanks to the following employees, researchers, and contractors who have helped the exploration project along the way: Jarred Zimmerman, Isabella Cross-Najafi, Phil Dalhof, Jake McCane, Renee Hofacker, Chris Gammons, Childs Geoscience Inc., Peter E. Walcott & Associates Limited, ALS Minerals, AK Drilling, and Groundhog Mining & Exploration Contractors.

References Cited

Berger, B.R., Hildenbrand, T.G., and O’Neill, J.M., 2011, Control of Precambrian basement deformation zones on emplacement of the Laramide Boulder Batholith and Butte mining district, Montana, United States: U.S. Geological Survey Scientific Investigations Report 2011-5016, 29 p.

Sotendahl, J.M., and Gammons, C.G., 2012, Economic geology of the Madison gold Au-Cu skarn, Silver Star, MT: Butte, Mont., Montana Tech of the University of Montana, Master’s Thesis, 12–51 p.

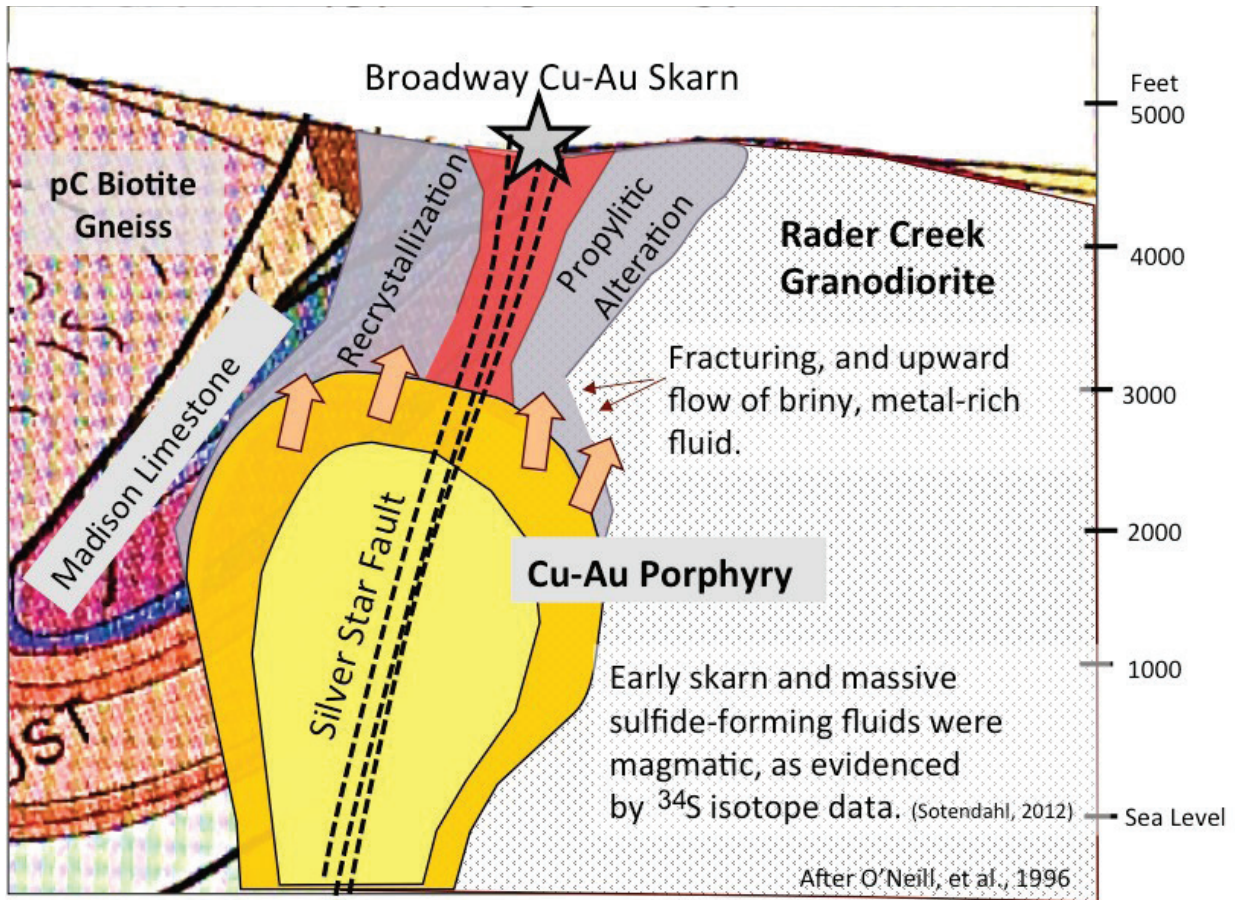


Figure 7. Depiction of the potential copper porphyry target (Childs Geoscience, written commun., 2017).



Conference attendees tour the Golden Sunlight Mine north of Whitehall, MT. Photo by A. Roth, MBMG.



Jenna Kaplan presents her paper at the symposium. Photo by A. Roth, MBMG.

Supergene Minerals from the Mayflower Mine, Madison County, Montana

Richard I. Gibson

Geologist, Butte, Montana, rigibson@earthlink.net

Introduction

The Mayflower Mine is located about 8 miles southeast of Whitehall, Montana, and was a major gold producer in Montana at the turn of the 19th century. Ore at the mine occurs in telluride minerals that formed during hydrothermal alteration of Cambrian Meagher carbonates. W.A. Clark purchased the Mayflower for \$150,000, and from 1896 to 1912, it produced about \$1,300,000 in gold. The Anaconda Company mined there from 1935 to 1942, and various entities have explored the property since the 1980s. Published work at the mine has focused on primary (hypogene) gold telluride mineralization (e.g., Spry and others, 1997; Zhang and Spry, 1994) at the mine site. This report is focused on supergene minerals that the author collected from mine dumps in 1971.

The Mayflower Mine occurs within the Willow Creek Fault Zone (WCFZ), a Proterozoic age east–west-trending lineament that defines the northern edge of the Dillon block (Archaean), and the southern margin of the Helena Embayment of the Belt Basin (Proterozoic). The WCFZ has been affected by subsequent tectonic events, such as thin-skinned (Sevier) contraction of Late Cretaceous to Paleogene age in the Southwest Montana Transverse Zone (SMTZ) (Schmidt and others, 1988) and recent Basin and Range block faulting (e.g., Stickney and others, 2000).

At the Mayflower mine, east–northeast trending reverse faults formed during SMTZ deformation. These faults juxtapose older Midproterozoic LaHood Formation (Belt Supergroup) rocks and Cambrian Flathead to Devonian Jefferson sandstones, shales, and carbonates over Cretaceous Elkhorn Mountains Volcanics (Klepper and others, 1957). The east–northeast-trending reverse faults likely served as conduits for mineralizing fluids that concentrated in oolitic and paleotidal facies of the Cambrian Meagher limestone.

Cocker (1993) recognized geochemical enrichments of Cu, Pb, Ag, Au, and V within the Meagher Formation controlled by lithology and proximity to the Mayflower Fault. Mn and Mg are enriched at greater distance, and Hg, Tl, As, and Zn are either constant or increase slightly with distance from the Mayflower Fault. The minerals identified below likely formed in the proximal zone based on the observations of Cocker (1993), and consist mostly of copper and lead minerals, vanadates, and one Cu-Mg carbonate mineral (Mcguinnessite).

Minerals

Confidently identified and/or confirmed by various analyses:

Hemimorphite $\text{Zn}_4\text{Si}_2\text{O}_7(\text{OH})_2 \cdot \text{H}_2\text{O}$

Vanadinite $\text{Pb}_5(\text{VO}_4)_3\text{Cl}$ - Wulfenite PbMoO_4

Descloizite $\text{PbZn}(\text{VO}_4)(\text{OH})$ - motttramite $\text{PbCu}(\text{VO}_4)(\text{OH})$

Mcguinnessite $\text{CuMgCO}_3(\text{OH})_2$ (fig. 1)



Figure 1. Mcguinnessite $\text{CuMgCO}_3(\text{OH})_2$

Likely but unconfirmed (only visually identified):

Tangeite $\text{CaCuVO}_4(\text{OH})$ - Volborthite $\text{Cu}_3\text{V}_2\text{O}_7(\text{OH})_2 \cdot 2\text{H}_2\text{O}$ (fig. 2)

Roscoelite (mica group) $\text{KV}_2^{3+}(\text{Si}_3\text{Al})\text{O}_{10}(\text{OH})_2$

Possible—Speculative, unknown:

Red-orange sub-vitreous orthorhombic(?) – compare Calderónite $\text{Pb}_2\text{Fe}^{3+}(\text{VO}_4)_2(\text{OH})$; Gottlobite $\text{CaMg}(\text{VO}_4)(\text{OH})$; casts similar to Sylvanite AgAuTe_4

Green to colorless, vitreous - austinite $\text{CaZn}(\text{AsO}_4)(\text{OH})$; duftite $\text{PbCu}(\text{AsO}_4)(\text{OH})$; amorphous (opaline?)

Dioptase $\text{CuSiO}_3 \cdot \text{H}_2\text{O}$

Epimorphs, hollow encrustations of brown, orange, green chalcedony-like material (fig. 3). Original crystals appear to be tetragonal disphenoids, possibly hexagonal or tetragonal scalenohedrons.

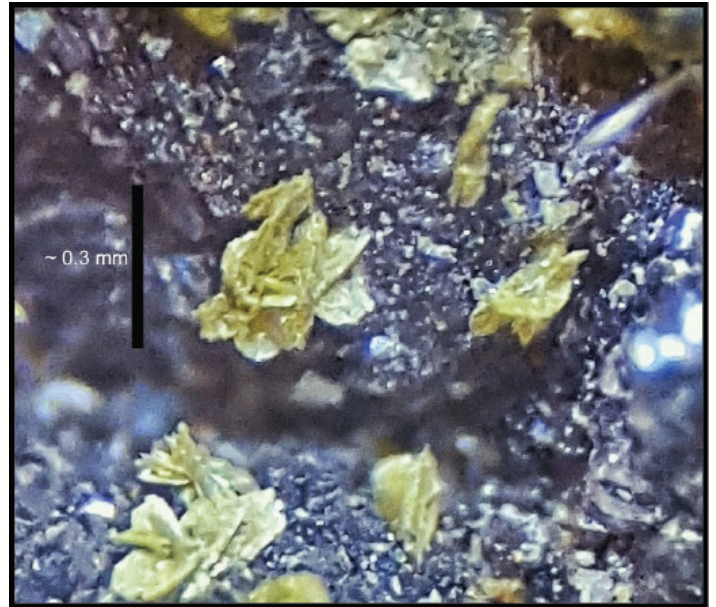


Figure 2. Volborthite $\text{Cu}_3\text{V}_2\text{O}_7(\text{OH})_2 \cdot 2\text{H}_2\text{O}$.

References Cited

Cocker, M.D., 1993, Primary element dispersion patterns in a carbonate-hosted, epithermal, high-grade, Au-Ag telluride system—Mayflower mine, Madison County, Montana, USA: *Journal of Geochemical Exploration*, 47(1–3), p. 377–390.

Klepper, M.R., Weeks, R.A., and Ruppel, E.T., 1957, *Geology of the southern Elkhorn Mountains, Jefferson and Broadwater Counties, Montana*: U.S. Geological Survey Professional Paper 292, 82 p.

Schmidt, C.J., O'Neill, J.M., and Brandon, W.C., 1988, Influence of Rocky Mountain foreland uplifts on the development of the frontal fold and thrust belt, southwestern Montana, *in* *Interaction of the Rocky Mountain Foreland and the Cordilleran Thrust Belt*, Schmidt, C.J., and Perry Jr., W.J., eds., *The Geological Society of America Memoir 171*, p. 171–201.

Spry, P.G., Foster, F., Truckle, J.S., and Chadwick, T.H., 1997, The mineralogy of the Golden Sunlight gold-silver telluride deposit, Whitehall, Montana, USA: *Mineralogy and Petrology*, 59(3–4), p. 143–164.

Stickney, M.C., Haller, K.M., and Machette, M.N., 2000, *Quaternary faults and seismicity in western Montana*: Montana Bureau of Mines and Geology Special Publication 114, scale: 1:750,000.

Zhang, X.M., and Spry, P.G., 1994, Petrological, mineralogical, fluid inclusion, and stable-isotope studies of the Gies gold-silver telluride deposit, Judith Mountains, Montana: *Economic Geology*, 89(3), p. 602–627.

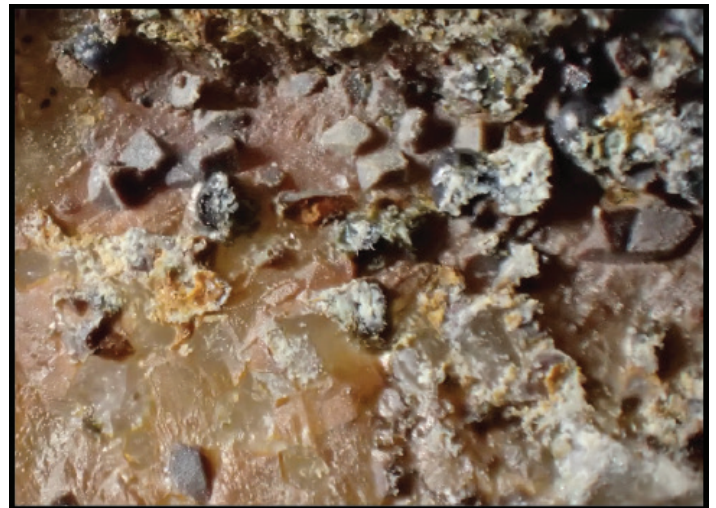


Figure 3. Epimorphs.

Copperopolis, Copper City, and Copper Cliff: Microminerals from Three of Montana's Obscure Copper Deposits.

Michael J. Gobla

Abstract

Although Montana is world famous for its enormous copper deposit at Butte, copper mining in the Treasure State was first undertaken at Copperopolis, in the Musselshell district in Meagher County, in 1866 when 5 tons of ore containing malachite, cuprite, and native copper was mined and shipped to the United Kingdom for processing. Copperopolis saw a number of ups and downs, but never materialized into a major producer. Copper City in Broadwater County is a skarn deposit that was discovered in 1874. In 1906 the Three Forks Copper Mining Company sunk a shaft on “one of the greatest undeveloped copper districts in the world.” Although the shaft at Copper City reached a depth of 600 feet, and some copper ore containing chalcopyrite and chalcocite was produced, the venture failed. The Copper Cliff in Missoula County was discovered in 1892. It forms a dramatic 150-foot-tall quartz cliff with blue and yellow colored streaks from mineral coatings. This district was also proclaimed to be the next great copper district of Montana. Several mining companies were formed to work the deposits, which contain malachite, azurite, native copper, and enargite, but they ended in failure. Although these copper camps were not economic powerhouses, they each have produced interesting microcrystal specimens. Hope of establishing a great mine remains. Copper Cliff is currently being explored for a deep porphyry copper deposit. There may yet be another major copper district in Montana.

Copperopolis

Copperopolis is located in the Musselshell mining district in Meagher County, where quartz veins intruded into Precambrian Belt Supergroup rocks (Blumer, 1971; fig. 1). The deposit was discovered by J.E. Hall and a partner named Hawkins who developed the Northern Pacific, the first mine to produce copper ore in the state of Montana. The mine shipped 5 tons of high grade ore to the United Kingdom for processing in 1866. By 1867 there were 60 men at work on the Northern Pacific, Copperopolis, Crittenden, Cole Sanders, St. John, Tuscarora, Boomerang, Canada, Musselshell, and a few other claims. The district began to decline when freighters began demanding \$100 per ton to transport the ore from the district. On May 25, 1868, an Indian raid resulted in

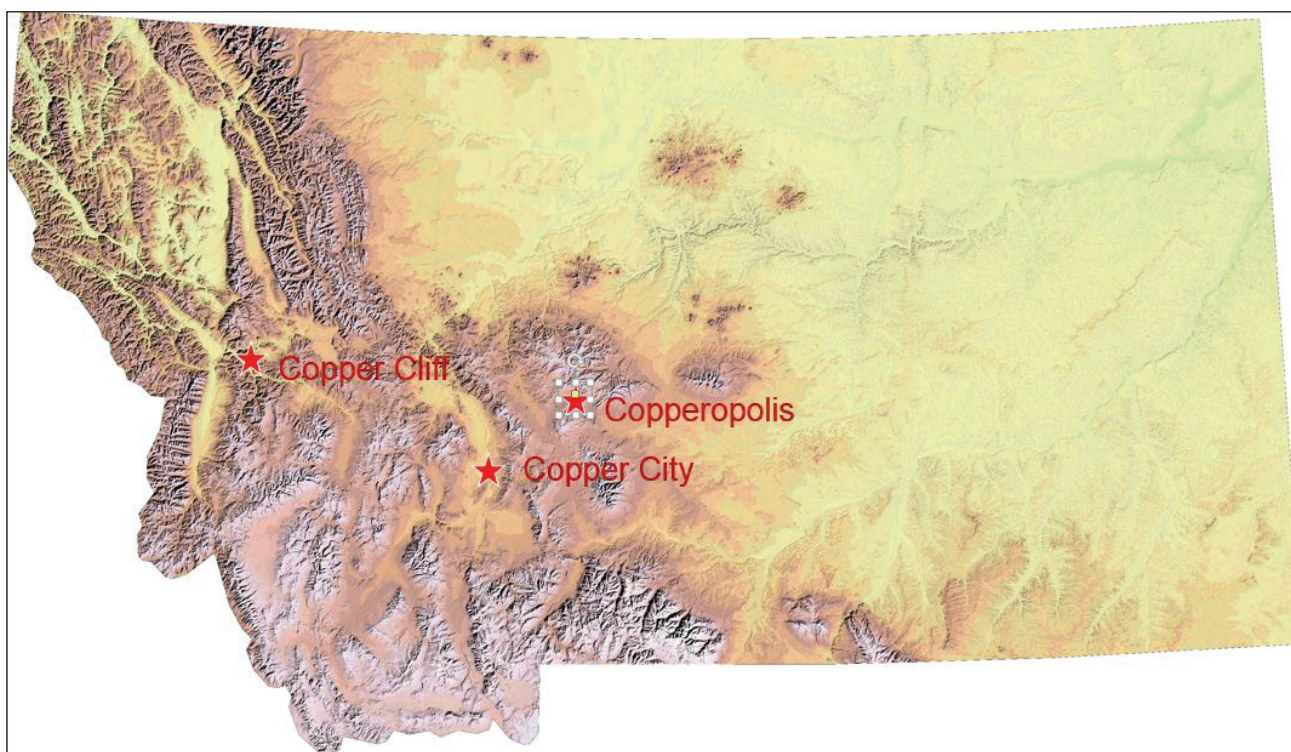


Figure 1. Map of Montana showing the location of Copperopolis, Copper City, and Copper Cliff.

loss of horses and wounding of several men by arrows. This raid led to further decline of the district (fig. 2).

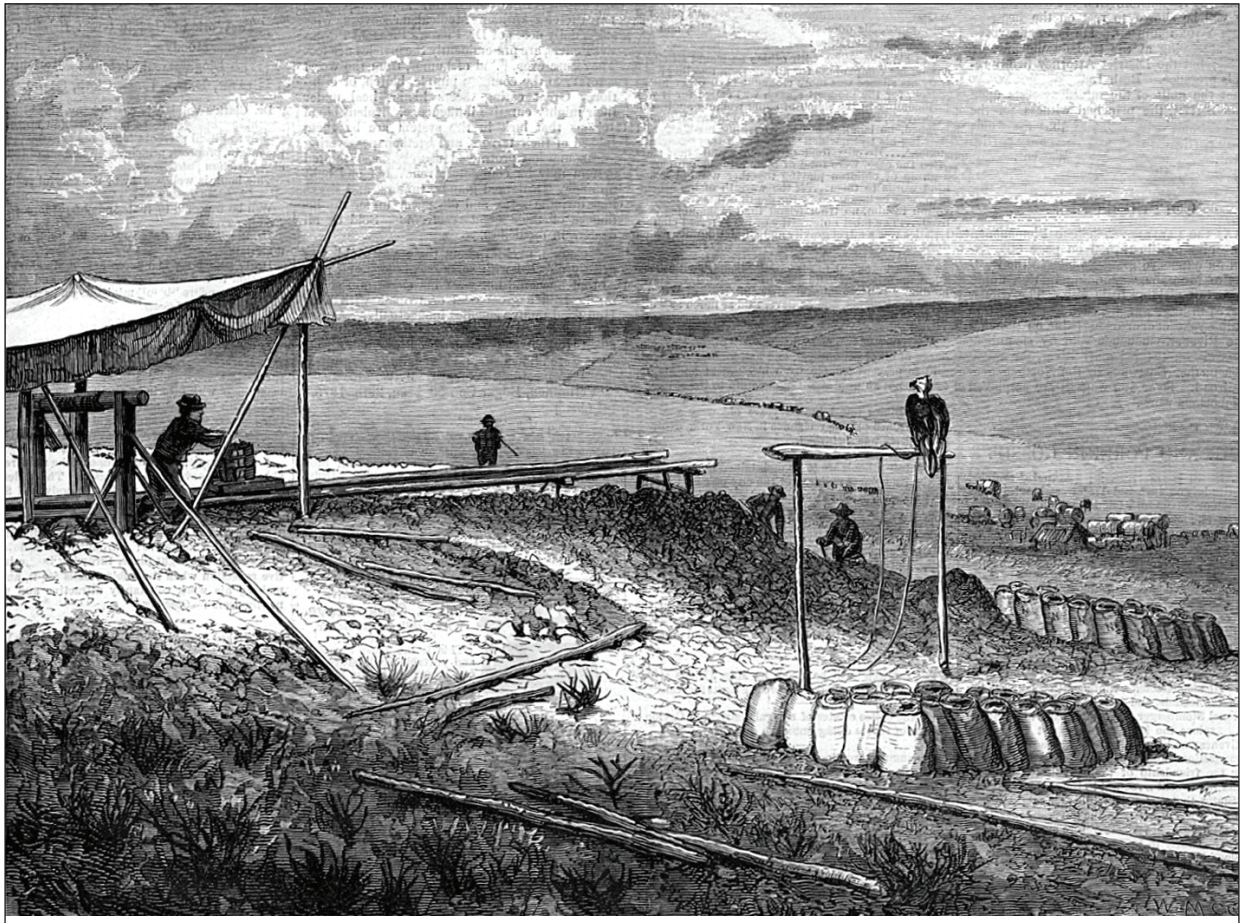


Figure 2. One of the earliest known illustrations of a mining operation in Montana is this sketch of the Northern Pacific mine at Copperopolis, Meagher County (Harpers Weekly, 1875).

In 1874 there was renewed interest when men named Ware and Kingsbury renewed working the Newland lead and produced 25 tons of one from a 45-foot shaft and shipped it to Baltimore, Maryland for reduction. They made a profit of \$55 per ton on the effort, but the mines again closed down as only the richest of ore could withstand the high shipping and processing costs.

In April 1883, Marcus Daly named his smelter town in Deer Lodge County Copperopolis, but was later informed by the postmaster that a post office by the name of Copperopolis had already been established in Meagher County in 1880. Daly decided to rename his town as Anaconda. In the 1890s, Copperopolis was revived and the arrival of the railroad in nearby Martinsdale in 1896 resulted in a mining boom. In 1900, Marcus Daly purchased the North Pacific and other mines at Copperopolis from J.E. Hall and so took title to the place with his favored name. With his financial backing, the Copperopolis Mining Company was created and W.W. McDowell and John Blewett were sent to develop the property. A workforce of 75 men was employed. The Northern Pacific shaft was deepened to 300 feet and the St. John and another shaft were put down to 200 feet in depth. Copperopolis turned into a real town with a hotel, livery, and 25 houses. Five teams of horses were used to haul the ore 27 miles to the railroad at Two Dot, Montana. Despite the frenetic development, by September the operations were closed down due to the difficulty and heavy expenses of pumping water from the mine. Marcus Daly passed away later in 1900, which stopped further development. The Daly Mining Company was organized to take over the Marcus Daly properties and McDowell negotiated to acquire the claims under a bond. Operations resumed with a mine superintendent named Gallagher. McDowell's operations shipped over 30 cars of ore, netting an average of \$2,000 per car. Lower copper prices led to the eventual closure in 1903. Margaret Daly deeded the claims to the Daly Mining Company on July 29, 1903.

Later attempts to work the mine were on a small scale, which included work in 1908 and 1910, and then

there was a period of steady production from 1914 to 1924. The shaft was deepened to 625 feet and over 2,000 feet of drifts were eventually driven in this mine. Detailed production records were not kept. A total of \$500,000 in copper ore is estimated to have been produced over the life of the mine (Roundup Record-Tribune, August 29, 1940; table 1).

Table 1. Minerals found at Copperopolis, Musselshell mining district, Meagher County, Montana.

Azurite	Copper*	Malachite*
Barite	Cuprite*	Pyrite
Calcite*	Hematite	Quartz*
Chrysocolla	Goethite	Tenorite

*Minerals in bold occur as microcrystals.

Malachite is abundant and takes many forms of primary contact twin microcrystals. The crystals are so well crystallized that they appear to be deep emerald green to nearly black in color. Malachite crystals of this form are rare, known mainly from a few localities in the Democratic Republic of Congo in Africa. The more familiar needle-shaped radiating crystals of malachite and botryoidal crusts do occur but are of uncommon occurrence at Copperopolis. Typically, malachite forms blocky-shaped microcrystals which resemble rhombohedral forms, but on closer examination are actually stubby contact twin crystals. Other forms resemble six-sided lozenge shapes, rectangular tablets, and occasionally the more prismatic contact twin forms. The malachite microcrystals commonly form small aggregates of intergrown crystals which, when broken open, exhibit an interior core of bright red cuprite containing small grains of native copper (figs. 3–5).



Figure 3. Aggregates of malachite microcrystals from Copperopolis showing typical rhombohedral-like forms which are actually monoclinic contact twins.

Cuprite microcrystals are rarely found (fig. 6). All of the cuprite is crystallized, but it typically takes the form of a complete filling in narrow veinlets, or as aggregates of microcrystals that have been completely overgrown by malachite microcrystals. Cuprite is also found to have been partially to completely replaced by chrysocolla forming pseudomorphs after octahedral microcrystals of cuprite. Malachite forms as epimorphs after cuprite octahedral forms. Azurite is very rare in occurrence, typically forming small grains. Native copper



Figure 4. Malachite microcrystals with a six-sided lozenge-shaped form, from Copperopolis.

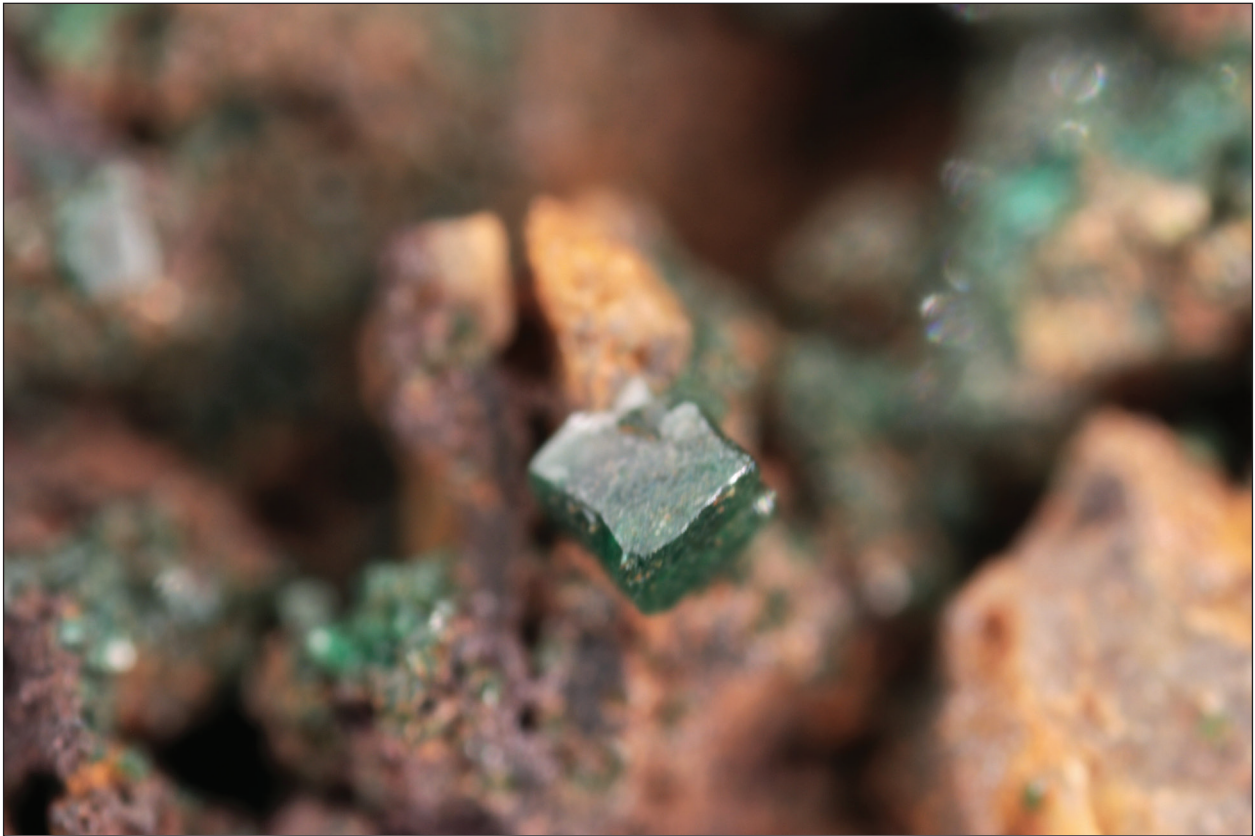


Figure 5. An unusual tablet-shaped malachite microcrystal with curved sides from Copperopolis.

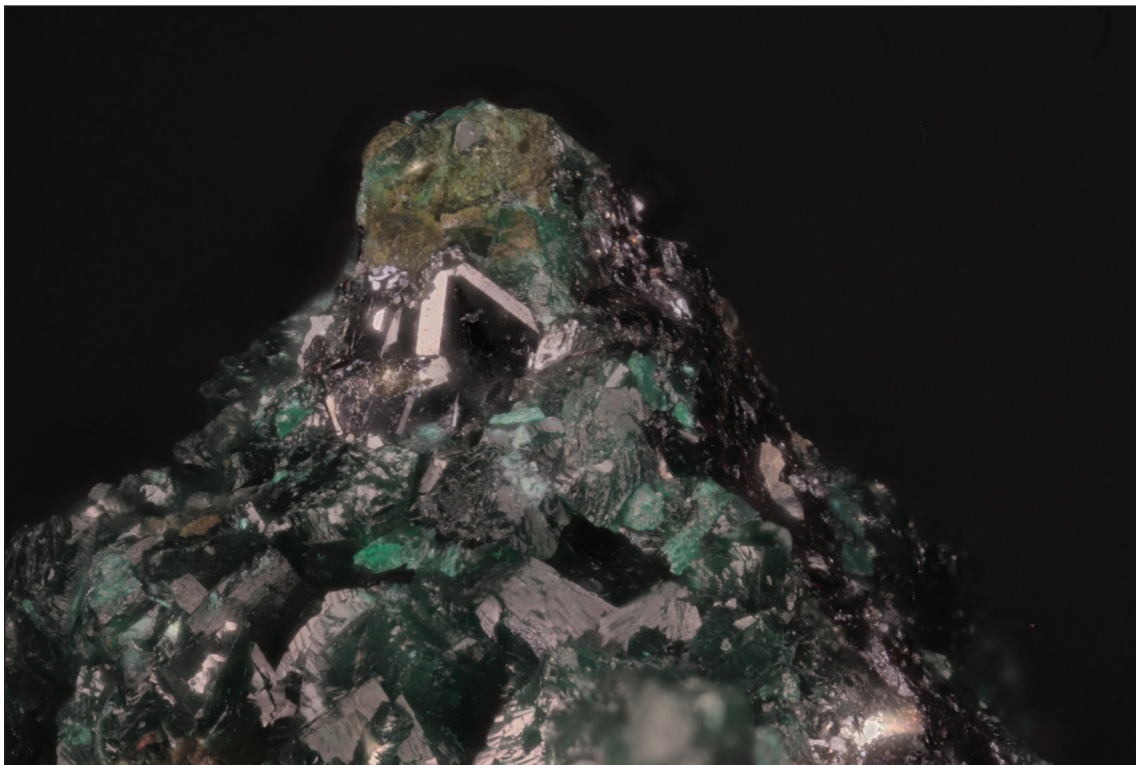


Figure 6. A cuprite microcrystal showing octahedral and cube forms with associated malachite microcrystals from Copperopolis.

occurs as small grains and microcrystals embedded in crystalline masses and veinlets of cuprite (fig. 7). Nearly all of the pyrite is massive, brecciated, and shot through with veinlets of goethite. Small masses of pyrite are oxidized and show iridescence resembling chalcopyrite and bornite. Although chalcopyrite and bornite are reported to occur (Roby, 1950), none has been observed, and past reports likely were misidentifications of tarnished pyrite, which is abundant at the site and strongly resembles the copper sulfides. Goethite also occurs as pseudomorphs after pyrite microcrystals and as small spheres and botryoidal crusts. Calcite forms colorless microcrystals in vuggy quartz and also occurs as massive cleavages intergrown with earthy red hematite along

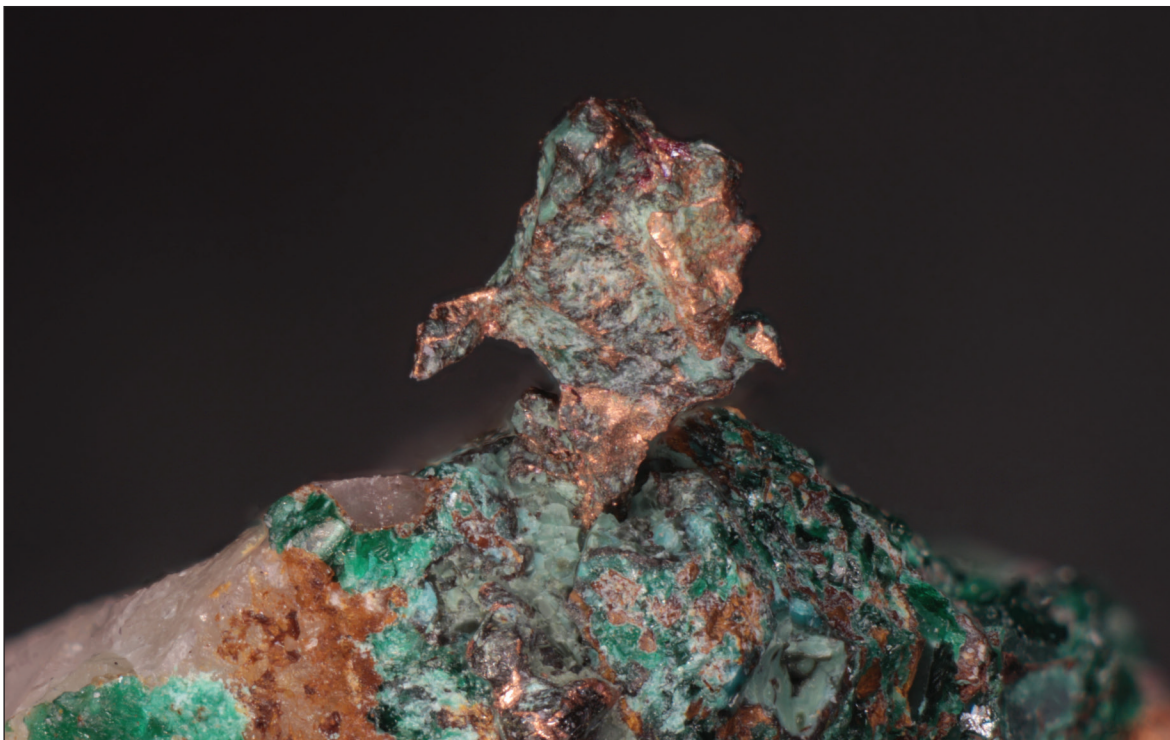


Figure 7. Native copper microcrystals, Copperopolis.

the cleavage planes, resulting in brown masses resembling siderite. Quartz forms milky white massive vein filling to occasional milky crystals to 2 inches in length, and as microcrystals lining vugs. The quartz microcrystals vary from colorless to white to pale blue to rare pale amethystine color and on rare occasion are associated with microcrystals of malachite.

Copper City

Located 7 miles north of Three Forks, the claims in the Emerson district are located in section 25, T. 3 N., R. 1 E., and can be reached by the Copper City Road, which is located about 4.5 miles north of I-90. Limestone has been altered to marble, forming a skarn deposit covering a large area. There are two locations where the rock has been excavated. One is an open cut located 0.5 miles NW of Copper City; the other is the site of the Pennsylvania mine shaft, where there are two waste rock dumps located about 1,500 feet NE of the buildings at Copper City. There are conflicting reports about the discovery. A newspaper article says that the Three Forks Copper Mining Company deposit was originally discovered by Montana Vigilante X Bielder, but it was never worked (The Sun, New York, NY, January, 10, 1910, p. 11). A later account says John Emerson discovered the deposit in 1874 (Richards, 1943). It is possible that both accounts are correct and that both men were involved. Ten mining claims were staked. Emerson extracted some high-grade gold ore and then sold the mine in 1879 to Samuel Seaman and John Hopping, who worked the mine for a few more years producing about \$14,000 (around 700 ounces) in gold (Richards, 1943; fig. 8).



Figure 8. The ghost town remains at Copper City, Broadwater County, Montana.



Figure 9. Waste rock at the Pennsylvania mine shaft north of Copper City, Broadwater County.

The property changed ownership a few times. It eventually became the property of Mr. Herbert G. Dunbar, who organized the Three Forks Copper Mining Company in 1906. He extended the shaft, and by 1916 it had reached the 400 foot level. The shaft eventually reached a depth of 600 feet with drifts on the 450, 500, and 550 foot levels. Sulfide copper ore was encountered at a depth of 325 feet (Weed, 1920). Ore production details have not been recorded. Operations ceased in 1921 and the earthquake of 1925 caused timbers in the shaft to fall, making the workings inaccessible. The Chemical Copper Company investigated the property under the Defense Minerals Exploration Administration in the 1950s. The results of their investigation were not encouraging, and the site has remained inactive (fig. 9).

A study of polished ore samples showed bornite as the principal copper mineral along with microscopic grains and veinlets of chalcopyrite, pyrite, and chalcocite (Richards, 1943; table 2). The most abundant minerals are massive brown vesuvianite and green diopside, some of which contains thin seams and coatings of chrysocolla. White to pale-blue-colored calcite oc-

Table 2. Minerals found at Copper City, Broadwater County, Montana.

Bornite*	Clintonite*	Magnetite*
Calcite*	Diopside*	Pyrite
Chalcocite	Fluorapophyllite*	Vesuvianite*
Chrysocolla	Grossular*	

*Minerals in bold occur as microcrystals.

curs as thin seams and small masses in the rock. The small masses of calcite in the silicate rock can be dissolved to reveal bornite, clintonite (crystals), diopside (crystals and microcrystals; fig. 10), magnetite (microcrystals), grossular (microcrystals), and vesuvianite (crystals and microcrystals; fig. 11). A small amount of calcite is found as microcrystals in small open vugs and in thin veins cutting through the brown vesuvianite. A single specimen of one of these calcite veins found by the author exhibited a vug containing few microcrystals of a zeolite min-



Figure 10. Diopside microcrystals from Copper City. Most of the diopside at Copper City is opaque, but occasionally transparent microcrystals such as these are found.



Figure 11. Vesuvianite microcrystal with calcite and chrysocolla, Pennsylvania mine, Copper City, Emerson district, Broadwater County, Montana.

erals that appears to be fluorapophyllite. Grossular is scarce and usually seen only as microcrystals; some have dark inclusions (probably magnetite) and as a result appear to be nearly black in color. A single large grossular crystal (approximately 2 cm in diameter and black in color) was collected from the area near the open cut and now is a part of the Montana Bureau of Mines and Geology Mineral Museum collection.

Copper Cliff



Figure 12. The Copper Cliff, Missoula County, Montana.

feet wide containing native copper; a second vein containing chalcopyrite and black copper sulfides was encountered at 100 feet in from the portal. By April 1893 they extracted over seven carloads of high-grade ore for shipping (The Daily Independent, Helena, April 17, 1893).

In 1896 they bonded the properties to H.L. Frank and Charles Smith of Butte, who put a force of men to work and extended an adit 800 feet into the Copper Cliff claim (The Anaconda Standard, January 29, 1896, p. 10). A townsite called Copper Cliff was located on a high plateau area located above the mine. In 1899 the 100-foot level adit cut into several feet of high-grade mineralization and specimens showing massive native copper were exhibited in Anaconda (The Anaconda Standard, May 8, 1899, p. 12). Although they shipped 15 cars of ore running from 14 to 28 percent copper, they spent \$80,000 without putting the mine on a paying basis.

In January 1900, Mr. Shipler arrived in Butte with two carloads of high-grade ore from Copper Cliff that he sold to a smelter. In March 1900, Sam J. Ritchey bonded the Copper Cliff mine. He stated that there is \$350,000 worth of ore available and that the ore assays from 17 to 23 percent and carries \$6 to \$8 per ton in gold (Daily Intermountain, April 12, 1900, p. 3). The shaft was extended to a depth of 185 feet (Daily Intermountain, June 26, 1900, p. 5). In sinking the shaft they cut a 24-foot ledge of copper, much of it in the native state, and below that was porphyry.

In late 1900, negotiations to sell the mine were initiated. At the end of 1901 an agreement was finally made with investors from London, England to purchase the Copper Cliff (Rosebud County News, January 2, 1902, p. 3). On September 11, 1903, a new company called the Copper Cliff Mines of Montana, Ltd. was organized in London, but since the initial purchase, the London owners never did any work on the property. The mine was next acquired by men associated with the Tacoma, Washington smelter. By 1905, 34 men were at work for the Copper Cliff Mining Company with ore being shipped to the Tacoma smelter. This operation did not last long.

In 1918 men from Butte acquired the property and formed the Potomac Copper Company (fig. 13). In 1919, the Potomac Copper Company did much development work at the mine. In May 1919 the company began construction of a new access road and purchased two compressors to install near the mine in order to facilitate driv-



Figure 13. Stock certificate from the Potomac Copper Company, which drove adits into the Copper Cliff and Leonard mines in 1919.

ing a new 1,200-foot-long adit about 800 feet below the cliff. They also drove an adit into the Leonard claim located higher on the mountain. In July they began construction of a boarding house, and at this time a fissure containing enargite was uncovered at the base of the cliff (Great Falls Daily Tribune, July 6, 1919, p. 11). The company was not mentioned after 1920, so it is presumed that they ran out of capital prior to sustaining profitable production of copper ores.

In 1940, 47 tons of ore were shipped from the Copper Cliff, with a total value of \$333, and the next year 15 tons were produced. In 1943 4 tons of ore were produced, and in 1944 5 tons of ore. Total production of the mining district between 1891 and 1960 is estimated at 259 ounces gold;

567 ounces silver; and 110,898 pounds copper (Sahinen, 1957).

The deposit consists of massive quartz containing copper minerals which are associated with a porphyritic intrusion into Belt Supergroup rocks. Currently the site is not accessible because it is being actively explored for a deep porphyry copper deposit.

Azurite is rare at the Copper Cliff mine and typically occurs as small massive grains. A single specimen of azurite microcrystals with chrysocolla was recovered (table 3).

Table 3. Minerals found at Copper Cliff, Missoula County, Montana.

Azurite*	Enargite*	Olivinite*
Chenevixite	Euchroite*	Quartz
Chrysocolla	Famatinite	
Copper	Malachite	

*Minerals in bold occur as microcrystals.

Chenevixite occurs as green crusts in vuggy quartz. It is often associated with microcrystals of olivenite.

Chrysocolla forms thin crusts, and is responsible for the blue stains on the cliff.

Malachite is found in small amounts as small grains, crusts, spheres, and occasional acicular microcrystals.

Enargite forms tiny microcrystals. Studies of polished sections of ore from the mine determined that the enargite is usually intergrown with small amounts of famatinite.

Euchroite was found several decades ago in one boulder from the Copper Cliff; these are some of the best crystals know for this mineral (fig. 14).

Olivinite forms elongated prismatic microcrystals of typical olive green color (fig. 15). The crystals are found in small vugs in quartz and are often coated by an orange clay. Some of the microcrystals have formed over massive crusts of bright green chenevixite.

About 400 feet higher on the mountain is the Leonard mine (later renamed as the Blue Bell). It was active in 1913, 1916–1918, and 1943–1945. It produced 45 tons of copper ore along with silver and lead (Sahinen, 1957). This mine has produced a few specimens of azurite microcrystals, malachite in small masses showing radiating form, and a few pseudomorphs of chrysocolla after azurite (figs. 16, 17).

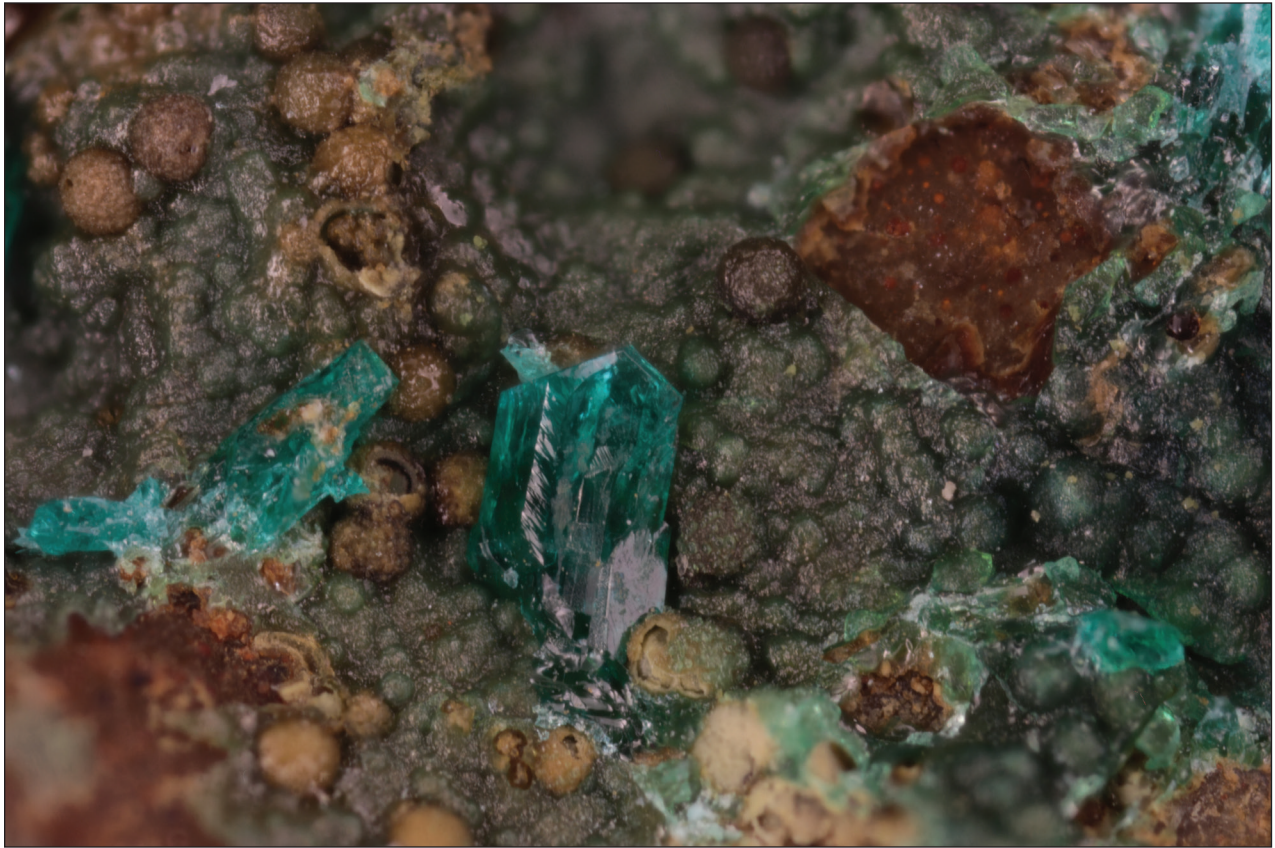


Figure 14. Euchroite microcrystal from the Copper Cliff mine, Missoula County, Montana.



Figure 15. Olivinite microcrystals from the Copper Cliff mine, Missoula County, Montana.

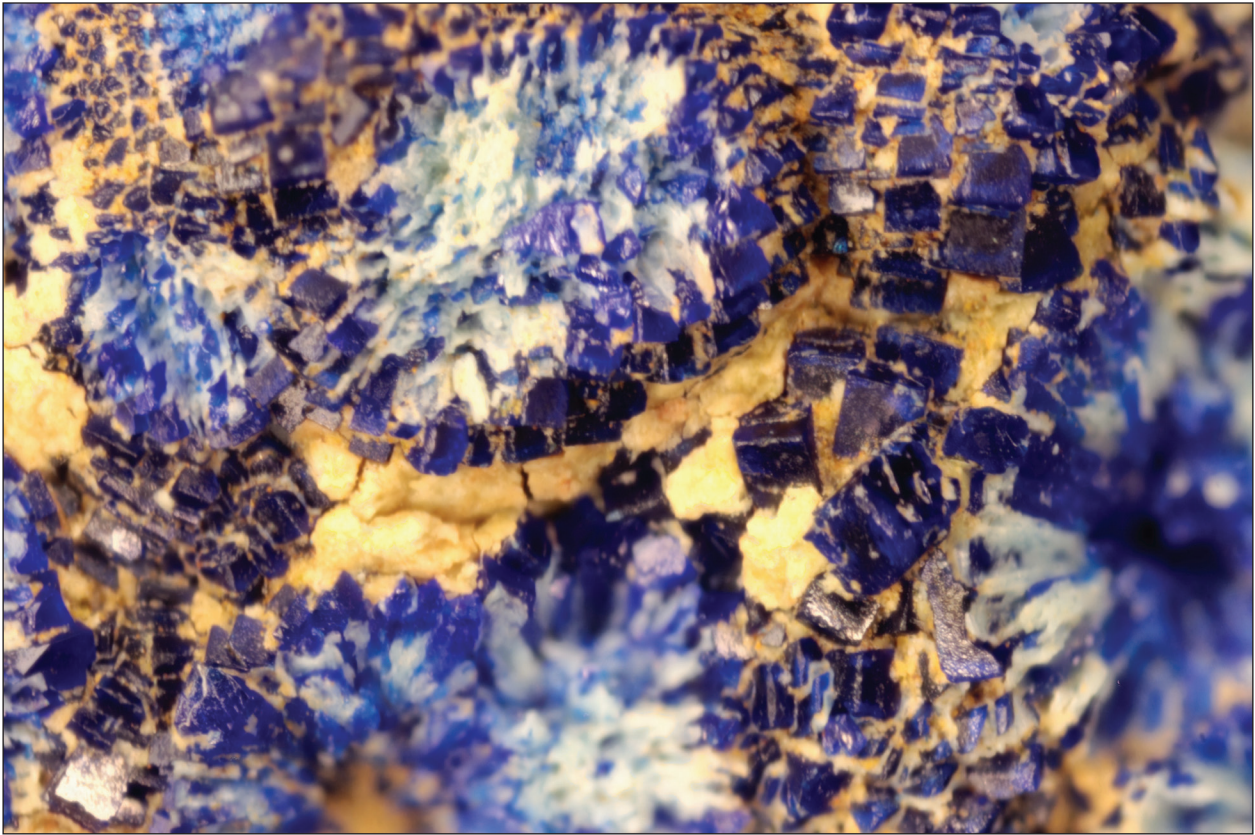


Figure 16. Azurite microcrystals, Leonard mine, Copper Cliff district, Missoula County, Montana.

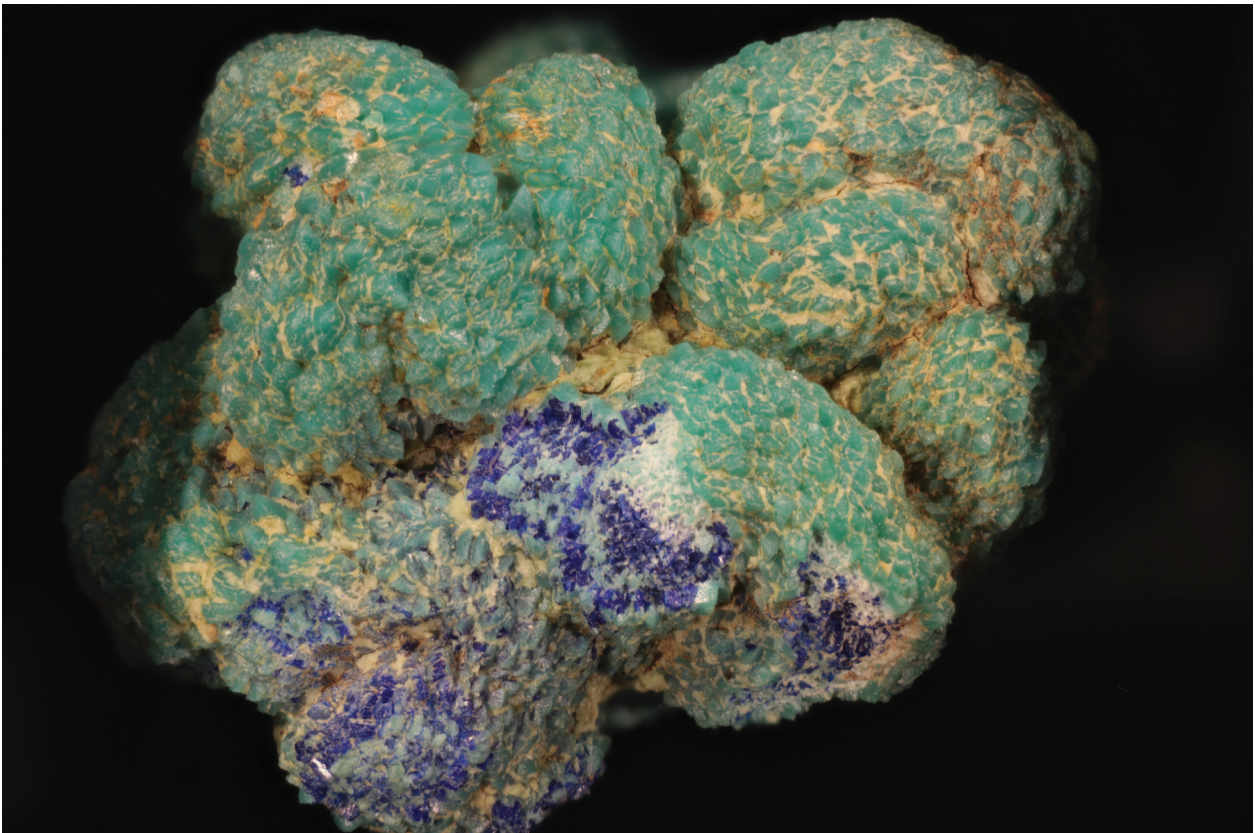


Figure 17. Chrysocolla pseudomorphs after azurite with some unaltered azurite microcrystals, Leonard mine, Copper Cliff district, Missoula County, Montana.

References

- Blumer, J.W., 1971, Geology of the Deadman Canyon-Copperopolis area, Meagher County, Montana: Butte, Mont., Montana Tech, M.S. Thesis, 68 p.
- Richards, J.C., 1943, Geology and ore deposits of the Pennsylvania mine, Three Forks, Montana: Butte, Mont., Montana Tech, M.S. Thesis, 39 p.
- Roby, R.N., 1950, Mines and mineral deposits (except fuels), Meagher County, Montana: U.S. Bureau of Mines Information Circular 7540, 40 p.
- Sahinen, U.M., 1957, Mines and mineral deposits, Missoula and Ravalli Counties, Montana: Montana Bureau of Mines and Geology Bulletin 8, 63 p.
- Stevens, H.J., 1903, The copper handbook, vol. IV.: Houghton, Mich., Stevens Copper Handbook Company.
- Weed, W.H., 1920, The mines handbook, vol. XIV: New York City, Stevens Copper Handbook Company.
-



Mike Gobla presents his paper at the symposium. Photo by A. Roth, MBMG

MBMG's Abandoned and Inactive Mines (AIM) Inventory and Sampling Program— 8,000 Mines and So Little Time

Phyllis Hargrave

Montana Bureau of Mines and Geology

In 1992, staff at the Montana Bureau of Mines and Geology (MBMG) began a systematic program to identify the “universe” of sites with possible human health, environmental, and/or safety problems either on or affecting National Forest lands. Later, the MBMG contracted with the BLM to conduct similar studies on their lands. For the next 11 years, the MBMG screened out sites deemed not likely to affect Federal lands, characterized those that possibly would (fig. 1A), visited these sites, and sampled them (water, soil, and waste rock) if warranted.

There were many surprises and enigmas in addition to the usual waste rock piles (fig. 1B), Lodgepole pines, and collapsed adits (fig. 1C). The AIM program produced 15 USFS volumes organized by Forest and by drainages, and one BLM report (see references). Volumes of the results are posted as pdfs on the MBMG publications catalog. Water sample results are entered in MBMG's Ground Water Information Center, GWIC.



Figure 1. (A) Adit discharge at the Iron Mountain Mine, Superior Ranger District, Lolo National Forest; (B) Waste dump at the Copper Queen Mine, Beartooth Ranger District, Custer National Forest; (C) Open adit at the Rock Island Mine, Superior Ranger District, Lolo National Forest.

References

- Hargrave, P.A., Bowler, T.B., Lonn, J.D., Madison, J.P., Metesh, J.J., and Wintergerst, R., 1998, Abandoned-inactive mines of the Blackfoot-Little Blackfoot River drainages, Helena National Forest: Montana Bureau of Mines and Geology Open-File Report 368, 228 p.
- Hargrave, P.A., English, A.R., Kerschen, M.D., Liva, G.W., Lonn, J.D., Madison, J.P., Metesh, J.J., and Wintergerst, R., 1999, Abandoned-inactive mines of the Kootenai National Forest administered land: Montana Bureau of Mines and Geology Open-File Report 395, 226 p., 1 sheet.
- Hargrave, P.A., Metesh, J.J., Kerschen, M.D., Liva, G.M., McDonald, C., and Wintergerst, R., 2000, Abandoned-inactive mines of the Lewis and Clark National Forest: Montana Bureau of Mines and Geology Open-File Report 413, 132 p.
- Hargrave, P.A., Kerschen, M.D., McDonald, C., Metesh, J.J., Norbeck, P.M., and Wintergerst, Robert, 2000, Abandoned-inactive mines program, Gallatin National Forest administered land: Montana Bureau of Mines and Geology Open-File Report 418, 199 p.
- Hargrave, P.A., Kerschen, M.D., McDonald, C., Metesh, J.J., and Wintergerst, R., 2003, Abandoned-inactive mines on Lolo National Forest administered land: Montana Bureau of Mines and Geology Open-File Report 476, 166 p.

- Hargrave, P.A., McDonald, C., Kerschen, M.D., Metesh, J.J., and Wintergerst, Robert, 2003, Abandoned-inactive mines on Bitterroot National Forest administered land: Montana Bureau of Mines and Geology Open-File Report 484, 93 p.
- Kerschen, M.D., Hargrave, P., McDonald, C., Metesh, J.J., and Wintergerst, Robert, 2000, Abandoned-inactive mines program, Custer National Forest administered land: Montana Bureau of Mines and Geology Open-File Report 421, 86 p., 4 appendices.
- Marvin, R.K., Metesh, J.J., Bowler, T.P., Lonn, J.D., Watson, J.E., Madison, J.P., and Hargrave, P.A., 1997, Abandoned/inactive mines of Montana, U.S. Bureau of Land Management: Montana Bureau of Mines and Geology Open-File Report 348, 544 p.
- Marvin, R.K., Hargrave, P.A., Lonn, J.D., Abdo, G.N., and Metesh, J.J., 1998, Abandoned-inactive mines of the southern Beaverhead-Deerlodge National Forest: Montana Bureau of Mines and Geology Open-File Report 379, 345 p.
- McDonald, C., Hargrave, P.A., Kerschen, M.D., and Metesh, J.J., 2002, Abandoned-inactive mines on the Flat-head National Forest administered land: Montana Bureau of Mines and Geology Open-File Report 462, 42 p., 4 appendices.
- Metesh, J.J., Lonn, J., Duaiame, T., Marvin, R.K., and Wintergerst, R., 1995, Abandoned-inactive mines program, Deerlodge National Forest, volume II: Cataract Creek drainage: Montana Bureau of Mines and Geology Open-File Report 344, 201 p.
- Metesh, J.J., Lonn, J.D., Duaiame, T.E, and Wintergerst, R., 1994, Abandoned-inactive mines program report, Deerlodge National Forest, Basin Creek drainage, volume I: Montana Bureau of Mines and Geology Open-File Report 321, 131 p.
- Metesh, J.J., Lonn, J., Madison, J.P., Marvin, R.K., and Wintergerst, R., 1995, Abandoned-inactive mines program, Deerlodge National Forest, volume III: Flint Creek/Rock Creek drainages: Montana Bureau of Mines and Geology Open-File Report 345, 219 p.
- Madison, J.P., Metesh, J.J., Lonn, J.D., Marvin, R.K., and Wintergerst, R., 1995, Abandoned-inactive mines program, Deerlodge National Forest, volume IV: Upper Clark Fork River drainage: Montana Bureau of Mines and Geology Open-File Report 346, 152 p.
- Metesh, J.J., Duaiame, T., Lonn, J.D., Madison, J.P., Marvin, R.K., and Wintergerst, R., 1998, Abandoned-inactive mines program, Deerlodge National Forest, volume V: Boulder/Jefferson River drainages: Montana Bureau of Mines and Geology Open-File Report 347, 179 p., 2 sheets.
- Metesh, J.J., Lonn, J., Marvin, R.K., Hargrave, P.A., and Madison, J.P., 1998, Abandoned-inactive mines program, Helena National Forest, volume I: Upper Missouri River drainage: Montana Bureau of Mines and Geology Open-File Report 352, 254 p., 2 sheets.

Geology, History, and Remediation in the Carpenter–Snow Creek Mining District, Neihart, Montana

Sara Edinberg

Hydrogeologist, Montana Department of Environmental Quality

The Carpenter–Snow Creek Mining District (fig. 1), located outside of Neihart, Montana, has a rich mining history that resulted from historic production of silver, lead, and zinc. The district is in the Little Belt Mountains southeast of Great Falls, considered the front, or border range, of the Rocky Mountains. The Little Belts formed during regional Cretaceous–Paleocene deformation. The mountains form a broad, dome-shaped uplift that is cored by Paleoproterozoic basement rocks that lie stratigraphically below the Belt series, and are intruded by

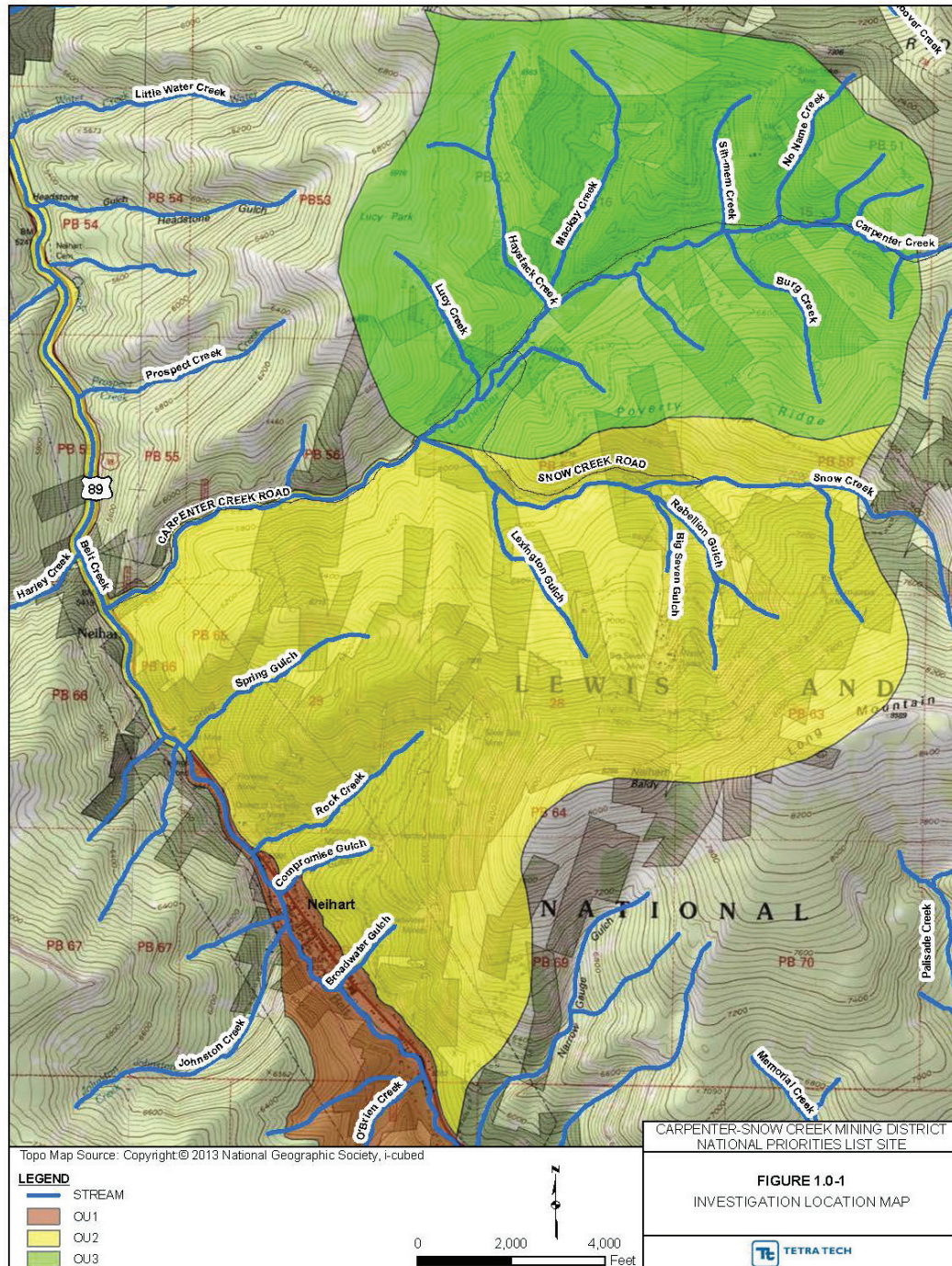


Figure 1. Map of the Carpenter–Snow Creek Mining District, divided into Operable Units (OUs) for the purposes of Superfund Cleanup. OU1 covers the town of Neihart; OU2 covers Snow Creek and the Neihart Slope; and OU3 covers Carpenter Creek and the Silver Dyke Mine.

Eocene laccoliths, bysmaliths, stocks, sills, dikes, and diatremes (fig. 2). Precambrian through Cretaceous sedimentary rocks cap the dome structure.

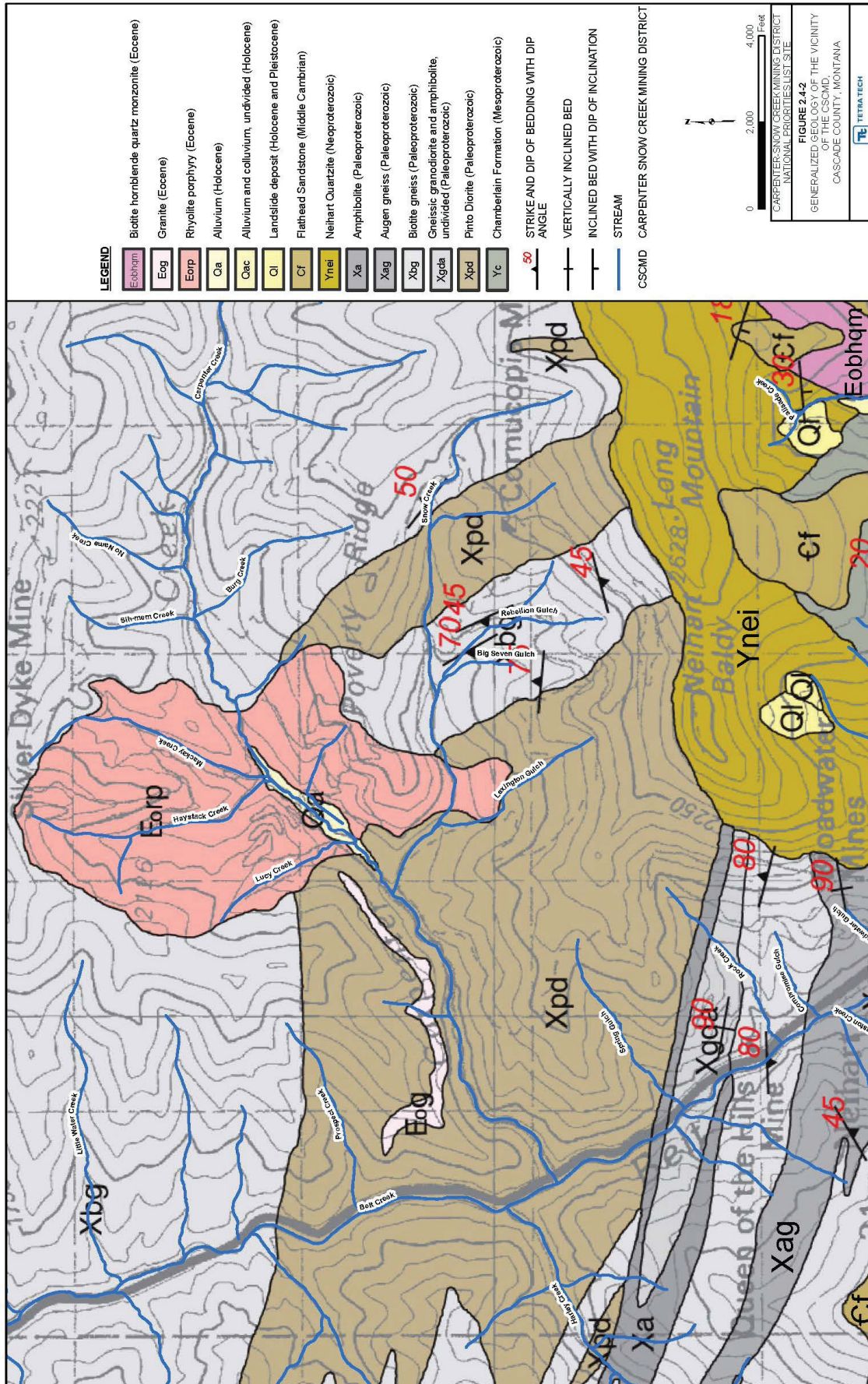


Figure 2. Geologic map of the Carpenter-Snow Creek Mining District. The town of Neihart is located at the south end of the map.

Ores formed at relatively shallow depths and are divided into three zones that are gradational to one another: Zone I ores are low-grade, and contain sulfides that formed at relatively high temperatures and contain proportionately high concentrations of copper; Zone II ores contain sulfides that formed in a moderate temperature environment and contain high lead, zinc, and silver concentrations; and Zone III ores were formed at the lowest temperatures and contain significant silver and gold, but little lead, zinc, or copper. The ore minerals are primarily galena, which was replaced by zinc, and then copper, as temperatures in the hydrothermal system increased.

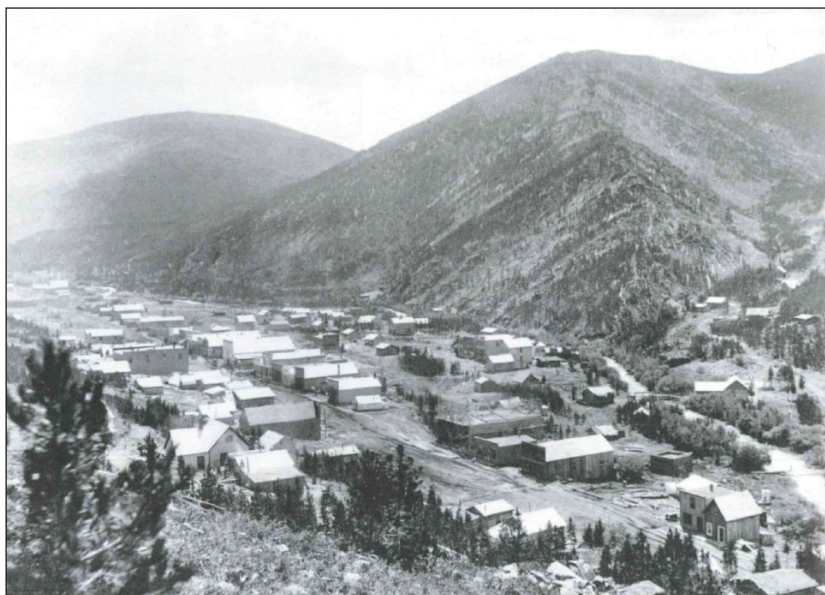


Figure 3. The town of Neihart at its peak, in the late 1880s.

several mines in the district reopened. This led to upgrades to the concentrating plant in Neihart, and construction of several new flotation plants.

The American Zinc, Lead and Smelting Company purchased the Silver Dyke mine (fig. 4) in upper Carpenter Creek in 1921. Open-pit mining resulted in the production of a glory hole (fig. 5), and tailings were deposited at an impoundment in a nearby drainage. The impoundment was breached in 1925 due to an earthquake, which resulted in widespread deposition of tailings along Carpenter Creek, and the construction of two tailings piles in the creek. Although the Silver Dyke was mined out by 1929, the site was the largest producer of ore in the Carpenter–Snow Creek district, with silver production second only to Silver Bow County (Butte District). The last major activity in the district occurred from 1930 to 1945, although some small-scale contract mine operations occurred in Snow Creek in the 1950s under the Defense Mining Exploration Act of 1950.

The Carpenter–Snow Creek Mining district was listed as a Federal Superfund site in 2001. Mining and milling in the area resulted in unsafe metal concentrations in soil, sediment, and surface and ground water. Elevated concentrations of metals are sourced from waste rock, tailings, and discharging mine adits located throughout the district. Since its listing in 2001, the Environmental Protection Agency (EPA), in cooperation

The first claim was made in the Carpenter–Snow Creek Mining district in 1881, but limited transportation hindered early development. Production in the district increased by 1888, when construction of the smelter at Great Falls was completed and a branch of the Great Northern Railroad extended into Neihart (fig. 3). A federal mandate that required the United States government to purchase silver led to a drop in silver prices, and subsequently the Panic of 1893. Although mining slowed during this time, production continued, and several new mines were successfully developed in the area. The district experienced a small boom between 1916 and 1919 that resulted from rising silver prices, and



Figure 4. View of the Silver Dyke Mill and associated tailings today. The glory hole can be seen to the left of the mill.



Figure 5. Ore minerals (galena and secondary copper) in the glory hole (Silver Dyke Mine).

with the Montana Department of Environmental Quality (DEQ) and Tetra Tech, Inc. (EMI Unit), has worked to characterize the site through a Remedial Investigation report. The report summarizes all completed investigations and provides information necessary to complete the Feasibility Study, and support remedial action decisions. A major removal action of the remaining tailings in the historically breached impoundment was completed in 2014. However, a vast amount of remediation work is needed to mitigate risks at the site associated with metals and arsenic contamination.

The Early History (1982-2000) of Butte Mine Flooding

John Metesh

Director, Montana Bureau of Mines and Geology

Introduction

More than a century of underground mining of a zoned porphyry copper deposit in Butte, Montana (fig. 1) resulted in thousands of miles of horizontal and vertical workings that required extensive dewatering. When pumping of the Butte underground mines ceased on April 22, 1982, water levels in the shafts rose more than 2,000 feet in the first 20 months and an additional 930 feet over the next 20 years. Water-chemistry monitoring of flooding shafts indicated considerable difference between mines as well as rapidly changing chemistry with respect to time. The mines, their workings (shafts, cross-cuts, drifts, stopes etc.), and their underground linkages were all mapped in detail during the life of the district. Water monitoring in the flooding shafts from 1982 to 2000 identified differences in shaft-water chemistry, and the rates at which shaft-water chemistry changed through time, in the mines. Chemical differences in shaft waters should reflect mineralogy, mine geometry, and groundwater flow paths through time and space at each mine.

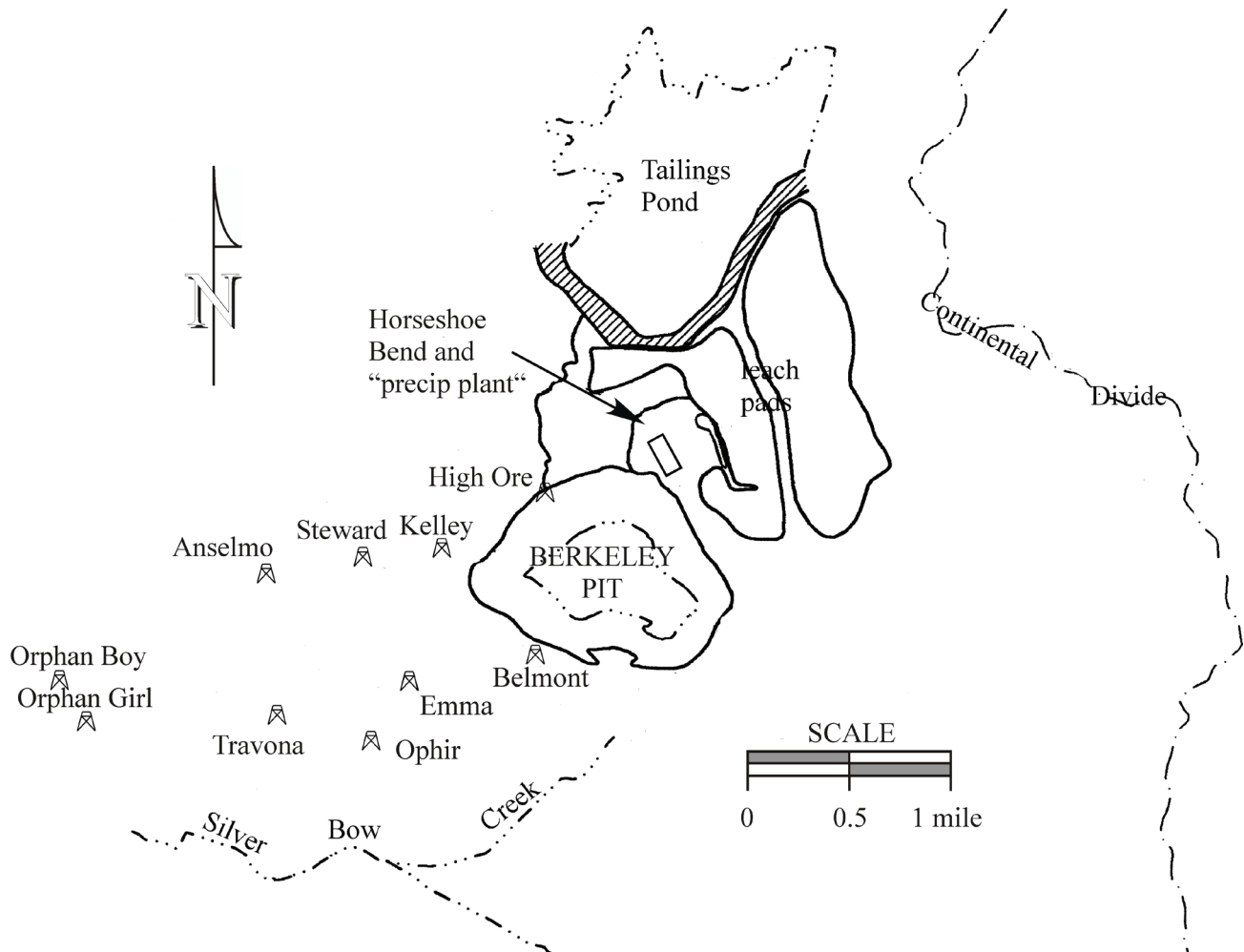


Figure 1. Flooding of the mines in Butte, Montana began with the shutdown of pumping at the Kelley and High Ore shafts in April 1982. Surface water, including discharge from Horseshoe Bend and the leach pads, was routed into the Berkeley Pit to prevent discharge to Silver Bow Creek.

Aspects of the Flow Model

Maps of the underground mine workings were used to estimate water volumes, water flow paths, and the influence that minerals from different parts of the district may have had on shaft-water chemistry from 1982 to 2000. A mine's geometry, and its position within the flooding system, were used to identify potential chemical source water flowing into the workings at each location. Geochemical-equilibrium models were constructed that reproduced observed water chemistry at six mine shafts into the ore body and the groundwater system. These results were used to determine groundwater flow paths for both early (1982–1984) and late (1984–2000) periods of Butte mine flooding.

Butte Mine Flooding: 1982–2000

An estimated 450 million cubic feet of surface water entered the workings via the Berkeley Pit during the first 20 months of flooding. The primary source of the Berkeley Pit water was an acid leaching operation identified through geochemical modeling of the mass balance of iron and copper in the receiving waters (fig. 2). Large, unpredictable fluctuations in water chemistry transitioned to stable, predictable trends after the initial effects of this surface-water inflow in the early period of mine flooding.

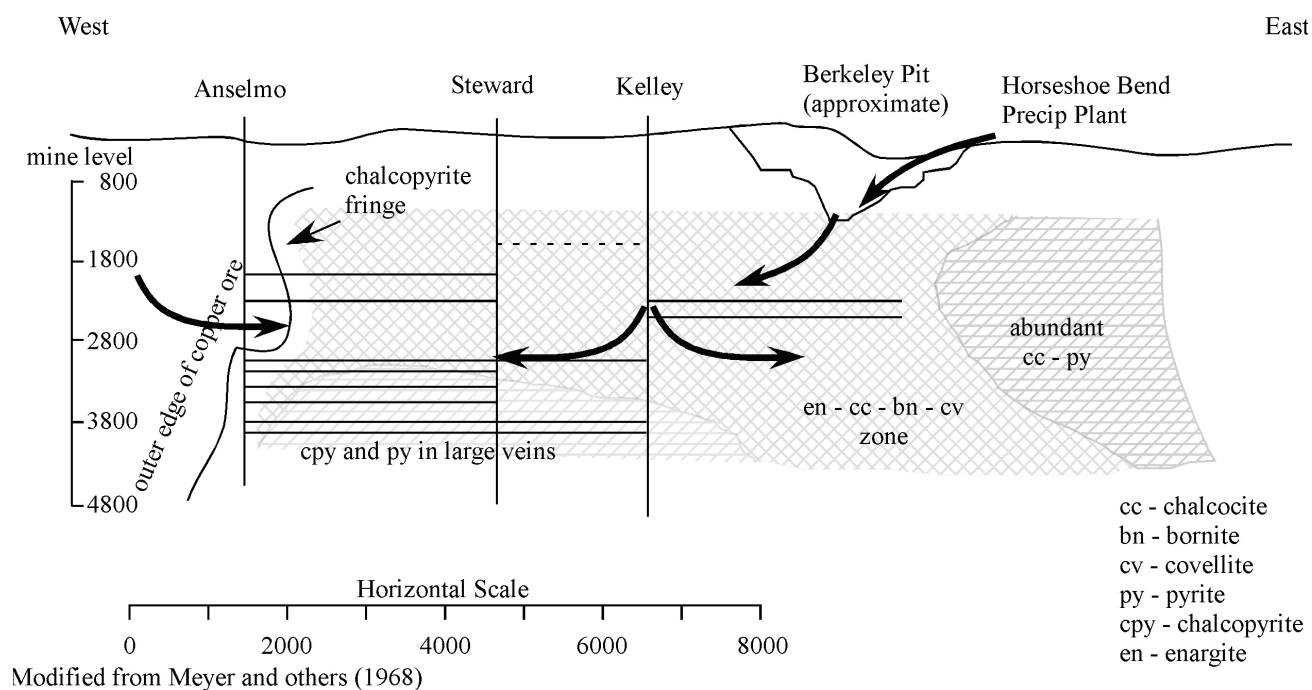
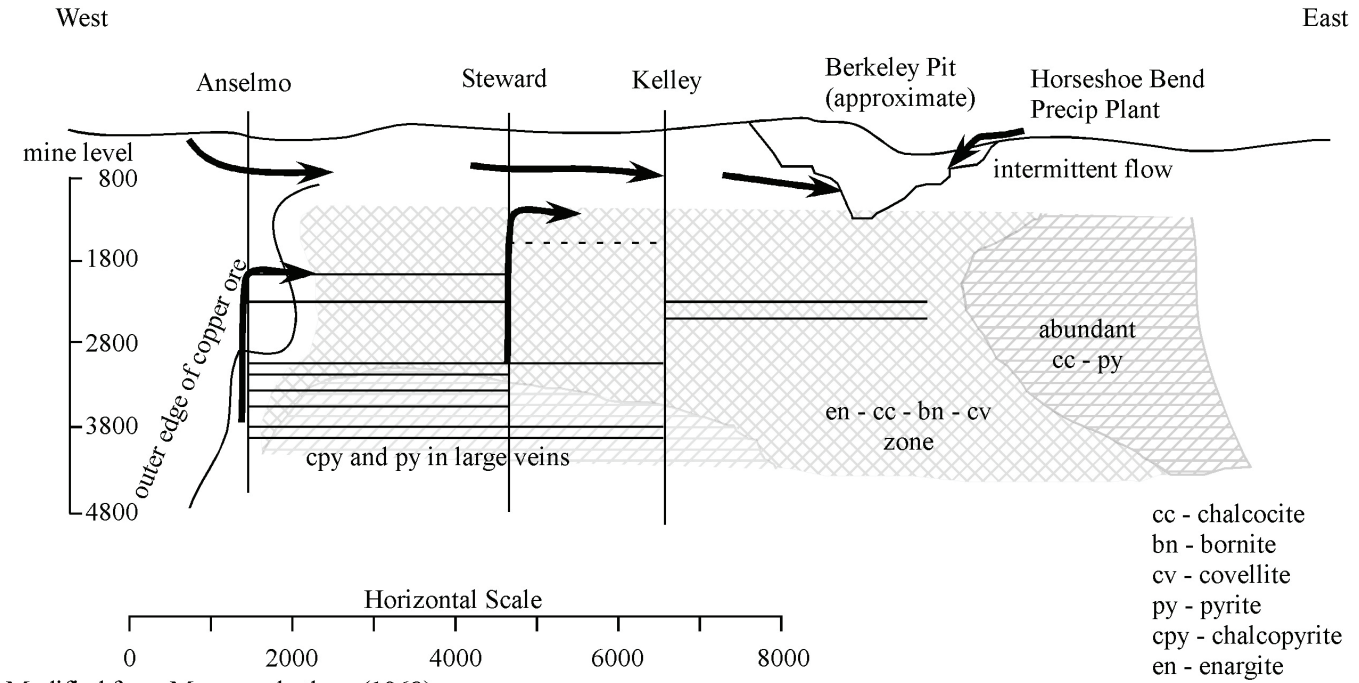


Figure 2. The conceptual model of the early period of flooding has waters entering the workings as groundwater from the edge of the district and as surface water from the Berkeley Pit. Flow arrows indicate the source and direction of waters filling the underground workings in the early period of flooding (1982 to 1984). Modified from Meyer and others (1968).

Geochemical modeling helped describe the redirection of flow paths that occurred in the later period (1984–2000) of flooding. After the first 20 months, water in workings generally flowed toward the Berkeley Pit, but vertical gradients within the workings were upward from the deeper workings and downward in the shallow bedrock aquifer (fig. 3).

Reference Cited

Meyer, C., Shea, E.P., and Goddard, C.C., 1968, Ore Deposits at Butte, Montana, *in Ore Deposits of the United States, 1933-1967, the Graton-Sales volume*, John D. Ridge, editor, American Institute of Mining, Metallurgy and Petroleum Engineering, Inc., New York, New York, Volume II, p. 1373-1416.



Modified from Meyer and others (1968)

Figure 3. The conceptual model of late flooding has waters continuing to enter the workings as groundwater from the edge of the district, but gradients prevent the flow surface water from the Berkeley Pit. Flow arrows indicate the source and direction of waters filling the underground workings in the later period of flooding (1984 to 2000). Water flows upward in the Anselmo and Steward shafts mixes with shallow waters, and then flows to the Kelley and Berkeley Pit.



Geologists attend the Map Chat at the Butte Brewing Company in uptown Butte, MT. Photo by A. Roth, MBMG.



MBMG's Director and Montana State Geologist John Metesh. Photo by A. Roth, MBMG.

Modeling Areas Susceptible to Ground Subsidence Due to Mine Drift and Shaft Collapse in Butte, Montana

Christopher P. Smith and Paul R. Thale
Montana Bureau of Mines and Geology

Abstract

Well-preserved historic mine maps are a valuable tool for identifying areas in historic mining communities that are susceptible to ground subsidence caused by mine drift and shaft collapse. Areas in uptown Butte, Montana have experienced ground subsidence due to hard rock mining that began in the 1870s, and subsequently produced thousands of miles of underground drifts and shafts. Block caving in these mine workings led to development of the Berkeley open pit mine (Berkeley Pit), which produced metals such as gold, silver, and copper from 1955 to 1982. We present here a three-dimensional model that displays all known underground drifts and shafts, and a map that shows all drifts and shafts located within 500 feet of the ground surface in uptown Butte. Areas susceptible to future ground subsidence lie above underground drifts and shafts that are within 500 feet of the ground surface.

Introduction

Ground subsidence caused by underground mine drift and shaft collapse is a common problem worldwide. Underground mining in Butte created over 5,600 miles of drifts and shafts beneath about 500 mine sites (Hoffman, 2001). Many of the underground features were consumed during development of the Berkeley Pit (fig. 1) beginning in 1955. Underground mining in the Berkeley Pit (fig.) ceased in the late 1970's and all operations in the pit closed by 1983 (Hoffman, 2001). Montana Resources (MR) currently mines a copper–molybdenum–porphyry deposit (Houston and Dilles, 2013) at the Continental Pit, and has since 1986. Despite a shift to open-pit mining, many underground drifts and shafts remain within 500 feet of the ground surface in uptown Butte (fig. 2).

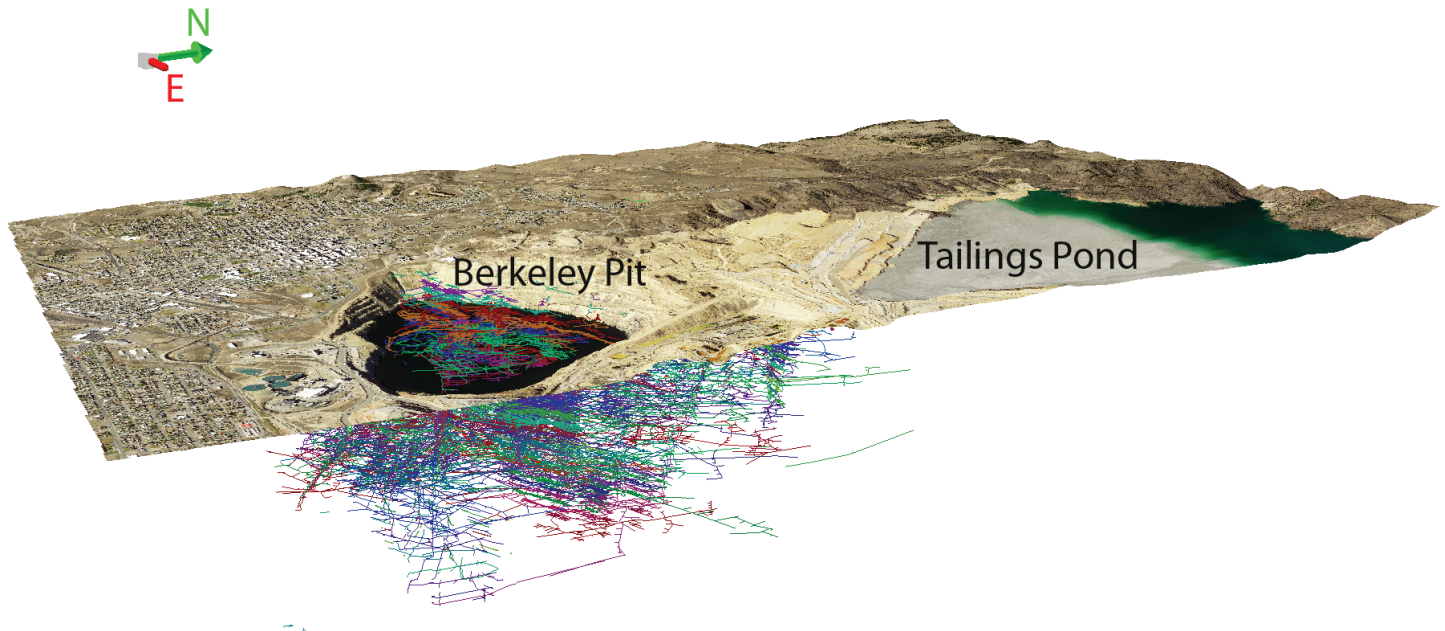


Figure 1. This three-dimensional model shows underground mine workings beneath uptown Butte. The image also shows drifts and shafts consumed during block caving and development of the Berkeley Pit. The Continental Pit (not shown), developed in 1986, is located immediately east of the Berkeley Pit. Model created using GIS.

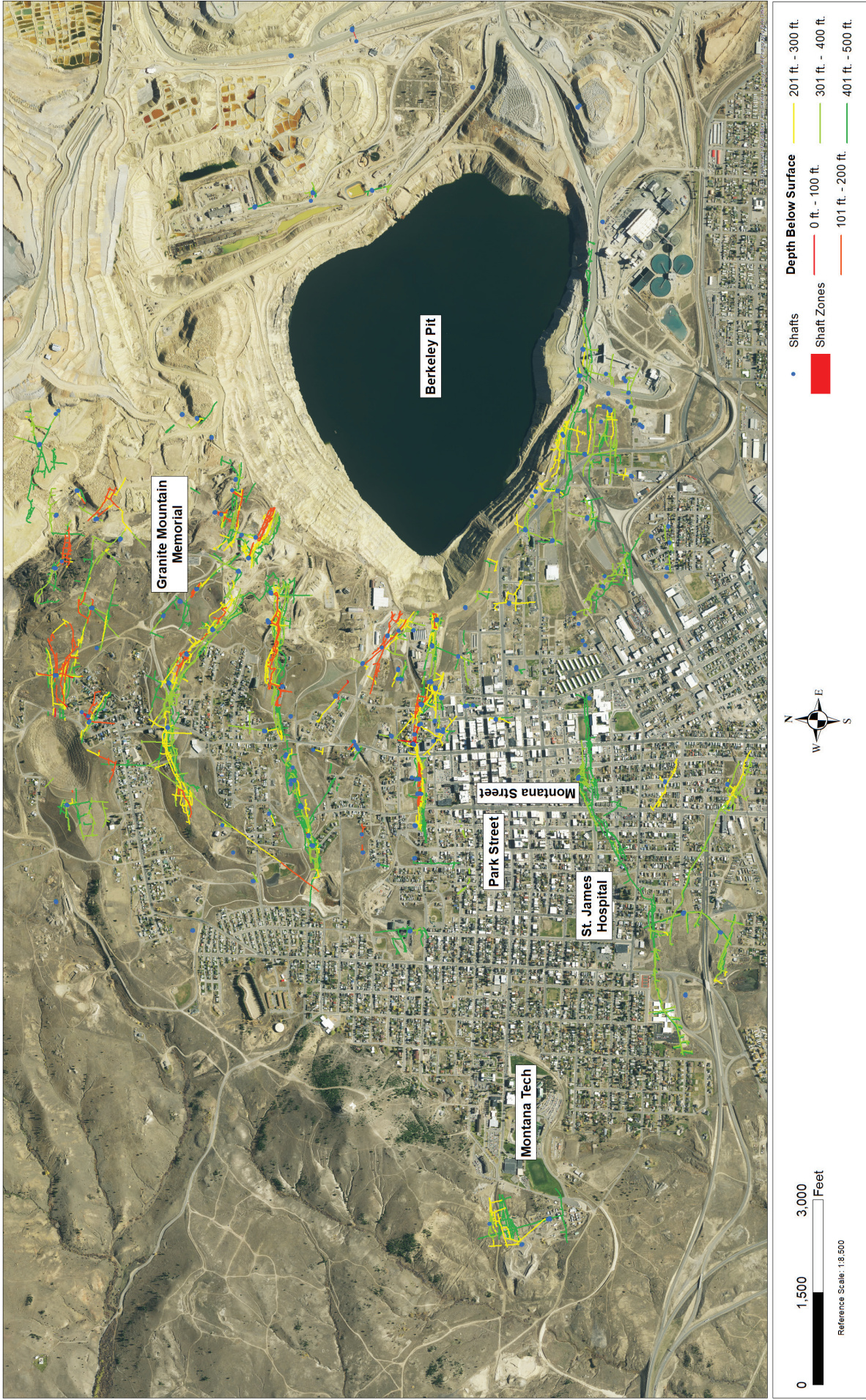


Figure 2. This map shows the depth and position of all mine drifts and shafts located within 500 feet of the ground surface at Butte, MT. These regions are particularly susceptible to ground subsidence caused by mine drift or shaft collapse.

Creating the Subsidence Models

We had to overcome challenges with spatial referencing in order to construct the 3D model of the Anaconda Copper Mining Company's (ACMC) mine drift and shaft locations (fig. 1), including: (1) Global spatial referencing—the elevation datum used to survey the ACMC's historic mine maps predated the National Geodetic Vertical Datum of 1929 (NGVD 29); and (2) local spatial referencing—the depth to drifts listed in ACMC stope books were in reference to the collar of the Alice Shaft (replaced with pit), or the collar of the Mountain Con. These factors eliminated the option of directly referencing the collar elevation in North American Vertical Datum of 1988 (NAVD 88) and applying a static correction to all drift elevations to project these data into NAVD 88. To overcome these issues, we digitized the ACMC historic mine maps and used known shaft locations to georeference them. A surface interpolated across the Alice Pit allowed us to estimate an elevation for the former Alice Shaft collar. We applied an approximate average elevation correction to all drifts in the ACMC stope books based on our estimate of the Alice Pit collar and the elevation of existing headframes.

Spatial analysis of the 3D model (fig. 1) using a 10-m Digital Elevation Model (DEM) allowed us to determine the depth below ground surface for each drift. We isolated the drifts located within 500 feet of the ground surface and displayed them over satellite imagery. This map shows one representation of areas susceptible to ground subsidence due to mine drift and shaft collapse in uptown Butte, Montana (fig. 2).

Results and Conclusions

Historic ACMC mine maps and a Geographic Information System (GIS) platform made it possible to conduct spatial calculations necessary to project subsurface data from an unknown local coordinate system to a recognized global coordinate system under uptown Butte, Montana. This allowed us to create spatial models, in 3D (fig. 1) and map view (fig. 2), that display locations identified as susceptible to ground subsidence due to mine drift or shaft collapse. Subsequent drilling intersected drifts shown in our models (T. Duaiame, written comm., 2017) and proves their locational accuracy.

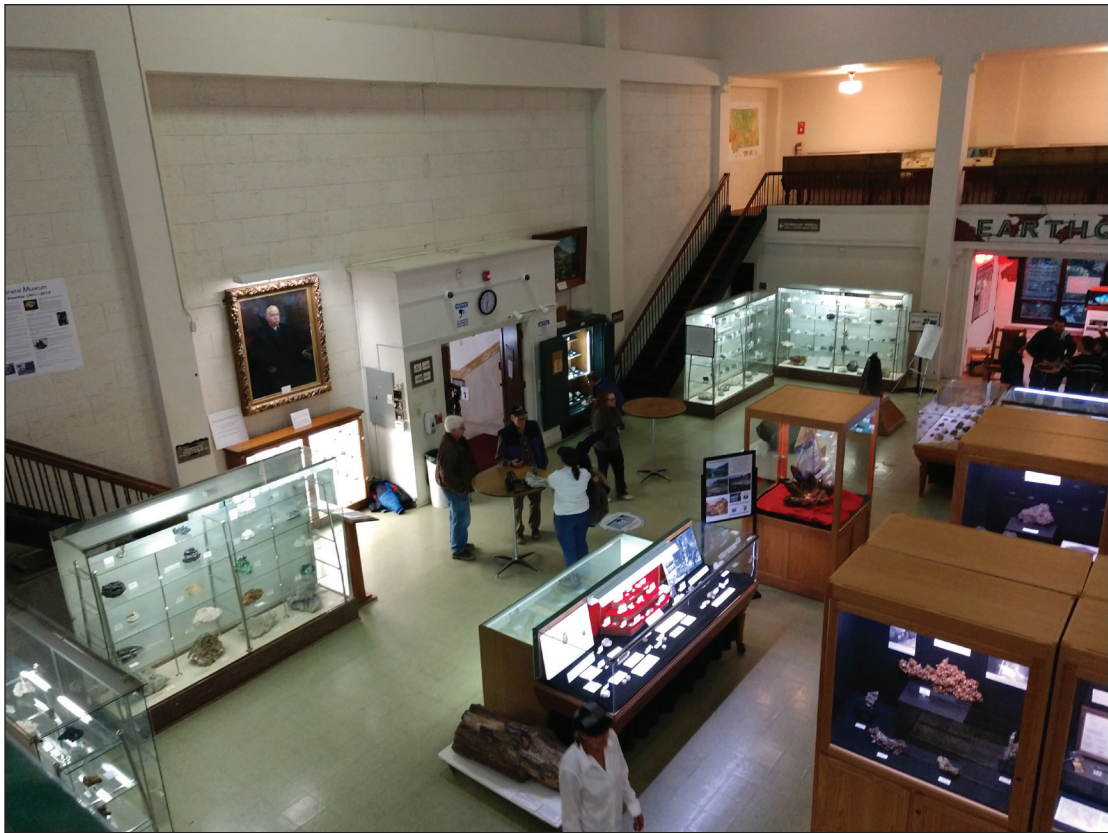
Our work highlights the importance and application of using archived data (ACMC mine maps and stope books) to address modern issues. Our models (figs. 1, 2) are currently used to address public questions about ground subsidence with visual representations. Our methods can be used to create similar models for any community in the world that has underground mine workings and archived mine data.

Acknowledgments

We would like to extend special thanks to Terence (Ted) Duaiame, MBMG, for presenting us with this challenging task.

References Cited

- Czehura, S.J., 2006, Butte: A world-class ore deposit: *Mining Engineering*, v. 58, p. 14–19.
- Hoffman, L., 2001, The mining history of Butte and Anaconda, *in* Mining History Association Annual Conference, 12th Annual, 2001: Montana Tech of the University of Montana.
- Houston, R.A., and Dilles, J.H., 2013, Structural geologic evolution of the Butte district, Montana: *Economic Geology*, v. 108, no. 6, p. 1397–1424.



Meet and Greet at the Mineral Museum on the Montana Tech campus. Photo by A. Roth, MBMG.



Poster session at Montana Tech. Photo by A. Roth, MBMG.

POSTERS AND ABSTRACTS



Montana Tech Geosciences—Geochemistry graduate student Shanna Law receives her award for “best student poster” at the symposium banquet. Photo by A. Roth, MBMG.



Montana Tech Professional and Technical Communications major Jonathan Dupuis (center) at the symposium banquet. Photo by A. Roth, MBMG.

Thermochemical Arsenite Reduction and the Origin of Hydrothermal Arsenide Minerals

Nick Allin

Experiments are being conducted to determine the relative rates of reduction of aqueous sulfate and aqueous arsenite ($\text{As}(\text{OH})_3, \text{aq}$), using foils of copper, nickel, or cobalt as the reductant, at temperatures of 150 to 300°C. At the highest temperature, sulfate was partly reduced to sulfide with precipitation of Cu_2S (chalcocite) on copper foil and NiS_2 (vaesite) + $\text{NiSO}_4 \cdot x\text{H}_2\text{O}$ on nickel foil. In the 300°C arsenite reduction experiments, Cu_3As (domeykite), Ni_5As_2 , and CoAs (langisite) formed. Whereas reduction of sulfate has not been observed below 250°C, reduction of arsenite by copper to form domeykite is rapid to at least 150°C. The implication is that a low-temperature fluid carrying both aqueous sulfate and arsenite will quickly precipitate metal-arsenide minerals at a reducing interface, whereas sulfate reduction is much slower, especially at temperatures below 250°C. This helps to explain the abundance of metal-arsenide minerals and relative lack of metal-sulfide minerals in certain ore deposit types, including unconformity-type U-Ni and “5-element suite” vein deposits.

An Occurrence of Cu-Ni-Co-Au-PGE in the Grouse Mountain Dike, Troy District, Lincoln County, Montana

John E. Etienne

Geologist, PO Box 1982, Hayden, ID 83835

This research into the copper–nickel–cobalt–gold–platinum–palladium potential of the Grouse Mountain Dike (GMD) started in 2004. Five mining properties were examined as part of this study, all occurring along the GMD. From southeast to northwest, the properties are the Bluebird, Black Horse (Highland Chief), Iron Mask (Eureka), Hiwatha, and the Copper King (Diamond H). All geochemical assays were completed by ALS Chemex, Vancouver, BC. The Cu-Ni-Co-Au-PGE mineralization typically displays copper oxides on exposed surfaces. Areas of GMD outcrop that more closely resemble a felsic intrusive rock were not observed hosting the Cu-Ni-Co-Au-PGE mineralization.

The Troy Mining District, in northwest Montana, has historically been explored for lead, zinc, silver, and copper since the late 1800s. Many prospects were located along the length of Grouse Mountain, 9 kilometers southwest of the town of Troy, mostly for lead, silver, and zinc, with sporadic occurrences of copper being reported over the years. Rowe (1928) mentions platinum being found in an unspecified location near Troy. Johns (1970) reported on nickel being found in a diorite sill northwest of Troy, while the U.S. Bureau of Mines (Brink, 1988) reported an occurrence of nickel in the generic “Troy Dike,” located in the general area of Grouse Mountain. More recently, in 1987, Newmont Exploration Limited, while examining the Iron Mask property on Grouse Mountain, collected samples from a prospect pit in an intensely altered part of the dike; two of these samples assayed 27.4 ppm (0.8 oz/ton) and 13.7 ppm (0.4 oz/ton) platinum with abundant copper and arsenic.

The Grouse Mountain area is underlain by slightly metamorphosed sediments and altered mafic to intermediate intrusives. The sediments are argillites and quartzites of the Proterozoic Belt Supergroup Prichard Formation. The Prichard has a dominantly northwest strike with dips ranging from 40° to 70° to the southwest (Phendler, 1982).

Intruding these sediments is a steeply southwest-dipping, coarse-grained mafic to intermediate intrusive known locally as the Grouse Mountain Dike. Original composition of the dike ranged from diabase to diorite, but hydrothermal and regional metamorphism has altered its composition to sericite, chlorite, biotite, and

carbonate (Gibson, 1948). The GMD is traceable for a total length of about 3,600 meters along a northwest strike. At the Iron Mask property the GMD is cut by a 1- to 2-meter-thick porphyritic quartz latite dike, called the “spotted porphyry” dike. While in some locations the GMD appears to cut across bedding and, technically, is a dike, in other locations it shows relative conformity to the enclosing Prichard Formation and so therefore is more sill-like. The dike is up to 76 meters wide.

At the Bluebird prospect, the GMD typically appears as a dark, greenish-gray, medium-grained, equigranular dike containing abundant fine-grained, disseminated sulfides, mostly pyrrhotite. Some areas of the dike above the main adit appear more felsic in composition. Assays of grab samples collected contained platinum and palladium, mostly in the 0.010–0.022 ppm range, but at the portal of the main adit, a malachite- and azurite-stained zone in the dike contained 0.05 ppm Au, 0.181 ppm Pt, 0.288 ppm Pd, 0.292% Cu, 0.101% Ni, and 168 ppm Zn. A grab sample of malachite-stained dike exposed in a road cut assayed 0.051 ppm Au, 0.035 ppm Pt, 0.071 ppm Pd, 0.397% Cu, and 891 ppm Ni.

The Black Horse prospect is an adit following an irregular quartz–calcite vein in the GMD. The vein itself contains irregular masses of sulfides, and grab samples show its platinum and palladium content generally <0.050 ppm, with copper, cobalt, nickel, and zinc in anomalous amounts. The surrounding altered dike contains fine-grained sulfides and higher platinum and palladium (0.052 and 0.072 ppm, respectively). Highest palladium values (0.154 ppm), along with elevated Au (0.097 ppm), Co (300 ppm), Cu (0.252%), Ni (0.219%), Pb (0.523%), and Zn (0.901%), came from a soft, hematitic-limonitic gouge zone near the face of the adit.

At the Iron Mask (Eureka) mine, multiple areas were examined. Near where the 1987 Newmont PGE samples were collected, a continuous series of 1-meter-long channel samples were collected across part of a prospect pit wall near the center of the GMD. Across 6 meters, the assays averaged 0.036 ppm Au, 650.7 ppm Co, 0.22% Cu, 0.146% Ni, 0.031 ppm Pt, and 0.041 ppm Pd. In 1992, several short diamond drill holes were completed under this pit. Only fragments of the core still exist, but one sample from 9.1 to 10.7 meter (30–35 foot) depth in DDH #3 contained 0.315 ppm Au, 476 ppm Co, 1.09% Cu, 0.546% Ni, 0.082 ppm Pt, and 0.029 ppm Pd from altered dike containing veinlets and disseminations of arsenopyrite, pyrrhotite, and chalcopyrite. To the southeast of this pit, grab samples yielded up to 2.27 ppm Au, 467 ppm Co, 0.2% Cu, 854 ppm Ni, 0.033 ppm Pt, and 0.214 ppm Pd in highly altered dike. To the northwest, the Copper adit was examined and a grab sample, collected from a 0.3-meter-wide zone of malachite-stained dike inside the tunnel, assayed 0.246 ppm Au, 219 ppm Co, 1.04% Cu, 0.217% Ni, 0.454 ppm Pt, and 1.12 ppm Pd. Inside the Eureka adit, a 0.3-meter-wide zone of malachite-stained dike and carbonate–quartz vein was grab sampled, returning 0.199 ppm Au, 1.91% Cu, 459 ppm Ni, 0.055 ppm Pt, and 0.089 ppm Pd. In the two samples of malachite-stained dike collected from underground, the copper-rich zones seem to be near the center of the GMD.

The GMD on the Hiwatha claim displays, in places, a felsic intrusive texture and does not appear to host any of the copper–nickel mineralization, but may host lead–zinc mineralization. A lead isotope date from this type of mineralization yielded a Proterozoic age (Marvin and Zartman, 1984).

The northwesternmost occurrence of the Cu-Ni-Co-Au-PGE mineralization is at the Copper King (Diamond H) claim. Here, at the collar of a collapsed shaft, is a 2- to 3-meter-wide zone of altered, brecciated GMD containing abundant limonite, goethite, malachite, and scattered fine-grained sulfides, mostly chalcopyrite. Four grab samples collected across this zone averaged 0.156 ppm Au, 289.9 ppm Co, 1.36% Cu, 0.35% Ni, 0.259 ppm Pt, and 0.393 ppm Pd.

Using surface field observations, plus limited underground exposures and remnants from short drill holes, the following description has been assembled for the Cu-Ni-Co-Au-PGE mineralization occurring on Grouse Mountain. The mineralized zones may appear as irregular-defined, malachite-stained, propylitically altered dike and carbonate–quartz veins (Iron Mask; Bluebird) or as a well-defined zone of brecciated, sheared, limonitic dike with malachite staining (Copper King). Both types of malachite-stained zones probably represent mineralization occurring along faults. Visible sulfides are arsenopyrite, pyrrhotite, chalcopyrite, and pyrite. The sulfides may occur as scattered grains or in veinlets cutting across the altered material. Boxwork and goethite veinlets are common in more altered outcrops. Structurally, the mineralization occurs near the middle of, and appears to

dip parallel to, the GMD. Base metal veins, with little PGE, nickel, or cobalt, commonly occur along the foot-wall contact of the dike or in its interior.

A nearby analogy to the Grouse Mountain Cu-Ni-Co-Au-PGE mineralization could be the Revais Creek Intrusive (RCI) located near Dixon, Montana. Most recent descriptions of the RCI (Mudge and others, 1976; Lauer, 1998; Wentland, 2007) have described the known high-grade PGE mineralization as being localized along fault zones at the contact between the intrusive and the host Proterozoic Belt Supergroup Ravalli Group. These mined high-grade zones tended to be crushed, clay-rich zones (Mudge and others, 1976). The RCI has been dated at 687–697 Ma, placing it in a series of Neoproterozoic intrusives related to the Windermere rifting event between 780 and 550 Ma (Burtis and others, 2007; Burtis, 2003). It is believed that the GMD may also be one of these Neoproterozoic intrusives, as it appears to be different from the nearby 1455–1469 Ma Purcell sills.

The RCI mineralization has been described as hydrothermal in origin (Lauer, 1998; Wentland, 2007). At the GMD, Pd is more abundant than Pt, and there is associated hydrothermal alteration and high Cu/Ni ratios, all of which are typical of PGE mineralization in gabbro-hosted hydrothermal deposits such as New Rambler, Wyoming (Hubert and others, 1988). Therefore, a hydrothermal origin for the GMD-hosted Cu-Ni-Co-Au-PGE mineralization is proposed.

References Cited

- Brink, S.E., 1988, Troy Dike: U.S. Bureau of Mines Minerals Availability System Mineral Property File #0300530249.
- Burtis, E.W., Sears, J.W., and Chamberlain, K.R., 2007, Age and petrology of Neoproterozoic intrusions in the northern Rocky Mountains, U.S.A.: Correlation with the Gunbarrel Magmatic Event, *in* Proterozoic geology of western North America and Siberia, SEPM Special Publication No. 86, p. 175–191.
- Burtis, E.W., 2003, Neoproterozoic sills and dikes in northwestern Montana: Implications for magmatic activity associated with early Windermere rifting: Missoula, University of Montana, unpublished MS thesis, 116 p.
- Gibson, Russell, 1948, Geology and ore deposits of the Libby quadrangle, Montana: U.S. Geological Survey Bulletin 956, p. 103–104.
- Hubert, L.J., Duke, J.M., Eckstrand, O.R., Lydon, J.W., Scoates, R.F.J., and Cabri, L.J., 1988, Geological environments of the Platinum Group elements: Geological Survey of Canada Open File 1440, 148 p.
- Johns, W.M., 1970, Geology and mineral deposits of Lincoln and Flathead Counties, Montana: Montana Bureau of Mines and Geology Bulletin 79, 182 p.
- Lauer, D.D., 1998, Hydrothermal copper and platinum group element mineralization in the Revais Creek intrusion, Flathead Indian Reservation, west-central Montana: Missoula, University of Montana, unpublished MS thesis, 107 p.
- Marvin, R.F., and Zartman, R.E., 1984, A tabulation of lead isotopic ratios for lead minerals from mines and prospects in the Belt-Purcell Basin in the United States and Canada: U.S. Geological Survey Open File Report 84-210, 15 p.
- Mudge, M.R., Harrison, J.E., Kleinkopf, M.D., and Ingersoll, R.G., 1976, Status of mineral resource information for the Flathead Indian Reservation, Montana: Bureau of Indian Affairs, Administrative Report BIA-22, 58 p.
- Phendler, R.W., 1982, Report on the Bluebird Property, Lincoln County, Montana: Private report for Grenoble Energy Limited, 18 p.
- Rowe, J.P., 1928, Minor metals and non-metallic minerals of Montana: *Engineering and Mining Journal*, v. 125, no. 20, p. 818.
- Wentland, D.T., 2007, Copper and platinum group element mineralization in the Revais Creek intrusion, Flathead Indian Reservation, Sanders County, Montana: Golden, Colo., Colorado School of Mines, unpublished MS thesis, 139 p.

Identifying Environmental Tracers Using Water Chemistry and Stable Isotopes, Moulton Road Area, Butte, Montana

Matt Berzel

Montana Bureau of Mines and Geology

This study was conducted to identify environmental tracers using water chemistry and stable isotopes in the Moulton Road area adjacent to the Yankee Doodle tailings impoundment north of Butte, Montana. The water level of the tailings lake is being raised as tailings slurry is pumped up to the impoundment, and numerous residential wells are located in close proximity. Although it has an alkaline pH (>9), the water in the tailings lake is much higher in some chemical constituents than the wells, and some of these constituents could be used as tracers to determine if lake water is migrating out of the impoundment due to the rising level. Tracers examined in this study include the O- and H-isotopic composition of water and the concentration and S- and O-isotopic compositions of dissolved sulfate. Although water in the tailings lake is partly evaporated, the contrast between the isotopic signature of the lake and the groundwater wells is relatively small, making it a less powerful tracer. On the other hand, sulfate concentrations are more than an order of magnitude higher in the lake than in the groundwater. Whereas the S-isotope compositions of dissolved sulfate in lake and groundwater samples are similar, the O-isotope compositions of sulfate for the two end members are very different (-2.8 and -14.0‰, respectively). A conservative mass balance model was used to predict changes in the concentration and isotopic composition of sulfate in background groundwater as water sourced from the tailings lake is mixed in. As little as 5% mixing of lake water is enough to cause a substantial shift in the $\delta^{18}\text{O}$ of dissolved sulfate in a long-term groundwater monitoring well.

This study also reports new data on the geochemistry of the active tailings slurry, the shallow sediment in the tailings lake, and the shallow sediment pore water of the lake. Acid-base accounting tests show that the solid fraction of the tailings slurry is net acidic, and will generate acid leachate if allowed to completely oxidize. The shallow sediment in the lake is also net acidic, but has somewhat higher neutralization potential compared to the slurry due to precipitation of calcite in the lake. Results from sediment pore water samplers (peepers) and piezometers show very little change in the chemistry of the pore water as the sediment is buried, at least to a depth of 8 feet. Vertical gradients in the pore waters are directed upwards, consistent with an increase in pore-water pressure as the tailings sediments consolidate.

Based on the results of this study it is recommended that $\delta^{18}\text{O}$ -sulfate should be added to the list of analytes obtained from long-term monitoring wells in the Moulton Road area. This parameter is the most powerful tracer of potential mixing of lake water and background groundwater.

Mapping Hydrothermal Alteration in the Belt Supergroup Using a pXRF

Philip Dalhof

This project aims to test the hypothesis that it is feasible to create a map using a portable x-ray fluorescence device (pXRF) as a field expedient tool with which to analyze and characterize terrains to identify geochemical anomalies of potential exploration value by conducting spot sampling of overlying soils (at the C horizon), and corroborating this data with geochemical modeling. Ideally, these models would help portray the geometry potassic, phyllic, or argillic zones of alteration caused by hydrothermal fluid flow, providing a new tool for understanding and visualizing both hydrothermal pathways and, potentially, the proximity of ore body emplacements on a regional scale. This map will also serve to validate the pXRF as a stand-alone tool capable of detecting faint chemical ratio and compositional changes in any terrain.

To ensure the presence of hydrothermal alteration in at least some of the 251 samples collected, the field site was a roughly 4-km² area, lithologically constrained to lay solely within the Belt Group, adjacent to the Golden Sunlight Mine.

GeoWrite: A Digital Field Notebook

Jonathan Dupuis

Jonathan developed GeoWrite for his senior project, as a requirement to complete his Professional and Technical Communications degree. GeoWrite functions as a pocket reference guide for geologists in the field, allowing them quick access to numerous ArcGIS maps and Microsoft OneNote. The app is a working mockup of what digital field journals may look like in the future. Feature enhancements may include automatic geotagging, cataloging photos, and the ability to choose specific maps and databases (e.g., mineral identification databases, geologic maps, subsurface mine workings, etc.).

Mineralogy and Stable Isotope Geochemistry of the Apex Gold Deposit near the Golden Sunlight Mine, Montana

Hamadou Gnanou and Christopher H. Gammons

Department of Geological Engineering, Montana Tech, Butte, Montana

The Golden Sunlight mine, located 50 km to the east of the famous Butte porphyry/lode deposits, is the largest gold mine in Montana, and has produced over 3 million ounces of gold in its 35-plus year history. Most of this gold has come from the Mineral Hill breccia pipe (MHBP), a west-dipping, cylindrical body of brecciated latite and country rock fragments of the Precambrian LaHood and Greyson Formations. The breccia pipe is late Cretaceous in age (84 ± 18 Ma, DeWitt and others, 1986), is silicified, pyrite-rich, and is mineralized with gold, silver, and minor base metals. Because the MHBP has largely been mined out, the current owners of the mine, Barrick Gold, have been exploring a new prospect, called Apex, to the north of the main MHBP ore body. This deposit exists near the unconformable contact between the Proterozoic Greyson Formation and the overlying Cambrian Flathead Formation. Both sedimentary units are mineralized, although exploration has focused more on structures in the Greyson. The purpose of the current study is to examine the mineralogy and stable isotope geochemistry of Apex to see how it relates to the MHBP.

Reflected and transmitted light microscopy and SEM-EDS analyses of polished core samples from Apex reveal a complex paragenesis of ore and gangue minerals that is similar to that described by previous workers for MHBP. Pyrite is the dominant sulfide, accompanied by common sulfides such as galena, sphalerite, chalcopyrite, bornite, and tetrahedrite-tennantite, as well as less common phases such as pearceite ($\text{Cu}(\text{Ag,Cu})_6\text{As}_9\text{S}_{11}$), tetradymite ($\text{Bi}_2\text{Te}_2\text{S}$), aikinite (CuPbBiS_3), goldfieldite ($\text{Cu}_{10}\text{Te}_4\text{S}_{13}$), and electrum (Au-Ag alloy). Gangue minerals include quartz, barite, anhydrite, adularia, dolomite, siderite, sericite, rutile, althausite, and magnetite. Analyses of drill core with a Terraspec Halo SWIR device reveal that illite, muscovite, and kaolinite are the dominant alteration minerals, with several detections of the NH_4 -rich K-feldspar, buddingtonite.

The S-isotope composition of pyrite in veins from the Apex deposit overlaps with pyrite from the MHBP (as determined by previous workers). In both deposits, there is a cluster of $\delta^{34}\text{S}$ values in the range of -10 to -5‰, with a tail to more positive values >0‰. The heavier S appears to be associated with sedimentary pyrite in the Precambrian Belt sediments, whereas the lighter S is of hydrothermal origin. The fact that the mineralogy and S-isotopic compositions at Apex and MHBP are similar implies that both deposits formed in the same ore-forming event. The unusual S-isotope composition of sulfides at Apex and MHBP may have been caused by assimilation of isotopically light sulfide at a deeper crustal level by ascending magmas and associated hydrothermal fluids that formed the mineral deposits.

Reference

DeWitt, E., Foord, E.E., Zartman, R.E., Pearson, R.C., and Foster, F., 1996, Chronology of Late Cretaceous igneous and hydrothermal events at Golden Sunlight gold-silver breccia pipe, southwestern Montana: U.S. Geological Survey Bulletin, v. 2155, 48 p.

Distribution of Sulfide Minerals in Metasedimentary Deposits of the Apple Creek Formation, Salmon River Mountains, Idaho

Francis Grondin

Montana Tech, Butte, Montana

The Idaho Cobalt Belt (ICB) is located in east-central Idaho and is a geologically complex and economically significant area within the Salmon River Mountains. The belt extends 60 kilometers and trends northwest–southeast, containing rich metallic deposits of cobalt, copper, and gold. Thirty hand samples were collected from the coarse and banded siltite units throughout the ICB, and distribution and characterization of sulfides within these units are the focus of this study. Not surprisingly, the distribution of sulfides (chalcopyrite, pyrite, cobaltite) varies spatially within and adjacent to the ICB. Most often sulfides occur disseminated within the siltites and decrease closer to the Idaho Batholith.

Using Fluid Inclusions and C, O, H and Sr Isotopes to Understand the Genesis of Dolomite-Hosted Talc Mineralization in Montana

Garrett W. Hill and Christopher H. Gammons

Department of Geological Engineering, Montana Tech, Butte, Montana

Talc and chlorite deposits of southwest Montana formed as hydrothermal replacements of Archean and/or early Proterozoic dolomitic marble and quartzo-feldspathic gneiss. Although the hydrothermal replacement model is generally accepted, less is known about the temperature, composition, and origin of the fluids involved in talc and chlorite formation. The current study is examining fluid inclusions in quartz associated with both talc and chlorite, stable hydrogen and oxygen isotopes of talc, chlorite, and quartz, and stable carbon, oxygen, and strontium isotopes of carbonate minerals. The deposits examined include the Yellowstone, Beaverhead, and Willow Creek talc mines, and the Antler chlorite mine.

Fluid inclusion studies of quartz and dolomite from Yellowstone shows moderately high salinity (14.5–21.7 wt% NaCl eq.) and a low homogenization temperature range of 101 to 125°C. These temperatures are not corrected for pressure. All the inclusions are simple two-phase, liquid-rich fluids; the lack of CO₂-clathrate or CO₂(l) phases indicates a low CO₂ partial pressure, which would favor talc formation at the expense of dolomite. Fluid inclusions from Antler have slightly higher homogenization temperatures of 177 to 239°C but lower salinities of 9.2–13.3 wt% NaCl eq. Bulk leachate analyses are in progress to learn more about the Ca-Na-K-Mg and Cl-Br ratios of the inclusion fluids. The O-isotope compositions of talc and quartz from the Yellowstone Mine are +2.1 to +3.8 and +11.1 to +15.9‰, respectively. Oxygen-isotope geothermometry based on coexisting talc + quartz gives temperature estimates of 146 to 218°C. The H-isotopic composition of Yellowstone talc ranges from -53 to -45‰. Using published isotope fractionation factors for talc–quartz–water, and assuming a temperature of formation of 150 to 250°C, the stable isotope data are consistent with the idea that the talc-forming fluids were sourced from meteoric water that subsequently became moderately saline through dissolution of evaporites and/or water–rock interaction. Another idea, that the fluids were sourced from evaporated seawater, is also being evaluated. Carbonate and strontium isotope analyses (in progress) may help to decide which hypothesis best fits the data.

Eocene Ignimbrite Flare-Up in the Northeastern U.S. Cordillera: Timing and Style of Volcanism in the Lowland Creek Volcanic Field of Southwestern Montana

Kaleb C. Scarberry

Montana Bureau of Mines and Geology

Abstract

The Eocene Lowland Creek Volcanic field is located north and west of Butte, Montana. The volcanic field formed in the Challis–Kamloops–Absaroka volcanic belt between about 53 Ma and 49 Ma following basement-cored deformation (Laramide orogeny) in southwestern Montana. Volcanic products include evolved composition rhyolite tuffs (fig. 1A), porphyry rhyodacite lavas (fig. 1B), and small piles of crystal-poor andesite lavas. The predominance of felsic compositions in these deposits is unusual compared to Eocene igneous rocks in Montana, which tend to be more mafic. Compositionally, the Lowland Creek deposits resemble younger rhyodacite lavas and tuffs of the ignimbrite flare-up in the Great Basin. This study favors a model in which the Lowland Creek Volcanic field erupted in a transtensional pull-apart basin during an early phase of southward-sweeping, ignimbrite flare-up volcanism. Volcanic activity, coincident with the onset of extension, likely records initiation of slab roll-back (Farallon plate) in the northeastern U.S. Cordillera.

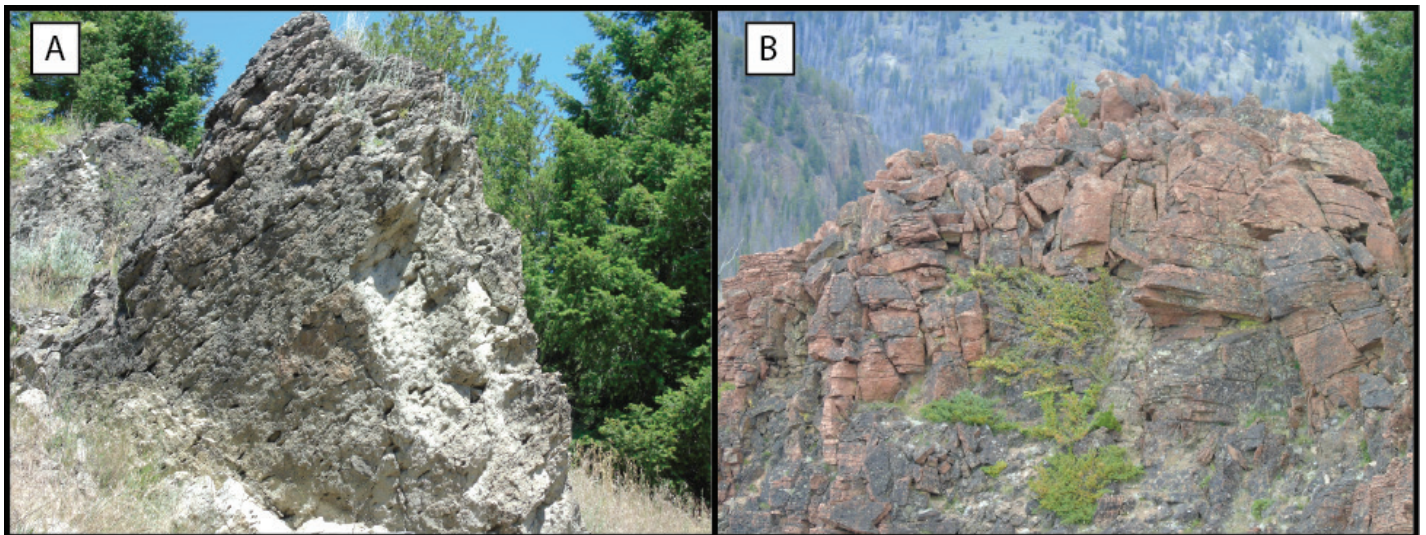


Figure 1. Lowland Creek Volcanics: (A) compaction foliation in non-welded rhyolite tuff in Hail Columbia Gulch, west of Butte; (B) flow-banded rhyodacite porphyry lavas on top of Sheepshead Mountain, north of Butte.

Hydrothermal Water-Rock Interactions: From Mineralogy to Water Chemistry

Shanna Law and Alysia Cox

Department of Chemistry and Geochemistry, Montana Tech, Butte, Montana

The aqueous compositions of hot springs are controlled by hydrothermal water–rock interactions at depth and are affected by thermophilic microbes living in the hydrothermal system. We investigated the controls on aqueous hydrothermal chemistry in the Rabbit Creek area of Yellowstone National Park (YNP). The EQ3/6 program modeled water–rock interactions and predicted aqueous chemical speciation of elements in a deeply sourced hot spring. Using EQ3/6, we reacted the summarized mineralogy of hydrothermally altered volcanic tuffs in YNP drill core Y-5 with local meteoric water chemistry. The EQ6 output represents the aqueous chemical speciation expected in a deeply sourced hot spring due only to local hydrothermal water–rock interactions. We also sampled and measured the aqueous geochemistry of a deeply sourced hot spring proximal to the drill core. This measured aqueous chemistry was speciated with EQ3. The EQ3 output represents the aqueous hydrothermal chemistry due to water–rock–microbe interactions. Preliminary model outputs suggested that water impacted by water–rock–microbe interactions has lower concentrations of most calcium species and manganese species than water impacted only by water–rock interactions. In contrast, both model outputs predicted concentrations on the same order of magnitude for most strontium species and barium species. Although trace metals are poorly represented in the model, trace metals measured in the Y-5 drill core compared to the deeply sourced hot spring water showed no apparent trends. Further iterations of these preliminary models and comparisons to other local hot springs are underway.

Montana Lamprophyre Occurrences

Jake McCane

Colorado State University, Fort Collins, Colorado

Lamprophyric rocks are rare, hypabyssal, potassic, igneous rocks that are closely associated with numerous world-class mineral deposits. The geologic community's understanding of the petrogenesis of lamprophyric rocks is the poorest of any igneous rock type and their relationships with other rock and magma types remains an enigma. There are two contrasting models for the petrogenesis of lamprophyres, magma mixing and mantle metasomatism. Work from Iddings (1895) and Prostka (1973) within Wyoming and Montana classified lamprophyres, analyzed petrographical relationships, and proposed a hybrid origin of these lamprophyres involving mixing of syenitic and mafic melts.

The purpose of this study is to: (1) stand as a case study, with focus on analyzing the petrogenesis of lamprophyres, which are known to be genetically related to numerous worldwide poly-metallic deposits; (2) test the validity of Prostka's proposed model for lamprophyres found throughout Montana against that of mantle metasomatism; (3) test if minerals within these lamprophyres are in geochemical equilibrium with the matrix; (4) provide better determinations of end member mixing; and (5) geochemically analyze mineral zonations, and hence constrain the nature of the components involved in a hybrid origin.

Prostka (1973) suggested that the textural and mineralogical features of 29 thin sections from the Absaroka Volcanic Province alluded to a hybrid origin of these lamprophyres. His model involves the invasion of a trachytic or syenitic magma into a mafic zone within a calc-alkaline pluton containing cumulates of labradorite, augite, olivine, hypersthene, and Fe-Ti oxides. Hybridization could also be obtained by this magma invading a gabbroic, mafic layered complex, or from syenitic magmas interacting with mafic and ultramafic rocks in the lower crust and upper mantle. In this model, the syenitic magma disaggregates the cumulate minerals and

partially assimilates them, thus becoming a mixture of crystals and a melt of lamprophyric composition. Prostka's study did not include geochemical or mineral chemical data to validate his magma mixing model of lamprophyres. Thus, a rare opportunity exists to analyze samples and test whether all crystals are comagmatic, and thereby assess which of the two contrasting petrogenetic models is more applicable to lamprophyres.

References

- Iddings, J.P., 1895, Absarokite–shoshonite–banakite series: *Journal of Geology*, v. 3, p. 935–959.
- Prostka, H.J., 1973, Hybrid origin of the absarokite–shoshonite–banakite series, Absaroka volcanic field, Wyoming: *Geological Society of America Bulletin*, v. 84, no. 2, p. 697–702.

Secondary Pb-Zn Mineralogy of the Summit Mine, Radersburg District, Broadwater County, Montana

Kyle Eastman and Nick Allin

Department of Geological Engineering, Montana Tech, Butte, Montana

Abstract

The Summit Mine is a Pb-Zn (Ag) carbonate replacement deposit (CRD-type) hosted in the Mississippian Madison Group limestone along the eastern limb of the Devil's Fence Anticline. During the first half of the 1900s, production was estimated at 5,000 tons of cerussite/smithsonite ore with grades to 10 oz/ton Ag and 10% Pb (Krohn and Weist, 1977). The Summit Mine is notable among mineral collectors as the source of some of the finest hemimorphite ($\text{Zn}_4\text{Si}_2\text{O}_7(\text{OH})_2 \cdot \text{H}_2\text{O}$) specimens in the U.S. Mineral identification was performed with a Thermo Scientific Niton XL3t GOLDD+ X-ray fluorescence spectrometer, an Olympus Terra X-ray diffractometer, and a Renishaw inVia Raman microscope. Complex secondary textures exist, with vuggy coliform and botryoidal Fe-oxides, jasperoids, and chalcedony dominant and intergrown with calcite, barite, and Pb, Zn, Cu, and V minerals. Hemimorphite occurs as elongate transparent colorless to pale blue bladed crystals, commonly with partial or complete pseudomorphism by chalcedony and druzy quartz. Descloizite ($\text{PbZn}(\text{VO}_4)(\text{OH})$) is the most common secondary vanadium mineral, and is often found intergrown with calcite. Boni and others (2007) used the (U-Th)/He method to date descloizite from the Otavi Mountainland region of Namibia, and this method could be applied at the Summit Mine to determine the age of secondary V mineral growth. Lesser amounts of mimetite and wulfenite were identified, in addition to the Zn-Cu carbonates rosasite and aurichalcite. This preliminary study indicates that the Summit Mine displays similar, but more complexly developed secondary mineralogy than other magmatic-hydrothermal CRDs in southwestern Montana, notably the Hecla District. Future work will investigate stable isotopes of S, C, and O, at the Summit Mine and other nearby CRDs, with the goal of determining the source of metals and nature of supergene fluids.

References

- Boni, M, Terracciano, R., Evans, N.J., Laukamp, C., Schneider, J., and Bechstadt, T., 2007, Genesis of vanadium ores in the Otavi Mountainland, Namibia, *Economic Geology* v. 102, p. 441–469.
- Krohn, D.H., and Weist, M.M., 1977, Principal information on Montana Mines, Montana Bureau of Mines and Geology Special Publication 75, 150 p.



Colorado State University Geology M.S. students Jake McCane (left) and Philip Dalhof (second from left) examine mafic intrusions on Bull Mountain north of Whitehall, MT with MBMG field geologists Petr Yakovlev (center) and Colleen Elliott (right). Photo by K. Scarberry, MBMG.

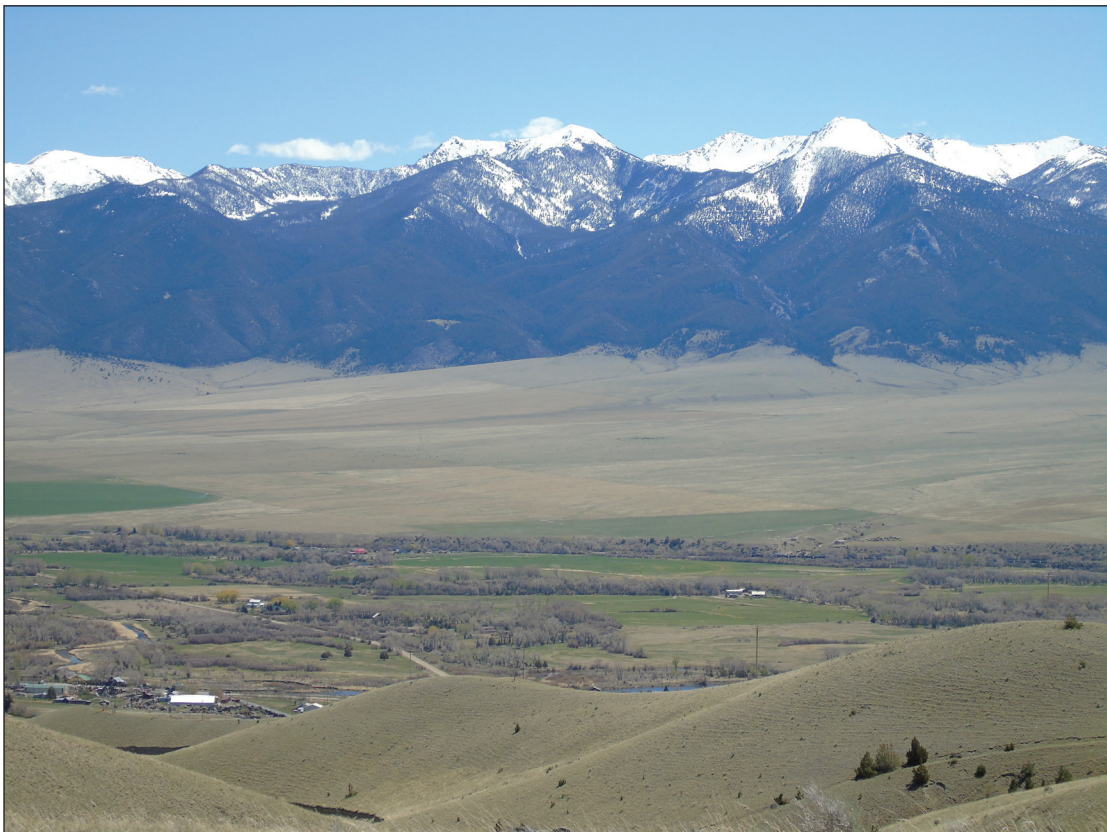


Montana Tech Geological Engineering M.S. student Nick Allin (left) discusses his research. Photo by A. Roth, MBMG.

FIELD TRIP: SILVER STAR



The Madison Au-Cu-Ag skarn at Silver Star, MT. Photo by K. Scarberry, MBMG.



The Tobacco Root Mountains from the Madison Au-Cu-Ag skarn at Silver Star, MT. Photo by K. Scarberry, MBMG.

Field Trip To The Madison Au-Cu Deposit, Silver Star, Montana

Jenna M. Kaplan¹ and Christopher H. Gammons²

¹*Broadway Gold Mining, Ltd.*

²*Department of Geological Engineering, Montana Tech*

Introduction to the Madison Gold Deposit

The Broadway Gold property sits on the intersection of two major structural zones that control regional mineralization. This property once was home to the historic Broadway mine, which was the largest gold producer in the Silver Star district, recovering an estimated 144,000 oz of gold between 1870 and 1942 (B. Price, written commun., 2005). The Broadway mine along with the Madison Gold deposit are localized along a mineralized skarn/jasperoid/massive sulfide body near the contact between limestone of the Mississippian Madison Group and granodiorite of the Cretaceous (80.4 ± 1.2 Ma, Lund et al., 2002) Rader Creek pluton. The Madison mine portal is located 250 meters to the north of the historic Broadway inclined shaft (fig. 1). The underground workings at the Madison mine, developed by Coronado Resources from 2008 to 2012, follow an elliptical decline that intercepts the down-dip extension of copper and gold mineralization that crops out at the surface in three small open pits (the Black, Victoria, and American Pit). The Broadway Gold property is owned by Broadway Gold Mining Ltd. who is currently conducting additional exploration techniques.

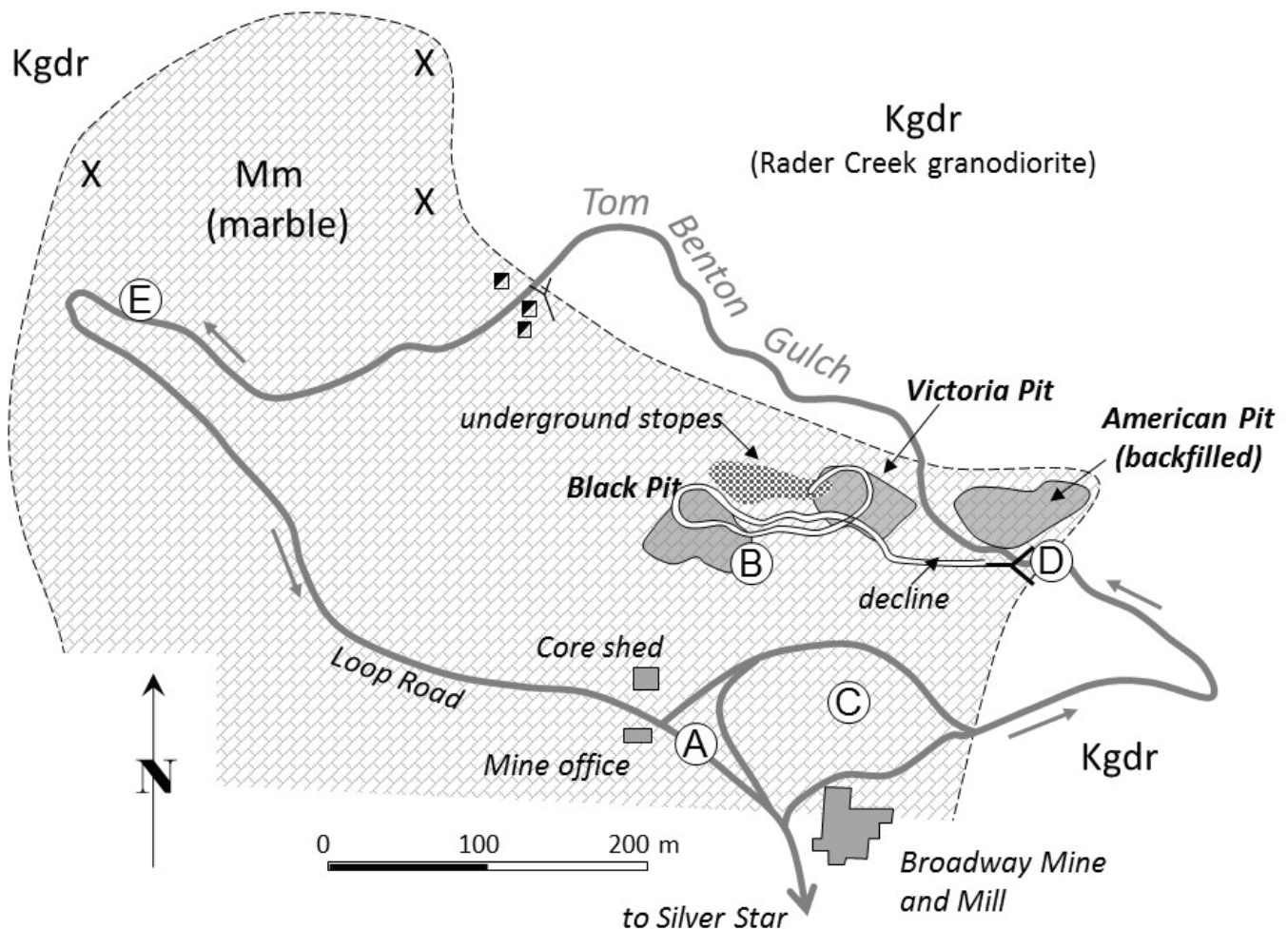


Figure 1. Map of mine workings and simplified geology near the Broadway and Madison Gold mines. Numbers refer to stops described in the text.

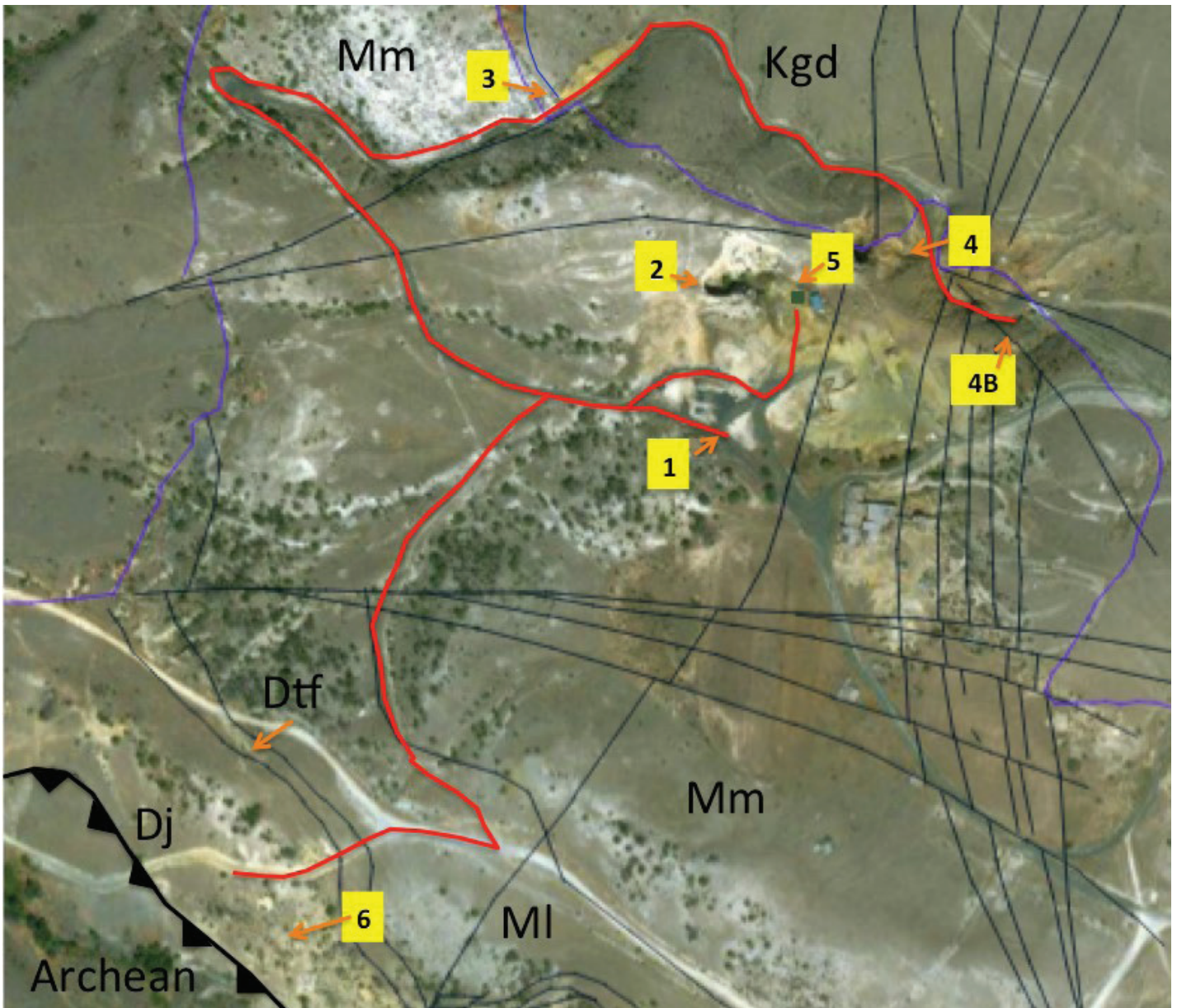


Figure 2. Simplified geologic base map with highlighted field trip route (red), faults (black), and major geologic units. Kgd, Rader Creek granodiorite; Mm, Madison Mission Canyon limestone; MI, Madison Lodgepole limestone; Dtf, Three Forks shale; Dj, Jefferson dolomite.

Field Trip Route

Stop 1: Boulders at the Mine Office

Boulders can be found lining the edge of the parking lot at the main office building, including: chalcocite, jasperoid, and skarn ore. This is also a good spot for discussing the regional geology of the district (fig. 3). The Madison Mine is located at the intersection of two major structural zones, the Great Falls Tectonic Zone and the Southwest Montana Transverse Zone (Perry Line), both which control regional mineralization (Berger and others, 2011). Southwestern Montana has experienced multiple major porphyry, skarn, and gold mineralizing events. The Madison Gold deposit is believed to be associated with a Cretaceous mineralization event. The major NW–SE-trending structures in the Silver Star district (fig. 3) may be related to similar NW-trending basement faults that control vein- and shear zone-hosted gold mineralization in the Tobacco Roots, as well as the Rochester district in the southwestern Highland Mountains. Old buildings from the historic Broadway mine form a picturesque foreground as one looks east across the Jefferson River Valley towards the Tobacco Root Mountains.

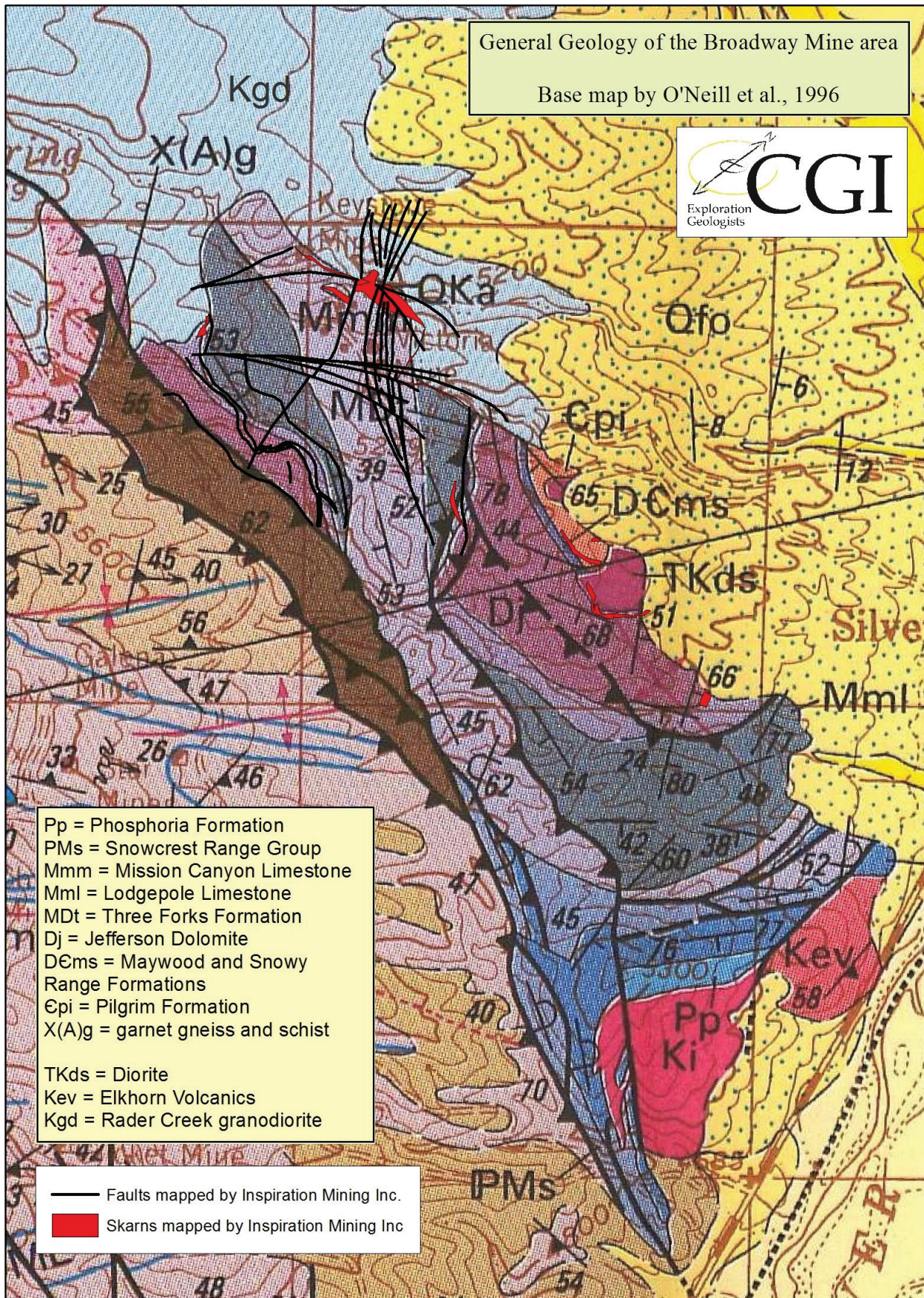


Figure 3. Geologic map of the Silver Star region from O'Neill and others (1996). Additional fault patterns were added from Inspiration Mines Inc. (1986). The Silver Star Fault, trending NW–SE, thrusts Archean basement rock on top of Proterozoic sediments (Childs and others, 2017).

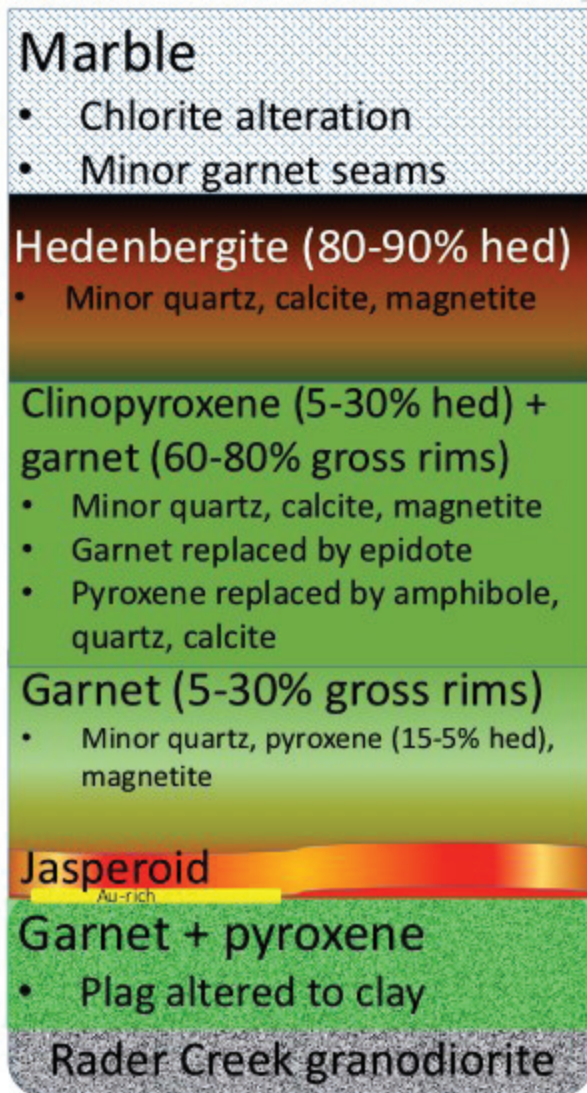


Figure 4. Schematic diagram showing typical mineral zonation within the Madison gold skarn. Hed. hedenbergite; gross, grossular (Zimmerman, 2017).

Stop 2: Black Pit

The Black Pit is named due to conspicuous outcrops of hedenbergite skarn along the southeastern rim of the pit. Hedenbergite ($\text{CaFeSi}_2\text{O}_6$) forms radiating clusters of prismatic crystals that can range up to 5 cm in length and is typically dark green to black in color. A metasomatic front is visible in the steep contact between hedenbergite and recrystallized limestone. The Black Pit was mined for the gold occurrence found in the brecciated, unaltered limestone found on the northern flank of the pit. Gold grades found in the fine matrix of the breccia run around 0.10 oz Au/ton (Price, written commun., 2005). The hedenbergite skarn was also mined for gold, although of lower grade. The breccia is clast-supported with a loose, sandy matrix and can include hedenbergite skarn clasts. It is possible that the breccia represents colluvium that filled a solution-collapse structure within the marble. If so, gold grades could be detrital in origin and were washed into the cracks from mineralized skarn. A hydrothermal origin has also been proposed. One of the best mineral collecting spots is within and around the Black Pit, with frequent jasperoid and sulfide-bearing skarn specimens. Figure 4 shows typical mineral zonation within the Madison gold skarn.

Stop 3: Altered Madison Limestone / Rader Creek Granodiorite

Driving down the road to Tom Benton Gulch, one will pass altered Madison limestone to the north. As you continue traveling east on the road, you will pass an old adit, sitting on a Au-bearing jasperoid body that is found in the contact between the Madison limestone and Rader Creek pluton. To the east, an outcrop that looks quite bedded is actually the Radar Creek granodiorite.

Stop 4: Jasperoid (Victoria and American Pit) / Skarn

The jasperoid forms in a steeply dipping, sinuous shape and consists of disseminated hematite, goethite, and limonite in a chalcedonic-silica cement. The jasperoid is commonly found brecciated and veined with sparry calcite. In some areas, the calcite veins were then completely replaced with native copper (grading up to 10%). One theory is that the bright red, hematitic jasperoid replaced sulfide minerals, whereas the yellow-brown jasperoid replaced silicate minerals in the prograde skarn. Although ore and waste look the same, the jasperoid was found to contain up to 1 opt Au. Sotendahl (2012) argued that the Silver Star jasperoid formed from the circulation of hot, oxidized groundwater that broke down the primary sulfide and skarn minerals, and redistributed copper to form pods of secondary chalcocite (figs. 5, 6). Due to gold's relative insolubility within oxidized fluids, the gold was most likely introduced into the jasperoid during skarn development. Gold grades found in the sulfide-bearing skarn are similar to those found in the jasperoid body.

You will first pass the Victoria Pit, located to the south. The mineralization below the Victoria is a gold-copper skarn and jasper deposit that extends for 1,600 feet along the intrusive-carbonate contact. The intrusive contact dips to the southwest at 20° – 70° . Rock type zonation away from the intrusion includes epidote endoskarn, jasper, garnet-pyroxene skarn, hedenbergite skarn, marble and polyolithic breccia, and marble (Price, written commun., 2005). Near the east end of the Victoria Pit, a jasperoid and hedenbergite outcrop exposes altered

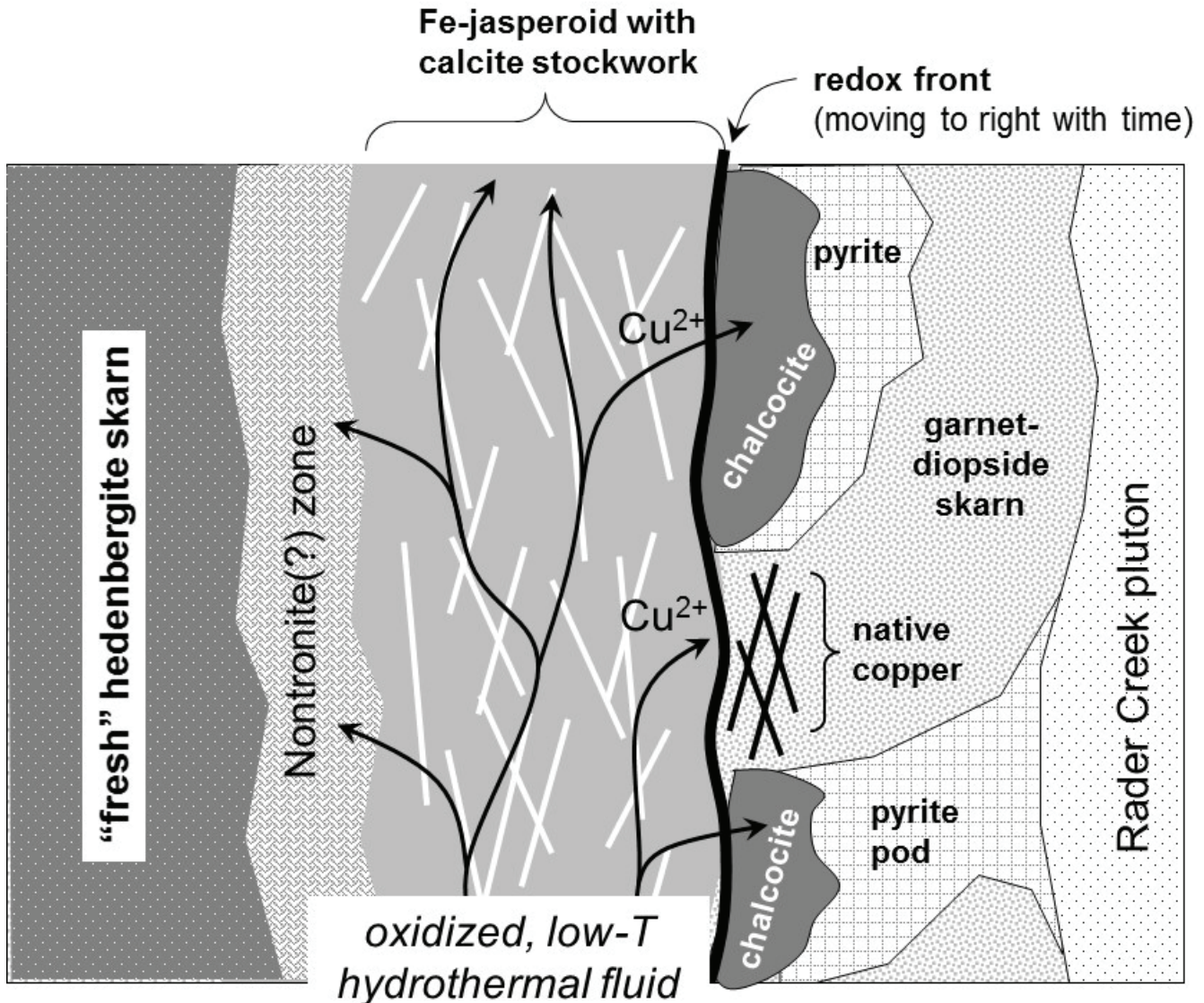


Figure 5. Schematic cross-section showing how late, oxidized fluids may have transformed prograde skarn into jasperoid with remobilization of copper.

hedenbergite to nontronite. Nontronite, an Fe(III)-rich smectite clay, is a common alteration product of hedenbergite (Eggleton, 1975) and is found lime-green in color and forms pockets and veinlets.

Continuing east on the road, you will pass another jasperoid body, the American Pit. Sulfide ores crop out at the surface in the American Pit and occur at depth below the Victoria Pit and Black Pit areas. High-sulfide skarns (up to 50% sulfides) and massive sulfides (up to 100% sulfides) were mined out of this pit (Price, written commun., 2005).

Traveling east of the American Pit, the Madison Mine portal can be found to the south. Directly north of the portal, a good outcrop of epidote-rich endoskarn developed in the Rader Creek granodiorite is exposed. Unaltered granodiorite crops out further east up the hill and valley. Garnet-diopside skarn can be found outcropping outside of the portal. The diopside is green and relatively fine-grained. The garnet is a pale brown and locally forms crystals up to 1 or 2 inches in diameter.

Stop 4B (dependent on daily operations): Underground Tour

	PROGRADE	RETROGRADE	OXIDATION &
	SKARN	SKARN	WEATHERING
pyrite			
pyrrhotite			
magnetite			
chalcopyrite			
bornite	??		
sphalerite		??	
galena			
electrum			
Bi-tellurides*	??		
hessite	??		
uraninite	??	??	
scheelite			
marcasite			
chalcocite			
copper			
cuprite			
tenorite			
gold			
silver			
CuI			
*includes tellurobismuthite (Bi ₂ Te ₃), tsumoite (BiTe), hedyite (Bi ₇ Te ₃)			
diopside			
garnet			
hedenbergite			
phlogopite			
chlorite			
nontronite			
hisingerite			
smectite			
kaolinite			
goethite			
hematite			
chalcedony			
calcite			

Figure 6. Ore and gangue mineral paragenesis at Madison Gold (from Sotendahl, 2012). Darker shading indicates a greater abundance of that mineral.

Stop 5: Core Shed

Time to take a look at some core highlights from the past year's drilling program. Broadway Gold's primary exploration drilling targets have been focused on defining the boundaries of the Au-bearing jasperoid and massive sulfide bodies that follow up on EM conductors, IP targets, surface mapping, and soil survey anomalies. The second drilling phase is focused on investigating the northwest Rader Creek / Limestone contact and potential copper porphyry target.

Stop 6: Replaced Sulfide Adits

If time allows, we can examine outcrops of the Jefferson dolomite to the southwest of the mine office. Several historic prospecting shafts are found within this Jefferson dolomite crest trending NW-SE across the property. The Jefferson Formation is found outcropping here as a ridge-forming, buff-orange dolomite that has undergone partial silicification. Elsewhere in southwest Montana, the Jefferson is dark gray or black in color, from disseminated hydrocarbons, and has a fetid smell when struck with a rock hammer. The anomalous color here is attributed to contact-metamorphism and hydrothermal alteration. Pseudomorphs of limonite after pyrite are locally visible. Most recent workers, including O'Neill and others (1996), interpret this area's overall structure as being an overturned syncline dipping southwest and dissected by faults (fig. 3).

References Cited

- Berger, B.R., Hildenbrand, T.G., and O'Neill, J.M., 2011, Control of Precambrian basement deformation zones on emplacement of the Laramide Boulder batholith and Butte mining district, Montana, United States: U.S. Geological Survey Scientific Investigations Report 2011-5016, 29 p.
- Eggleton, R.A., 1975, Nontronite topotaxial after hedenbergite: *American Mineralogist*, v. 60, p. 1063–1068.
- Lund, K., Aleinkoff, J.N., Kunk, M.J., Unruh, D.M., Zeihen, G.D., Hodges, W.C., du Bray, E.A., and O'Neill, J.M., 2002, Shrimp U-Pb and $^{40}\text{Ar}/^{39}\text{Ar}$ age constraints for relating plutonism and mineralization in the Boulder batholith region, Montana: *Economic Geology*, v. 97, p. 241–267.
- O'Neill, J.M., Klepper, M.R., Smedes, H.W., Hanneman, D. L., Frazer, G.D., and Mehnert, H.H., 1996, Geologic map and cross sections of the central and southern Highland Mountains, southwestern Montana: U.S. Geological Survey, Miscellaneous Investigations Series, Map I-2525.
- Sotendahl, J.M., 2012, Economic geology of the Madison Gold gold-copper skarn, Silver Star, Montana: Butte, Mont., Montana Tech, M.S. thesis.
- Zimmerman, Jarred. Weekly Report, July 31 to August 4, 2017.

Additional References

- Childs Geoscience and Broadway Gold Mining, 2017, "Pure New Investment Opportunity in Montana's Prolific Copper-Gold Camp," 2 July 2017, Silver Star, MT: unpublished report.
- DEQ, 2017, Silver Star District. <http://deq.mt.gov/Land/abandonedmines/linkdocs/126tech> [Accessed January 2018]
- Foote, M.W., 1986, Contact metamorphism and skarn development of the precious and base metal deposits at Silver Star, Madison County, Montana: Laramie, Wyo., University of Wyoming, Ph.D. thesis, 233 p.
- Gammons, C.H., Sotendahl, J.M., and Everett, D., 2010a, Secondary enrichment of copper at the Madison Gold skarn deposit, Silver Star District, Montana: *Northwest Geology*, v. 39, p. 15–24.
- Gammons, C.H., Sotendahl, J.M., and Cox, B.E., 2010b, Geology and mineral deposits in the northern Highland Mountains, Montana: A field trip crossing the Great Divide (twice): *Northwest Geology*, v. 39, p. 69–80.
- Kaplan, Jenna M., Weekly Report, April 1 to April 12, 2017.
- Sahinen, U.M., 1939, Geology and ore deposits of the Rochester and adjacent mining districts, Madison County, Montana: Montana Bureau of Mines and Geology Memoir 19, 53 p.



MBMG field geologist Kaleb Scarberry at the Golden Sunlight Mine north of Whitehall, MT. Photo by A. Roth, MBMG.



Montana Tech Geological Engineering M.S. student Francis Grondin discusses his poster with Philip Persson at the poster session. Photo by A. Roth, MBMG.

PRESENTER BIOGRAPHIES



Map Chat at the Butte Brewing Company in uptown Butte, MT. Photo by A. Roth, MBMG.



Colorado State University Geology M.S. student Jake McCane in the Boulder batholith near Boulder, MT. Photo by K. Scarberry, MBMG.

Allin, Nick

Originally from northern New Jersey, he earned a B.S. in Geology at Juniata College in Huntingdon, PA in 2016. He is currently a Masters student in the Geological Engineering department at Montana Tech, looking to graduate in 2018. His research interests include experimental high temperature aqueous geochemistry, geometallurgy, and economic geology.

Berg, Richard B.

Dick earned a B.S. in geology from Beloit College in 1959 and a Ph.D. in geology at the University of Montana in 1964. After teaching geology for two years at the State University College at Plattsburgh, N.Y., he joined the Montana Bureau of Mines and Geology in 1966. While at the Montana Bureau of Mines and Geology, he published reports and articles on bentonite, common clays, building and decorative stone, talc, chlorite, barite, zeolites, vermiculite, and sapphires. During a year as a visiting geologist at the Illinois Geological Survey, he published a report on tripoli in southern Illinois. In recent years, he authored or coauthored many geologic maps covering areas in central and western Montana and publications on Montana sapphires. His current research is on Montana sapphires. Dick has carefully avoided administrative obligations in favor of field studies.

Berzel, Matt

Matt started work at the MBMG in 2009 as a Professional Scientist working on surface water and groundwater research for the Environmental Program on the Butte and Anaconda area Superfund sites as well as other acid mine drainage and abandoned mine sites. He received a B.S. in Environmental Engineering from Montana Tech of the University of Montana and worked as an engineer specializing in storm-water runoff control and hydraulic systems designs. He received an M.S. in Hydrogeological Engineering at Montana Tech of the University of Montana in the summer of 2017. Matt is a registered Professional Engineer in the State of Montana.

Brimhall, George H.

George now manages Clementine Exploration following professorships at The John Hopkins University (1976-1978) and UC Berkeley (1978-2011), with earlier employment with the Anaconda Company (1972-1976) as the Steward Mine Geologist and Project Geologist for exploration of the deep porphyry copper-molybdenum mineralization. He received the Lindgren Award of the Society of Economic Geology in 1980 for his research and exploration management of the Pre-Mainstage Cu-Mo mineralization at Butte. He was awarded the Noyce Prize for excellence in undergraduate teaching at UC Berkeley, and was elected to the National Academy of Engineering in 2001.

Dalhof, Philip

Philip is currently a graduate student at Colorado State University in Fort Collins, studying Economic Geology under Dr. John Ridley.

Dupuis, Jonathan

Jonathan is a senior in Montana Tech's Professional and Technical Communication program. He works as a data preservationist working with the Montana Bureau of Mines and Geology, and digitally restoring and preserving historic mining documents. He also works as a local K-8 technology teacher in Divide, Montana through an internship through his PTC department.

Eastman, Kyle

Kyle has a M.S. in geology from Montana Tech of the University of Montana, and a B.S. in geology from Northern Arizona University. He has worked for the National Park Service at Oregon Caves National Monument, and for the Bureau of Land Management at Grand Canyon - Parashant National Monument. Kyle has been an avid mineral collector since an early age, and this passion brought him to study supergene mineralogy and ore-forming processes.

Edinberg, Sara

Sara graduated with a B.S. in Geology from Colorado State University, and earned an M.S. in Hydrogeology from Montana Tech of the University of Montana. She has worked as a Hydrogeologist in the Remediation Division of the Montana DEQ since July 2016. She oversees the remediation of the Colstrip Fly Ash Ponds at the Colstrip Steam Electric Station, and works as a technical expert on groundwater contamination for several other sites, including the Smurfit-Stone Paper Mill and the Carpenter-Snow Creek Mining District federal Superfund sites.

John E. Etienne

John graduated from the University of Montana with a degree in Geology. He earned his Masters of Science in Economic Geology from Eastern Washington University in 1987. He worked as a field geologist on precious metal deposit development in Nevada, Colorado, and Montana. Since 2006, John has worked with New Jersey Mining Company, leading geologic field work on the company's existing gold property development and production. He presently is responsible for ore control in the open pit and underground mining at the company's Golden Chest project near Murray, Idaho.

Gabelman, John W.

John graduated from Colorado School of Mines with Geol. Eng. in 1943, Ms. Geol. Eng. In 1948, and DSc. in 1949. He worked as an engineer and geologist for several companies before joining the Atomic Energy Commission in 1954 as District Geologist. He served as Geologic Advisor to the Raw Materials Representative for Latin America out of Lima, Peru, and Chief of Resource Appraisal in Washington headquarters, 1961-75. He joined Utah International as Manager of Exploration Research in 1983. He then founded Gabelman Associates, remaining active in uranium, gold, and oil/gas exploration in the western U.S. He retired to Butte in 2003.

Gammons, Christopher H.

Chris is a Professor in the Geological Engineering Dept. at Montana Tech. He grew up in Massachusetts and got a BS degree at Bates College in Maine and a PhD at Penn State. Before coming to MT Tech in 1997, he worked as a post-Doc at Monash University (Melbourne), the Swiss Federal Inst. Of Technol., and McGill University in Montreal. He also worked a couple years as an exploration geologist for the Anaconda Company. He does research in geochemistry and mineral deposits.

Gibson, Richard I.

Dick was born in Arkansas and grew up in Michigan. He studied geology at Indiana University, and Indiana's geologic field station in the Tobacco Root Mountains led to his love for Montana. After four years analyzing the mineralogy of kidney stones, he began a 40-year+ career as a geophysicist specializing in gravity and magnetic interpretation in the oil business. After teaching 14 summers and living at the Indiana geologic field station for four years as their caretaker, he moved to Butte in 2003, where he's been involved in Butte History,

from tours and museums to writing books, newspaper columns, and appearing in the Clark-Daly episode of the 2015 American Titans series on the American Heroes Channel. He's been a Geologist Study Leader for Smithsonian Journeys in Iceland, Alaska, and Western USA, and is the author of the History of The Earth Perpetual Calendar (a book and 380-episode podcast series) and "What Things Are Made Of: America's Global Dependency for Nearly Everything." He's the co-founder of the Tobacco Root Geological Society, and he's been collecting minerals since sometime before age 7.

Gnanou, Hamadou

Hamadou is a graduate student at Montana Tech and his study is focused on Geology. Hamadou got his undergraduate degree in Geology at University of Ouagadougou (Burkina Faso) and his Post-bac at Montana Tech. His career goal is to become an exploration geologist with a good understanding of economic geology and ore deposits. He is currently pursuing his master's degree in Geosciences and expects to graduate in Spring 2018. He previously worked as an exploration geologist with a junior mining company Sarama Resources before coming to Montana Tech to pursue his graduate studies.

Gobla, Michael J.

Mike is a geotechnical engineer with the Bureau of Reclamation in Denver, Colorado. He has degrees in mining engineering from the Colorado School of Mines and New Mexico Tech. His professional accomplishments include the design of major mine reclamation projects including the Summitville Mine in Colorado and the Gilt Edge Mine in South Dakota. For the past 40 years, Mike has been a mineral collector specializing in Montana mineralogy and mining history.

Grondin, Francis

Francis moved to Butte from Johnson City, Tennessee to start his graduate degree in Geo-sciences at Montana Tech. He earned his Undergraduate degree of Geology from Tennessee Technological University. The move out west was an easy choice, as he wanted to experience new opportunities and geology. He is learning new techniques, gaining new experiences, to become a well-rounded, experienced geologist. My passion is fieldwork and research. Nothing better than a breath of fresh air and a field book in hand.

Hargrave, Phyllis

Phyllis has a B.S. in geology from St. Lawrence University, and a M.S in geology from Montana College of Mineral Science and Technology (now Montana Tech), where she mapped a portion of the Lowland Creek Volcanics north of Butte for her thesis. Her experience has ranged from uranium exploration in Virginia and Colorado, New Mexico, and Wyoming, gold exploration in Montana (Phelps-Dodge, Placer Dome, & several small companies). In 1994, she joined MBMG and for 10 years was involved in the Abandoned and Inactive Mines Program - a contract with the BLM and the USFS to inventory abandoned mine locations and assess and prioritize their reclamation. Her later work for the Bureau includes conducting a placer deposit inventory, geologic mapping, hydrology and editing Bureau publication. Phyllis is a long-time member of the Tobacco Root Geological Society and serves as an editor for Northwest Geology.

Kaplan, Jenna M.

Jenna was born and raised in Chicago, Illinois. She received her bachelors in geology from Indiana University. She completed her masters from Montana Tech with a focus in ore deposit geology. Jenna went on to work as a field geologist for the Forest Service focusing in abandoned mine reclamation. She is currently working as the project geologist for Broadway Gold Mining at the Madison Au-Cu-Ag skarn deposit.

Korzeb, Stanley L.

Stan earned a B.S. in geology from the University of Massachusetts (Amherst, MA) and an M.S. in geology from Miami University (Oxford, OH). Stan is an Internationally Registered Professional Geologist through the Society of Mining Metallurgy and Exploration. He was a geologist with the Resource Evaluation branch at the US Bureau of Mines in Denver, Colorado for 15 years. Stan consulted for three companies in the Kilometer 88 District, Venezuela, then worked two years as Chief Geologist at an operating zinc mine in Sierra Mojada, Mexico, and was Vice-President of Exploration for five years at Texas Rare Earth Resources in Denver, Colorado. He became an exploration manager at the Pend Oreille mine in Metaline Falls, Washington and, for the past three years, worked at the Montana Bureau of Mines and Geology as its Economic Geologist.

Law, Shanna

Shanna has a B.S. in Environmental Geology from Juniata College and is currently working towards her M.S. in Geosciences – Geochemistry from Montana Tech. She is an active scientist of the Laboratory Exploring Geobiochemical Engineering and Natural Dynamics (LEGEND) under Dr. Alysia Cox at Montana Tech. Shanna expects to graduate in May 2018. Her academic interests include water-rock and water-rock-microbe interactions, and she aims to build a career in geochemistry and biogeochemistry.

McCane, Jake

Jake is a Colorado State University graduate student originally from Seattle, Washington. His research interests lie mainly in petrology and economic geology. In the future, Jake plans to work in the mining industry, focusing on mineral exploration. If the opportunity arises, he would gladly work abroad.

Metesh, John

John graduated from Montana State University in 1986, with an Earth Science degree (Geology). He earned a Master's degree in Geological Engineering from the Montana School of Mineral Science and Technology (Montana Tech) in 1990, and a Doctorate in Geology from the University of Montana in 2004. John joined the Montana Bureau of Mines and Geology 28 years ago as a Research Hydrogeologist, became Research Division Chief, Assistant Director, and, in 2012, Director and State Geologist. His research areas include mine water geochemistry/modeling and groundwater flow modeling.

Mosolf, Jesse G.

Jesse is a field geologist at the Montana Bureau of Mines and Geology. Jesse is a Montana native who holds a B.S. in Chemistry from MSU-Bozeman, a M.S. in Geology from UCLA, and a Ph.D. in Geological Sciences from UCSB. His research focuses largely on the tectonics of the North and South American Cordilleras where he has participated in several field-based projects in Bolivia, Chile, Peru, Mexico, Nevada, and Montana.

Persson, Philip M.

Philip was born in Uppsala, Sweden and became interested in minerals and geology at an early age after discovering pyrite crystals in an outcrop behind his parent's house near Stockholm. After moving to the USA in 1993 and ending up near Franklin, New Jersey, his obsession with all things mineral-related really took off, and thanks for the encouragement of his parents and the local mineral clubs, he soon accumulated a large collection of both self-collected and purchased minerals, and also began selling minerals on eBay and at local shows. After moving to Colorado in 2005 and obtaining a BA in geology from the University of Colorado at Boulder in 2012, he worked in the mining industry as an exploration geologist on projects in places such as Nevada, Idaho, and

Arctic Sweden. He obtained a master of science in geology with a focus on economic geology from the Colorado School of Mines in 2017, and has co-authored papers in the *American Mineralogist* and *Mineralogical Magazine*. He recently started a new job as a sales and marketing coordinator for Collector's Edge Minerals in Golden, Colorado. As a secret fan of black ugly minerals and sulfides, he is thrilled to be in Butte Montana for the 2017 MBMG Mining & Mineral Symposium and looks forward to presenting his master's thesis research.

Scarberry, Kaleb C.

Kaleb is a field geologist hired by the MBMG in 2012. He earned his doctorate in geology from Oregon State University in 2007 and spent the next five years teaching field geology and structural geology at Colorado State University. His current research focuses on Late Cretaceous – Tertiary volcanic stratigraphy, geochronology, and precious metal ore deposits.

Schubert, Benjamin

Ben obtained a Bachelor's Degree in Geological sciences from Rutgers University in New Brunswick, NJ in 2013, and a Master's Degree in Geological Sciences from Montana Tech in 2017. He possessed a strong interest in geology since early childhood and worked towards his goal of becoming a professional geologist since his education first started. He has been a member of numerous geological groups and societies, including the Montana Tech Geology Club and Ore Ganguer. He currently resides and works as a Lab Technician in Lexington, KY where he performs soil analyses at L. E. Gregg Associates.

Smith, Christopher P.

Christopher is a GIS Analyst at the Montana Bureau of Mines & Geology (MBMG) in Butte, Montana. Mr. Smith has been employed as a student employee with the MBMG since 2014. As a GIS Analyst he is responsible for geologic and other map & dataset development, high level development of geospatial databases, QA/QC, and relational database development & management. Mr. Smith is currently pursuing a B.S in Geophysical Engineering and Applied Mathematics at Montana Tech of the University of Montana.

Smith, Garrett

Garrett Smith is a geochemist currently working for the DEQ's Hard Rock Mining Bureau in Helena. He was born and raised in New Mexico, but returned to his ancestral roots in Montana after high school. He completed his undergraduate and graduate degrees at Montana Tech, with an emphasis in stable isotope geochemistry. Prior to his current position, Garrett was an assistant research professor with the Montana Bureau of Mines and Geology in Butte.

Thale, Paul R.

Paul is a GIS Specialist at the Montana Bureau of Mines & Geology (MBMG) in Butte, Montana. Mr. Thale has been with the MBMG since 1999. His responsibilities include GIS analysis and geospatial database production, QA/QC, data migration, data maintenance, IT support, & network infrastructure. He also trains staff & students in the use of ESRI software for geologic mapping and analysis. More recently he has been engaged with publishing geospatial data using ESRI map services and geodata services.

Zieg, Jerry A.

Jerry is a native of Meagher County (White Sulphur Springs) and received a graduate degree in geology from the University of Montana in 1981. He worked with Cominco American Inc. for 24 years as an exploration geologist, during which he participated in the 1985 discovery of the Johnny Lee deposit at Black Butte. He helped form Tintina Resources Inc. specifically focused on development of the Johnny Lee deposit.



Precambrian Belt Supergroup strata exposed in pit walls at the Golden Sunlight Mine north of Whitehall, MT. Photo by A. Roth, MBMG.



Clockwise from top left: MBMG's Data Preservation program leader Peggy Delaney, MBMG's Director and Montana State Geologist John Metesh, MBMG geologist Dick Berg, and Yvonne Metesh at the "Map Chat" at the Butte Brewing Company in uptown Butte. Photo by A. Roth, MBMG.

